

# The Online Journal Of Science and Technology

*Volume 2 Issue 4*  
*October 2012*

Prof. Dr. Aytekin İşman  
**Editor-in-Chief**

Prof. Dr. Mustafa Şahin DÜNDAR  
**Editor**

Assist. Prof. Dr. Evrim GENÇ KUMTEPE  
Assist. Prof. Dr. Hayrettin EVİRGEN  
Assist. Prof. Dr. Mustafa GAZİ  
Inst. Metin ÇENGEL  
**Associate Editors**



**Copyright © 2012 - THE ONLINE JOURNAL OF SCIENCE AND TECHNOLOGY**

All rights reserved. No part of TOJSAT's articles may be reproduced or utilized in any form or by any means, electronic or mechanical, including photocopying, recording, or by any information storage and retrieval system, without permission in writing from the publisher.

Published in TURKEY

**Contact Address:**

Prof. Dr. Aytekin İŞMAN- TOJSAT, Editor in Chief Sakarya-Turkey

**Message from the Editor-in-Chief**

The Online Journal of Science and Technology (TOJSAT) reflect rapid development on diffusing valuable researches from interdisciplinary fields through academic papers. The journal aims to underline the significance of merging academic disciplines and different practices in the field of science and technology. In this respect, selected papers from the field of science and technology need to be original, different practice on the base of qualitative and quantitative researches, especially mix approach.

As this issue promotes how the journal is developing as regards its vision and mission, there are valuable researches and their studies that contributed to the journal. Therefore, I would like to thank to editorial board, reviewers and the researchers for their valuable contributions to the journal and this issue.

**October, 01, 2012**

**Prof. Dr. Aytekin İŞMAN**

**Editor-In-Chief**

**Message from the Editor**

Almost two years have been past since the journals' first issue published on-line. Now, we have published the fourth issue of second volume.

In this issue of journal, selected papers such as Prediction of Slope Stability Using Statistical Method and Fuzzy Logic; The Role of Desalinated Water in Integrated Water Resource Management in Abu Dhabi Emirate-UAE; Cubic Transformational High Dimensional Model Representation; Effects on The Students' Personal Competences of the Usage of PBL Methodologies in Professional Reality Simulation Environments: Students, Teachers, Graduates and Employers' perceptions; Geochemical distribution of heavy metals in soils and stream sediments of Omiyale and environs, Ibadan, southwestern Nigeria will be published.

I will thank to the readers for supports by sending their valuable scientific works to publish in our journal. See you in 3rd International Science, Technology and Engineering Conference 2012 held in Dubai, United Arab Emirates.

**October, 01, 2012**

**Prof. Dr. M. Şahin DÜNDAR**

**Editor, TOJSAT**

**Editor-in-Chief**

Prof. Dr. Aytekin İŞMAN - Sakarya University, Turkey

**Editor**

Prof. Dr. Mustafa Şahin DÜNDAR - Sakarya University, Turkey

**Associate Editors**

Assist. Prof. Dr. Hayrettin EVİRGİN, Sakarya University, Turkey

Assist. Prof. Dr. Mustafa GAZİ, Eastern Mediterranean University, TRNC

Assist. Prof. Dr. Evrim GENÇ KUMTEPE, Anadolu University, Turkey

Inst. Metin ÇENGEL, Sakarya University, Turkey

**Editorial Board**

Ahmet AKSOY, Erciyes University, Turkey	Berrin ÖZÇELİK, Gazi University
Ahmet APAY, Sakarya University, Turkey	Can KURNAZ, Sakarya University, Turkey
Ahmet BİÇER, Gazi University, Turkey	Eralp ALTUN, Ege University, Turkey
Ali DEMIRSOY, Hacettepe University, Turkey	Fatma AYAZ, Gazi University, Turkey
Ali Ekrem OZKUL, Anadolu University, Turkey	Burhan TURKSEN, TOBB University of Economics and Technology, Turkey
Ali GUNYAKTI, Eastern Mediterranean University, TRNC	Galip AKAYDIN, Hacettepe University, Turkey
Alparslan FIGLALI, Kocaeli University, Turkey	Gilbert Mbotho MASITSA, University of The Free State - South Africa
Arif ALTUN, Hacettepe University, Turkey	Gregory ALEXANDER, University of The Free State - South Africa
Aydın Ziya OZGUR, Anadolu University, Turkey	Hasan Hüseyin ONDER, Gazi University, Turkey
Bekir SALIH, Hacettepe University, Turkey	Hasan KIRMIZIBEKMEZ, Yeditepe University, Turkey
Belma ASLIM, Gazi University, Turkey	Hüseyin YARATAN, Eastern Mediterranean University, TRNC
Bilal GÜNEŞ, Gazi University, Turkey	Iman OSTA, Lebanese American University, Lebanon
Bilal TOKLU, Gazi University, Turkey	Kenan OLGUN, Sakarya University, Turkey
Cafer CELİK, Ataturk University, Turkey	Mehmet CAGLAR, Eastern Mediterranean
Ergun KASAP, Gazi University, Turkey	
Fatma ÜNAL, Gazi University, Turkey	

Gürer BUDAK, Gazi University, Turkey	University, TRNC
Harun TAŞKIN, Sakarya University, Turkey	Muharrem TOSUN, Sakarya University, Turkey
Hasan DEMIREL, Eastern Mediterranean University, TRNC	Murat TOSUN, Sakarya University, Turkey
Hikmet AYBAR, Eastern Mediterranean University, TRNC	Mustafa DEMİR, Sakarya University, Turkey
Hüseyin EKİZ, Sakarya University, Turkey	Mustafa GAZİ, Near East University, TRNC
Hüseyin Murat TÜTÜNCÜ, Sakarya University, Turkey	Mustafa KALKAN, Dokuz Eylul University, Turkey
Işık AYBAY, Eastern Mediterranean University, TRNC	Nureddin KIRKAVAK, Eastern Mediterranean University, TRNC
İbrahim OKUR, Sakarya University, Turkey	Oğuz SERİN, Cyprus International University, TRNC
İlyas ÖZTÜRK, Sakarya University, Turkey	Selahattin GÖNEN, Dicle University, Turkey
İsmail Hakkı CEDİMOĞLU, Sakarya University, Turkey	Senay CETINUS, Cumhuriyet University, Turkey
Latif KURT, Ankara University, Turkey	Sevgi AKAYDIN, Gazi University, Turkey
Levent AKSU, Gazi University, Turkey	Ali ÇORUH, Sakarya University, Turkey
Mehmet Ali YALÇIN, Sakarya University, Turkey	Antonis LIONARAKIS, Hellenic Open University, Greece
Mehmet TURKER, Gazi University, Turkey	Canan LACIN SIMSEK, Sakarya University, Turkey
Mehmet YILMAZ, Gazi University, Turkey	Cüneyt BİRKÖK, Sakarya University, Turkey
Metin BAŞARIR, Sakarya University, Turkey	Emine Sercen DARCIN, Sakarya University, Turkey
Murat DIKER, Hacettepe University, Turkey	Ercan MASAL, Sakarya University, Turkey
Mustafa GAZI, Eastern Mediterranean University, TRNC	Ergun YOLCU, Istanbul University, Turkey
Mustafa GUL, Turkey	Elnaz ZAHED, University of Waterloo, UAE
M. Şahin DÜNDAR, Sakarya University, Turkey	Fatime Balkan KIYICI, Sakarya University, Turkey
Nabi Bux JUMANI, Allama Iqbal Open University, Pakistan.	Gülay BİRKÖK, Gebze Institute of Technology, Turkey
Orhan ARSLAN, Gazi University, Turkey	Hasan OKUYUCU, Gazi University, Turkey
Orhan TORKUL, Sakarya University, Turkey	Hayrettin EVİRGİN, Sakarya University, Turkey
Osman ÇEREZCİ, Sakarya University, Turkey	

Rahmi KARAKUŞ, Sakarya University, Turkey	İsmail ÖNDER, Sakarya University, Turkey
Recai COŞKUN, Sakarya University, Turkey	Kenan OLGUN, Sakarya University, Turkey
Recep İLERİ, Bursa Orhangazi University, Turkey	Melek MASAL, Sakarya University, Turkey
Ridvan KARAPINAR, Yüzüncü Yıl University, Turkey	Muhammed JAVED, Islamia University of Bahawalpur, Pakistan
Sevgi BAYARI, Hacettepe University, Turkey	Mustafa YILMAZLAR, Sakarya University, Turkey
Süleyman ÖZÇELİK, Gazi University, Turkey	Nilgun TOSUN, Trakya Üniversitesi, Turkey
Tuncay ÇAYKARA, Gazi University, Turkey	Nursen SUCSUZ, Trakya Üniversitesi, Turkey
Türkey DERELİ, Gaziantep University, Turkey	Phaik Kin, CHEAH Universiti Tunku Abdul Rahman, Malaysia
Ümit KOCABIÇAK, Sakarya University, Turkey	Rıfat EFE, Dicle University, Turkey
Yusuf KALENDER, Gazi University, Turkey	Şenol BEŞOLUK, Sakarya University, Turkey
Vahdettin SEVİNÇ, Sakarya University, Turkey	Uner KAYABAS, Inonu University, Turkey
Zekai SEN, Istanbul Technical University, Turkey	Vasudeo Zambare, South Dakota School of Mines and Technology, USA
Abdülkadir MASKAN, Dicle University, Turkey	Yusuf KARAKUŞ, Sakarya University, Turkey
Ahmet Zeki SAKA, Karadeniz Technical University, Turkey	Yusuf ATALAY, Sakarya University, Turkey
Ali GUL, Gazi University, Turkey	Yüksel GÜÇLÜ, Sakarya University, Turkey
Atilla YILMAZ, Hacettepe University, Turkey	

## Table of Contents

### AUTOMATION OF PHARMACY INVENTORY MANAGEMENT

*Zekerijah Šabanović* ..... 1

### CUBIC TRANSFORMATIONAL HIGH DIMENSIONAL MODEL REPRESENTATION

*Erdoğan Şen and Kamil Oruçoğlu* ..... 5

### EFFECTS ON THE STUDENTS' PERSONAL COMPETENCES OF THE USAGE OF PBL METHODOLOGIES IN PROFESSIONAL REALITY SIMULATION ENVIRONMENTS: STUDENTS, TEACHERS, GRADUATES AND EMPLOYERS' PERCEPTIONS

*Margarida M. Pinheiroa, Cláudia S. Sarricob and Rui A. Santiagoc*..... 11

### EXPERT IDEA ON LIQUID LIMIT AND PLASTIC LIMIT ESTIMATION WITH SOIL RESISTIVITY PROFILE

*Zamri Chik, S.M. Taohidul Islam, Hilmi Sanusi and Mohd. Marzuki Mustafa*..... 19

### FATE OF FLUOMETURON DISSOLVED IN NATURAL WATERS AND EXPOSED TO SOLAR LIGHT

*Sabrina Halladja, Abdelaziz Boulkamh and Claire Richard*..... 24

### GEOCHEMICAL DISTRIBUTION OF HEAVY METALS IN SOILS AND STREAM SEDIMENTS OF OMIYALE AND ENVIRONS, IBADAN, SOUTHWESTERN NIGERIA

*Laniyan, T. A, Omosanya, K.O, Adesanya and O. O* ..... 30

### GLOBAL STABILITY AND SETTLEMENT OF SEGMENTAL RETAINING WALLS REINFORCED WITH GEOGRID

*Anuar Kasa, Zamri Chik and Mohd Raihan Taha*..... 41

INFLUENCE OF PROCESS CONDITIONS ON GLYCEROL ESTERIFICATION CATALYZED BY TETRA-NBUTYLAMMONIUM-MODIFIED MONTMORILLONITE CATALYST <i>Iman Hashemizadeh and Ahmad Zuhairi Abdullah</i> .....	47
ISOLATION AND CHARACTERIZATION OF ANTIVIRAL PROTEIN FROM SALSOLA LONGIFOLIA LEAVES EXPRESSING POLYNUCLEOTIDE ADENOSINE GLYCOSIDE ACTIVITY <i>Zenab Aly Torky</i> .....	52
NOVEL CHIRAL COMPOUND: (R) AND (S) 1-(2-BENZYLOXY-3-METHOXYPHENYL)-2,2,2-TRICHLOROETHYL BENZENSULFONATE, SYNTHESIS AND CHARACTERIZATION <i>Mohammed Hadi Al-Douh</i> .....	59
PREDICTION OF SLOPE STABILITY USING STATISTICAL METHOD AND FUZZY LOGIC <i>Tarig Mohamed, Anuar Kasa and Muhammad Mukhlisin</i> .....	68
REMOVAL OF CR(III) IONS FROM TANNERY WASTE WATER THROUGH FUNGI <i>Amna Shoaib</i> .....	74
STEADY-STATE ELECTRON DRIFT VELOCITY AT DIFFERENT TEMPERATURES IN ALXGA1-XN AND INXGA1-XN ALLOYS: MONTE <i>Hamdouné, A, and Bachir, N</i> .....	79
THE POTENTIAL FOR CLIMATE CHANGE MITIGATION IN SOLID WASTE DISPOSAL: A CASE STUDY OF LAGOS LANDFILLS <i>Aboyade, A.O, Rabiou, A. and Amigun, B.</i> .....	84
THE ROLE OF DESALINATED WATER IN INTEGRATED WATER RESOURCE MANAGEMENT IN ABU DHABI EMIRATE-UAE <i>Muthanna Al-Omar</i> .....	90



# Automation of Pharmacy Inventory Management

Zekerijah Šabanović

Medical Faculty of Tuzla, University of Tuzla, Bosnia and Herzegovina  
zekerijah.sabanovic@untz.ba

**Abstract:** Pharmacy inventory management (PIM) comprises business activities which are connected with the size and placement of stocked drugs. To manage minimal and maximal drugs stock, orders dynamics etc., pharmacies must track expiration dates of each drug in stock. Outdated drugs can't be counted as stock and produce lot of costs, especially for their disposal. The most number of pharmacies in Bosnia use European Article Numbering (EAN13) barcode by which is impossible to define drug expiration dates. Radio Frequency Identification (RFID) enables full automatization of PIM, but it is still not in use, mostly because of high costs of implementation of this system.

In our research we have observed 52 Bosnian pharmacies and presented another approach to barcode technology which can be used in automatization of PIM. As the base we have used existing EAN13 code, adding 6 digits for expiration dates. We have successfully created and tested program for extraction of EAN13 and expiration dates from that barcode using separate files in database to keep inputs, outputs and stocks of each item by expiration dates.

**Key words:** Pharmacy Inventory Management, Automatization, Barcode Technology, Radio Frequency Identification (RFID), Clarion Programming Language

## Introduction

Inventory management is the systems and processes of maintaining the appropriate level of stock in a warehouse. The activities of inventory management involves in identifying inventory requirements, setting targets, providing replenishment techniques and options, monitoring item usages, reconciling the inventory balances, and reporting inventory status (Sysoptima, 2005). The main activities (amongst the others) are: inventory planning and demand forecasting, inventory monitoring and balance reconciliation and inventory reporting. There is different types of costs that take part in inventory cost structures: ordering (or setup) cost, carrying (or holding) cost (cost of capital, cost of storage, cost of obsolescence, deterioration, and loss), stock out cost, item costs, shipping costs and other cost subject to volume discounts.

To have a successful pharmacy inventory management, it is very important (especially for drugs) to track and control of the expiration dates. As researches show (Charlotte A. S., 2002) (McCarthy G., 2005): Much of the pharmaceutical waste occurring at a pharmacy was due to expired pharmaceuticals. The development of reverse distribution companies has enabled pharmacies to ship all outdated drugs as products back through these firms for the purpose of returning them to the manufacturer for credit. Any outdated items that do not meet the manufacturers' return policy become waste at the reverse distributor which becomes the waste generator, since this is where the decision to discard the item is made.

The most number of pharmacies in Bosnia (in the Europe also) use EAN13 barcode as the standard by which is impossible to define expiration dates. Pharmacies in Bosnia mostly follow expiration dates manually. Employees walk around from shelf to shelf and write down quantity with separate expiration dates of each lot (or item) and send this, paper based reports to the managers. They enter the data into computers (mostly in Excel), analyze them and make appropriate decisions connected with orders, prices, sales etc. This approach to the pharmacy inventory management is less successful.

## 1. THE ROLE OF INFORMATION TECHNOLOGY

### 1.1. Barcode Technology

There are two main types of barcodes which are used in enterprises: linear (1D) and two-dimensional (2D). The usage of first one is much cheaper and simple but it can present smaller number of human readable codes. Linear barcodes are used widely and there is a lot of types of them like: UPC, CodaBar, Code 25, 39, 128, Pharmacode, European Article Numbering -EAN, etc. There is a lot areas for use of barcode technology like: inventory management, stock control, manufacturing, patient identification, drug identification, purchased items scanning, work orders scanning, equipment tracking, document management, entertainment (tickets with barcode) etc. (Šabanovic Z., Osmanbegović E., 2010). EAN13 barcode is used as a standard in most European countries.

### 1.2. Radio Frequency Identification (RFID)

The purpose of an RFID system is to enable data to be transmitted by a portable device (using radio frequency), called a tag, which is read by an RFID reader and processed according to the needs of a particular application. The data transmitted by the

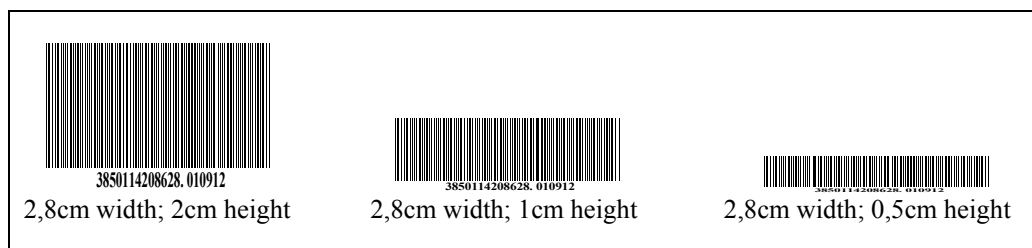
tag may provide identification or location information, or specifics about the product tagged, such as price, color, date of purchase, etc. RFID technology has been used by thousands of companies for a decade or more. RFID quickly gained attention because of its ability to track moving objects. There are a lot of current and potential uses of this technology (Association for Automatic Identification and Mobility, 2010) like: asset tracking, manufacturing, supply chain management, retailing, payment systems, security and access control.

## Material and Methods

In September 2011. we have observed 52 small and middle size pharmacies in North Eastern of Bosnia and Herzegovina. Tracking of drug expiration dates is very important for all of them. For simulation and testing purpose we have generated extended barcode which includes EAN13 barcode and 6 digits for expiration date (with point as delimiter) (Picture 1, Picture 2). Through experiments, as the most appropriate we have found Codabar which can accept up to 30 numeric digits. We have printed barcodes in 600\*600 dpi in various sizes (width from 10cm to 2cm) using Datamax I-4604 thermal printer which is used for label printing applications that demand high-resolution graphics, two-dimensional barcodes or very small labels. For barcode scanning we have used two types of barcode scanners: Metrologic mk9590-61a38 (lower resolution reader) and 3800g Linear & PDF Image Reader (2dimensional and high resolution reader).

In Clarion programming language we have created form for extended barcode scanning and routine for EAN13 and expiration date extraction from it (Šabanović, Z., Osmanbegović, E., 2010). Separate files (tables) were added to the relational database to keep expiration dates and quantity for each item (with different expiration date).

Picture 1. Samples of smallest extended barcodes (Codabar) that can be decoded



Picture 2. Sample of drug with extended barcode (front side) and EAN13 (top side)



## 3. RESULTS

By analyzing of data from 52 observed pharmacies we have found that 100% of observed pharmacies use barcode technology for point of sale purposes, 17,3% generates and prints barcodes (EAN13 only 11,5% of pharmacies), 88,5% of pharmacies track expiration dates manually (Table1). In observed pharmacies there is no any specific Decision Support Systems – DSS, built to help and automate pharmacy inventory management. There is no usage of RFID technology in pharmacies inventory management

**Table 1.** Usage of barcode technology (52 observed pharmacies)

Description	Number of pharmacies	Percentage
Point of Sale (POS) usage of barcode technology	52	100,0%
Other uses of Barcode (inventory management)	7	13,5%
Barcode generate and print	9	17,3%
EAN13 generate and print	6	11,5%
Manual tracking of drugs expiration dates	46	88,5%
Usage of RFID	0	0,0%
Computer generated drugs orders	11	21,2%
Usage of specific DSS in pharmacy inventory management	0	0,0%
Usage of Excel in pharmacy inventory management	36	69,2%

Picture 3. Form for extended barcode scanning

During testing of form and program routine made in Clarion (Sofvelocity Inc., 2011) (Picture 3, Picture 4) we didn't find any errors in drugs expiration dates extraction and storing them in the database. Barcode can be printed in a minimal size 2,8cm of width (Picture 1). Smaller barcode pictures cannot be scanned and decoded. Files/tables which keep expiration dates have been successfully added in existing relational database Sofvelocity Inc., 2011) (Diagram 1)

Picture 4. Routine for EAN13 and drugs expiration date extraction

```

Extract_EAN_ExpiryDate  ROUTINE

  IF barcode = '' then exit.

  extract_date# = 0; EAN13 = ''; exp_date = 0; Day'' = ''
  Month'' = ''; Year'' = ''

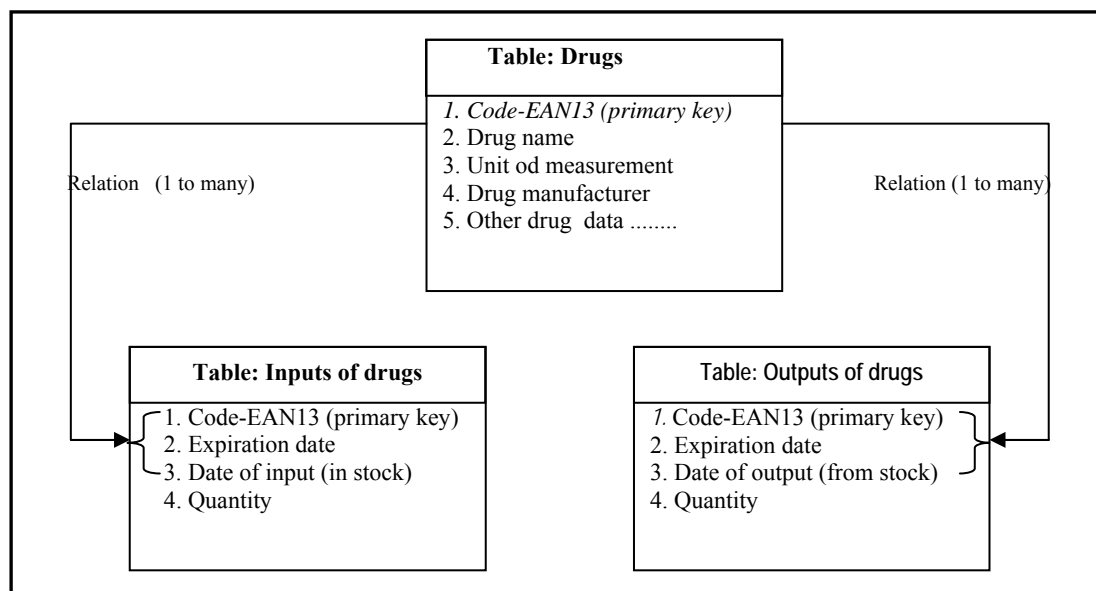
  LOOP x# = 1 TO LEN(CLIP(barcode))

    IF SUB(barcode,x#,1) = '.' ? Delimiter (here point)
      extract_date# = 1
      CYCLE
    -
    IF extract_date# <> 1 ? EAN13 extraction
      EAN13[x#] = SUB(barcode,x#,1)
    ELSE ? Expiry Date Extraction
      Day'' = sub(barcode,x#,2)
      Month'' = sub(barcode,x#+2,2)
      Year'' = sub(barcode,x#+4,2)
      BREAK
    -
  -
  Date'' = clip(Day'') & '.' & clip(Month'') & '.' & clip(Year'')
  exp_date = DEFORMAT( Date'', @d5.)

  DISPLAY

```

Diagram 1. A part of database created to store drug expiration dates of inputs and outputs



## Conclusions

Based on our research we can conclude that barcode technology is used regularly in most Bosnian pharmacies but they cannot track expiration dates automatically. Extended barcode (which shouldn't be printed on the same side with existing EAN13) is cheap and very successful solution for drugs expiration dates tracking. This barcode can be even smaller since many drugs has only month and year as expiration date (for ex. 12.2012), so for coding is necessary additional 4 digits. Even with full expiration date we can make barcode smaller using ordinal numbers of days in year (3 digits) and one digit for year (for example 0042 - extracted drug expiration date is 04.01.2012).

On the drugs manufacturers side extended barcode should be printed on the package of each item (for point of sale purposes). In the hospital, wholesale and community pharmacies with smaller changes in their pharmacy information systems (software and databases) they should be able to track drugs expiration dates (with single barcode scan of drugs inputs and outputs) increasing level of automatization of pharmacies inventory management (planning of drugs stock, determining of drugs prices, generating drugs orders automatically and decision making process).

## References

- Association for Automatic Identification and Mobility. (2010) *Technologies: Bar Code & RFID* Retrieved from <http://www.aimglobal.org/technologies/barcode/>
- Charlotte, A. S. (2002) *Managing Pharmaceutical Waste*. Journal of the Pharmacy Society of Wisconsin. Retrieved from [www.premierinc.com/safety/topics/epp/downloads/PSW\\_article.pdf](http://www.premierinc.com/safety/topics/epp/downloads/PSW_article.pdf)
- McCarthy, G. (2005) *Managing Pharmaceutical Waste*. Connecticut Hospital Roundtable. Retrieved from [www.ct.gov/dep/lib/dep/p2/institution/pharmaceutical\\_waste.pdf](http://www.ct.gov/dep/lib/dep/p2/institution/pharmaceutical_waste.pdf)
- Sofvelocity Inc. (2011) *Clarion Language Programming*, Pompano Beach, Florida.
- Softvelocity Inc. (2011) *Data Modeller*, Pompano Beach, Florida.
- Sysoptima, (2005) . *Inventory Management Overview - Demand Forecasting, Inventory Monitoring and Inventory Reporting*. Retrieved from [http://www.sysoptima.com/scm/inventory\\_management.php](http://www.sysoptima.com/scm/inventory_management.php)
- Šabanović, Z., Osmanbegović, E., (2010) *The role of barcode technology in inventory management*. Conference proceedings. Management, izobraževanje in turizem. Portorož. Slovenia.

# Cubic Transformational High Dimensional Model Representation

Erdoğan Şen <sup>†,◊</sup> and Kamil Oruçoğlu <sup>†</sup>

<sup>†</sup> Istanbul Technical University Mathematics Engineering Department, Maslak, 34469, Istanbul, TURKEY  
senerdogan@itu.edu.tr, koruc@itu.edu.tr

<sup>◊</sup> Namik Kemal University Mathematics Department, 59030, Tekirdag, TURKEY  
esen@nku.edu.tr

**Abstract.** This work focuses on the development of a multivariate function approximating method by using cubic Transformational High Dimensional Model Representation (THDMR). The method uses the target function's image under a cubic transformation for High Dimensional Model Representation (HDMR) instead of the function's itself.

**Keywords:** Cubic Equation, Transformational High Dimensional Model Representation, Multivariate Functions, Approximation

## Introduction

When a natural event is analyzed, the number of factors affecting the event is higher than calculated. General way to overcome this is to eliminate or ignore some of factors which will be less effective. However as the investigated event complicates, the number of affecting factors increases. Nowadays computer technology cannot be suitable to the calculation limitations on this type of problems. High Dimensional Model Representation (HDMR) is perhaps the most fruitful solution to those multidimensional problems. Various HDMR versions were suggested in order to tackle with different problem types encountered. Factorized HDMR is one of them. The main problem with FHDMR is that unlike additivity measures of HDMR, multiplicativity measures of FHDMR is unfortunately not well ordered. This led to the Logarithmic HDMR. The main idea behind Logarithmic HDMR was to initially transform what is basically a function of multiplicative nature to one that is of additive nature. This would enable us to expand the transformed problem using plain HDMR and then transform back the individual terms. Previous works was focused on the HDMR constancy optimization under an affine transformation (Yaman, 2008 and Yaman, Demiralp, 2009), conic transformation (Gündoğar, Baykara, Demiralp, 2010 and Gündoğar, Baykara, Demiralp, 2011) and quartic transformation (Şen, 2011). We shall consider in this work a cubic transformation and attempt to find optimal parameters for such a transformation leading to a new approximation.

## Transformational high dimensional model representation

Let us consider a function  $f(x_1, x_2, \dots, x_N)$  of  $N$  independent variables  $x_1, x_2, \dots, x_N$  which has a non-additive structure. A transformation  $T$  can be chosen which yields a new multivariate function  $\varphi(x_1, \dots, x_N)$

$$Tf(x_1, x_2, \dots, x_N) \equiv \varphi(x_1, x_2, \dots, x_N) \quad (1)$$

If we apply the HDMR expansion to  $\varphi$  we will get

$$\varphi(x_1, \dots, x_N) = \varphi_0 + \sum_{\beta=1}^N \varphi_{\beta}(x_{\beta}) + \dots + \varphi_{1\dots N}(x_1, \dots, x_N).$$

Additivity measures  $\sigma_i(\varphi)$ s can be defined for this expansion in the usual HDMR manner.

$$\sigma_0(\varphi) = \frac{\|\varphi_0\|^2}{\|\varphi\|^2}, \sigma_1(\varphi) = \sigma_0(\varphi) + \sum_{\beta=1}^N \frac{\|\varphi_{\beta}\|^2}{\|\varphi\|^2}, \sigma_2(\varphi) = \sigma_1(\varphi) + \sum_{\substack{\beta_1, \beta_2=1 \\ \beta_1 < \beta_2}}^N \frac{\|\varphi_{\beta_1 \beta_2}\|^2}{\|\varphi\|^2}, \dots \quad (2)$$

These measures will be different from those obtained by applying HDMR expansion to the original function  $f$ . Obviously the difference will be dependent on the specific choice of the transformation  $T$ . Since the basic philosophy of HDMR is to be able to represent the function with as few and as less variate terms as possible, we would prefer  $\sigma_0$  and  $\sigma_1$  to be as close to 1 as possible. In this study we choose to deal only with  $\sigma_0$  and attempt to maximize it.

### Cubic Transformational high dimensional model representation

A polynomial can be used as THDMR's operator for choosing the transformation suggested in (1). Here the degree of the polynomial will be taken to be three. The linear combination coefficients of the cubic will be assumed to vary with independent variables. They will be regarded as operators dependent on the algebraic operators each of which multiplies its operand with a different independent variable. This gives flexibility to the relevant transformation and they can be selected so as to approximate the HDMR expansion optimally.

$$Tf(x_1, \dots, x_N) = \varphi(x_1, \dots, x_N) = a_0(x_1, \dots, x_N) + a_1(x_1, \dots, x_N)f + a_2(x_1, \dots, x_N)f^2 + a_3(x_1, \dots, x_N)f^3.$$

Since only  $\sigma_0(\varphi)$  will be under consideration,  $\varphi$  will be approximated by the constant component  $\varphi_0$

$$\varphi = a_0 + a_1f + a_2f^2 + a_3f^3 \approx \varphi_0$$

which gives the approximate equality

$$\begin{aligned} f_1 &\approx \sqrt[3]{-A + \sqrt{A^2 + B^3}} + \sqrt[3]{-A - \sqrt{A^2 + B^3}} \\ f_2 &\approx \left(-\frac{1}{2} + i\frac{\sqrt{3}}{2}\right) \sqrt[3]{-A + \sqrt{A^2 + B^3}} + \left(-\frac{1}{2} + i\frac{\sqrt{3}}{2}\right)^2 \sqrt[3]{-A - \sqrt{A^2 + B^3}} \\ f_3 &\approx \left(-\frac{1}{2} + i\frac{\sqrt{3}}{2}\right)^2 \sqrt[3]{-A + \sqrt{A^2 + B^3}} + \left(-\frac{1}{2} + i\frac{\sqrt{3}}{2}\right) \sqrt[3]{-A - \sqrt{A^2 + B^3}}, \end{aligned} \quad (3)$$

where

$$i^2 = -1, \quad A = \frac{1}{2} \left( \frac{a_0 - \varphi_0}{a_3} - \frac{a_2 a_1}{a_3^2} + \frac{2a_2^3}{27a_3^3} \right) \text{ and } B = \frac{1}{3} \left( \frac{a_1}{a_3} - \frac{a_2^2}{3a_3^2} \right).$$

In this work we will consider only  $f_1$ . The other roots may be considered analogically. The aim here is to find convenient forms for  $a_0, a_1, a_2$  and  $a_3$  that maximize  $\sigma_0$  in (2). To this end  $a_0, a_1, a_2$  and  $a_3$  will be taken in  $L_2$  class. Hence orthonormal basis of the Hilbert space  $H^{(N)}$  will be taken into consideration. Orthonormality will be defined in terms of the inner product as

$$(u_j, u_k) = \int_V dV W(x_1, \dots, x_N) u_j(x_1, \dots, x_N) u_k(x_1, \dots, x_N) = \delta_{jk}, \quad 1 \leq j, k \leq \infty$$

where  $V = [a_1, b_1] \times \dots \times [a_N, b_N]$  represents the hyperprism which is the HDMR construction domain and  $W(x_1, \dots, x_N)$  the multiplicative weight function used in HDMR. The individual weight functions will be chosen as constants, normalized over the corresponding domain and  $dV$  is the product of individual differentials  $dx_1 \dots dx_N$ .

$$W(x_1, \dots, x_N) = \prod_{\beta=1}^N W_{\beta}(x_{\beta}) = \prod_{\beta=1}^N \frac{1}{b_{\beta} - a_{\beta}}$$

Although the basis mentioned above has an infinite number of elements, in practice a finite number of elements will be taken into consideration.

$$a_0(x_1, \dots, x_N) = \sum_{j=2}^m a_j^{(0)} u_j, \quad a_1(x_1, \dots, x_N) = \sum_{k=1}^n a_k^{(1)} u_k, \quad a_2(x_1, \dots, x_N) = \sum_{l=1}^p a_l^{(2)} u_l, \quad a_3(x_1, \dots, x_N) = \sum_{s=1}^t a_s^{(3)} u_s. \quad (4)$$

With these expressions in hand, the constancy measurer  $\sigma_0(\varphi)$  will be a function of the parameters  $a_j^{(0)}, a_k^{(1)}, a_l^{(2)}, a_s^{(3)}$  where

$$2 \leq j \leq m, 1 \leq k \leq n, 1 \leq l \leq p, 1 \leq s \leq t.$$

Thus

$$\sigma_0(\varphi) = \sigma_0(\varphi, a_2^{(0)}, \dots, a_m^{(0)}, a_1^{(1)}, \dots, a_n^{(1)}, a_1^{(2)}, \dots, a_p^{(2)}, a_1^{(3)}, \dots, a_t^{(3)}).$$

Using (4)  $\varphi$  can be expressed as

$$\varphi(x_1, \dots, x_N) = \sum_{j=2}^m a_j^{(0)} u_j + \left( \sum_{k=1}^n a_k^{(1)} u_k \right) f + \left( \sum_{l=1}^p a_l^{(2)} u_l \right) f^2 + \left( \sum_{s=1}^t a_s^{(3)} u_s \right) f^3 \quad (5)$$

To obtain the constant HDMR term  $\varphi_0$  both sides of (5) are to be integrated with respect to  $x_1, \dots, x_N$  over  $V$  under the weight function  $W$ .

$$\begin{aligned} \varphi_0 = & \sum_{j=2}^m a_j^{(0)} \int_V dV \left( \prod_{\beta=1}^N W_{\beta}(x_{\beta}) \right) u_j + \sum_{k=1}^n a_k^{(1)} \int_V dV \left( \prod_{\beta=1}^N W_{\beta}(x_{\beta}) \right) u_k f + \\ & \sum_{l=1}^p a_l^{(2)} \int_V dV \left( \prod_{\beta=1}^N W_{\beta}(x_{\beta}) \right) u_l f^2 + \sum_{s=1}^t a_s^{(3)} \int_V dV \left( \prod_{\beta=1}^N W_{\beta}(x_{\beta}) \right) u_s f^3 \end{aligned}$$

Defining vectors  $\eta$  and

$$\eta = \left( a_2^{(0)}, \dots, a_m^{(0)}, a_1^{(1)}, \dots, a_n^{(1)}, a_1^{(2)}, \dots, a_p^{(2)}, a_1^{(3)}, \dots, a_t^{(3)} \right), \tau = \left( \tau_2^{(0)}, \dots, \tau_m^{(0)}, \tau_1^{(1)}, \dots, \tau_n^{(1)}, \tau_1^{(2)}, \dots, \tau_p^{(2)}, \tau_1^{(3)}, \dots, \tau_t^{(3)} \right)^T$$

With the elements of vector  $\tau$  defined as

$$\begin{aligned} \tau_j^{(0)} &= \int_V dV \left( \prod_{\beta=1}^N W_{\beta}(x_{\beta}) \right) u_j = (u_j, h), \quad \tau_k^{(1)} = \int_V dV \left( \prod_{\beta=1}^N W_{\beta}(x_{\beta}) \right) u_k f = (u_k, f), \\ \tau_l^{(2)} &= \int_V dV \left( \prod_{\beta=1}^N W_{\beta}(x_{\beta}) \right) u_l f^2 = (u_l, f^2), \quad \tau_s^{(3)} = \int_V dV \left( \prod_{\beta=1}^N W_{\beta}(x_{\beta}) \right) u_s f^3 = (u_s, f^3), \end{aligned} \quad (6)$$

where

$$2 \leq j \leq m, 1 \leq k \leq n, 1 \leq l \leq p, 1 \leq s \leq t.$$

$h(x_1, \dots, x_N)$  appearing in the first inner product in (6) is a function which has the constant value 1 for all  $x_{\beta}$  in the hyperprism domain  $[a_1, b_1] \times \dots \times [a_N, b_N]$ .  $\varphi_0$  can now be written as an inner product  $\varphi_0 = \eta \tau$ . Since  $\varphi_0$  has a constant value, the square of its norm will be equal to the square of the function  $\varphi_0$ .

$$\|\varphi_0\|^2 = (\eta \tau)(\eta \tau)^T = \eta \tau \tau^T \eta. \|\varphi\|^2$$

On the other hand can be expressed in terms of the above defined vector  $\eta$  and a square matrix  $C$  which can be expressed in terms of its blocks as

$$C = \begin{pmatrix} K & L & N & S \\ L^T & M & P & T \\ N^T & P^T & R & Y \\ S^T & T^T & Y^T & Z \end{pmatrix}$$

where

$$\begin{aligned} K_{jk} &= (u_j, u_k), \quad 2 \leq j, k \leq m, \quad L_{jk} = (u_j, f u_k), \quad 2 \leq j \leq m, 1 \leq k \leq n, \\ M_{jk} &= (u_j, f^2 u_k), \quad 1 \leq j, k \leq n, \quad N_{jk} = (u_j, f^2 u_k), \quad 2 \leq j \leq m, 1 \leq k \leq p, \\ R_{jk} &= (u_j, f^4 u_k), \quad 1 \leq j, k \leq p, \quad P_{jk} = (u_j, f^3 u_k), \quad 1 \leq j \leq n, 1 \leq k \leq p, \\ S_{jk} &= (u_j, f^3 u_k), \quad 2 \leq j \leq m, 1 \leq k \leq t, \quad T_{jk} = (u_j, f^4 u_k), \quad 1 \leq j \leq n, 1 \leq k \leq t, \\ Y_{jk} &= (u_j, f^5 u_k), \quad 1 \leq j \leq p, 1 \leq k \leq t, \quad Z_{jk} = (u_j, f^6 u_k), \quad 1 \leq j, k \leq t. \end{aligned}$$



$C$  is a symmetric, positive definite matrix. Norm square of  $\varphi$  can be expressed in terms of  $C$  and  $\eta$  as

$$\|\varphi\|^2 = \eta C \eta^T.$$

So the constancy measurer  $\sigma_0$  becomes

$$\sigma_0 = \frac{\|\varphi_0\|^2}{\|\varphi\|^2} = \frac{\eta \mu \mu^T \eta^T}{\eta C \eta^T}. \quad (7)$$

Our aim is to maximize  $\sigma_0$  which can be written as a Rayleigh quotient as

$$\sigma_0 = \frac{y^T C^{-1/2} \tau \tau^T C^{-1/2} y}{y^T y}$$

where  $y = C^{1/2} \eta^T$ . However, a Rayleigh quotient takes its maximum value at the maximum eigenvalue of its kernel, in this case  $C^{-1/2} \tau \tau^T C^{-1/2}$ . Similarly  $y$  is the eigenvector corresponding to the maximum eigenvalue. An analysis of the kernel will give the maximum eigenvalue and the corresponding eigenvector of it. They are respectively,

$$\sigma_0 = \tau^T C^{-1} \tau, \quad y = C^{-1/2} \tau.$$

The equation for  $y$  gives us the vector  $\eta^T$  in (7) that maximizes  $\sigma_0$  as

$$\eta^T = C^{-1/2} y = C^{-1} \tau.$$

Utilizing these equalities we can construct a function for  $\varphi_0$ . To complete this we can express  $\varphi_0, a_0, a_1, a_2$  and  $a_3$  in terms of matrix algebraic entities.  $\varphi_0$  can be written in compact form as

$$\varphi_0 = \eta \tau = \tau^T C^{-1} \tau.$$

We define a vector  $\xi$  with  $(m+n+p+t-1)$  elements  $\xi = [\xi_2, \dots, \xi_m, \xi_1, \dots, \xi_n, \xi_1, \dots, \xi_p, \xi_1, \dots, \xi_t]^T$  and express  $a_0, a_1, a_2$  and  $a_3$  more compactly as

$$a_0 = \eta^{(0)} \xi^{(0)}, a_1 = \eta^{(1)} \xi^{(1)}, a_2 = \eta^{(2)} \xi^{(2)}, a_3 = \eta^{(3)} \xi^{(3)}.$$

Here the vectors  $\eta^{(0)}, \eta^{(1)}, \eta^{(2)}, \eta^{(3)}$  and  $\xi^{(0)}, \xi^{(1)}, \xi^{(2)}, \xi^{(3)}$  are explicitly defined as

$$\eta^{(0)} = [a_2^{(0)}, \dots, a_m^{(0)}], \eta^{(1)} = [a_1^{(1)}, \dots, a_n^{(1)}], \eta^{(2)} = [a_1^{(2)}, \dots, a_p^{(2)}], \eta^{(3)} = [a_1^{(3)}, \dots, a_t^{(3)}],$$

$$\xi^{(0)} = [\xi_2, \dots, \xi_m]^T, \xi^{(1)} = [\xi_1, \dots, \xi_n]^T, \xi^{(2)} = [\xi_1, \dots, \xi_p]^T, \xi^{(3)} = [\xi_1, \dots, \xi_t]^T.$$

To proceed we define  $(m+n+p+t-1) \times (m+n+p+t-1)$  projection matrices  $P_1, P_2$  and  $P_3$  as

$$P_1 = \sum_{\beta=1}^{m-1} e_\beta e_\beta^T, P_2 = \sum_{\beta=m}^{m+n-1} e_\beta e_\beta^T, P_3 = \sum_{\beta=m+n}^{m+n+p-1} e_\beta e_\beta^T$$

Where  $e_\beta$  is the unit vector in  $(m+n+p+t-1)$  dimensional space. Utilizing these projection operators  $a_0, a_1, a_2$  and  $a_3$  can be approximated as

$$a_0 = \eta P_1 \xi = \tau^T C^{-1} P_1 \xi, a_1 = \eta P_2 \xi = \tau^T C^{-1} P_2 \xi,$$

$$a_2 = \eta P_3 \xi = \tau^T C^{-1} P_3 \xi, a_3 = \eta (I - P_1 - P_2 - P_3) \xi = \tau^T C^{-1} (I - P_1 - P_2 - P_3) \xi$$

where  $I$  identity matrix. If now these substitutions are introduced into (3) we obtain



$$\begin{aligned}
f_1 \approx & -\frac{1}{2} \left[ \frac{\frac{\tau^T C^{-1} P_1 \xi - \tau^T C^{-1} \tau}{\tau^T C^{-1} (I - P_1 - P_2 - P_3) \xi} - \frac{\tau^T C^{-1} P_3 \xi \tau^T C^{-1} P_2 \xi}{[\tau^T C^{-1} (I - P_1 - P_2 - P_3) \xi]^2} + \frac{2[\tau^T C^{-1} P_3 \xi]^3}{27[\tau^T C^{-1} (I - P_1 - P_2 - P_3) \xi]^3} \right] + \\
& + \frac{1}{4} \left[ \frac{\frac{\tau^T C^{-1} P_1 \xi - \tau^T C^{-1} \tau}{\tau^T C^{-1} (I - P_1 - P_2 - P_3) \xi} - \frac{\tau^T C^{-1} P_3 \xi \tau^T C^{-1} P_2 \xi}{[\tau^T C^{-1} (I - P_1 - P_2 - P_3) \xi]^2} + \frac{2[\tau^T C^{-1} P_3 \xi]^3}{27[\tau^T C^{-1} (I - P_1 - P_2 - P_3) \xi]^3} \right]^2 + \\
& + \frac{1}{27} \left[ \frac{\frac{\tau^T C^{-1} P_2 \xi}{\tau^T C^{-1} (I - P_1 - P_2 - P_3) \xi} - \frac{[\tau^T C^{-1} P_3 \xi]^2}{3[\tau^T C^{-1} (I - P_1 - P_2 - P_3) \xi]^2} \right]^3 \\
& + \frac{1}{2} \left[ \frac{\frac{\tau^T C^{-1} P_1 \xi - \tau^T C^{-1} \tau}{\tau^T C^{-1} (I - P_1 - P_2 - P_3) \xi} - \frac{\tau^T C^{-1} P_3 \xi \tau^T C^{-1} P_2 \xi}{[\tau^T C^{-1} (I - P_1 - P_2 - P_3) \xi]^2} + \frac{2[\tau^T C^{-1} P_3 \xi]^3}{27[\tau^T C^{-1} (I - P_1 - P_2 - P_3) \xi]^3} \right] - \\
& - \frac{\tau^T C^{-1} P_3 \xi}{3\tau^T C^{-1} (I - P_1 - P_2 - P_3) \xi},
\end{aligned}$$

To simplify this expression we can use a spectral decomposition of  $C^{-1}$  as

$$C^{-1} = \sum_{\beta=1}^{m+n+p+1} \frac{1}{\lambda_{\beta}} \varphi_{\beta} \varphi_{\beta}^T$$

where  $\lambda_{\beta}$  is an eigenvalue of  $C$  and  $\varphi_{\beta}$  is an eigenvector corresponding to the eigenvalue  $\lambda_{\beta}$ . A good approximation will be to use the minimal eigenpairs of  $C$  as  $C^{-1} = \lambda_{\min}^{-1} \varphi_{\min} \varphi_{\min}^T$ .

## Conclusion

In this study we inserted certain flexibilities into the approximation. Because we want to improve its quality. Hence we applied HDMR on the image of the original function under a third degree transformation. The coefficients of the transformation are chosen to make the error of HDMR approximation as small as possible and this increases the efficiency of the method.

## References

- Şen, E. (2011). On Quartic Transformational High Dimensional Model Representation. *Numerical Analysis and Applied Mathematics ICNAAM 2011 American Institute of Physics Conference Proceedings*, 1389 ( pp.2044-2047). Halkidiki, Greece.
- Yaman, İ., (2008). Construction of New Rational Approximation Based on Transformational High Dimensional Model Representation and Efficient Usage of Them by Fluctuation Approximation. Ph.D Thesis, İstanbul Technical University Informatics Institute.

Yaman, İ., Demiralp, M. (2009), A New Rational Approximation Technique Based on Transformational High Dimensional Model Representation. *Springer U.S.line* Volume 52, No. 3 (pp.385-407), ISSN: 1017-1398 (Print) 1572-9265 (Online).

Demiralp, M. (2003). High Dimensional Model Representation and its Applications. *Tools for Mathematical Modelling*, 9, (pp.146-159).

Demiralp, M. (2006). Transformational High Dimensional Model Representation. *ICCMSE (International Conference of Computational Methods in Engineering)*, Crete, Greece.

Gündoğar Z., Baykara, N.A., Demiralp, M. (2010). Basic Features of Conic Transformational High Dimensional Model Representation. *Int. Conf. on Numerical Analysis and Applied Mathematics*, Rhodes, Greece.

Gündoğar, Z., Baykara, N.A., Demiralp, M. (2011). Conic Transformational High Dimensional Model Representation in Comparison with Hermite-Padé Approximants, *Proceedings of the Int. Conf. on Applied Informatics and Computing Theory*, Prague, Czech Republic, (pp.45-51).

# Effects on The Students' Personal Competences of the Usage of PBL Methodologies in Professional Reality Simulation Environments: Students, Teachers, Graduates and Employers' perceptions

Margarida M. Pinheiro<sup>a</sup>, Cláudia S. Sarrico<sup>b</sup> and Rui A. Santiago<sup>c</sup>

<sup>a</sup>ISCA-UA - Higher Institute of Accounting and Administration and GOVCOP - Research Unit for Governance, Competitiveness and Public Policies, UA - University of Aveiro, Aveiro, Portugal  
margarida.pinheiro@ua.pt

<sup>b</sup>ISEG –School of Economics and Management, UTL - Technical University of Lisbon, Lisbon, Portugal and CIPES - Centre for Research in Higher Education Policies, Matosinhos, Portugal  
cssarrico@iseg.utl.pt

<sup>c</sup>DCSPP - Department of Social, Political and Territorial Sciences, UA -University of Aveiro, Aveiro, Portugal and CIPES - Centre for Research in Higher Education Policies, Matosinhos, Portugal  
rui.santiago@ua.pt

**Abstract:** Trying to ensure that every student who enters the work market bears a set of personal attributions acknowledged as essential, higher education institutions (HEIs) have been being confronted with the need to activate new ways to produce and disclosure knowledge, compatible with the transition from an educational to a work environment. This research analyses the effects on the development of the students' personal competences of the PBL methodologies in a simulation environment for the business reality. Setting off from a case study of a vocational HEI, we resorted to the interview technique with teachers and employers and the questionnaire technique with the students and graduates. Students, graduates and teachers support that the PBL methodologies contribute for the further development of personal competences, mainly at the level of resource use (management, planning and work methodology) and at the level of knowledge construction (critical analysis, grounds for decisions and initiative). By the employers, one can easily detect a persistent trend not to acknowledge the PBL methodologies as directly responsible for an improvement of the graduates' personal competences, with the exception of the valorisation of more consistent grounds and more confident attitudes.

**Key words:** Students' personal competence, PBL Methodology

## Introduction

The society's current conditions require an extraordinary educational commitment in favour of the training for the new generations. The higher education system itself does not go unharmed by the social, political and economical transformations we experience. Bearing this context in mind as a reference, it is possible to realize a society which generates challenges over a set of professional, but also personal and social competences. The expectation that the graduates will be able to evidence a vast set of much needed attributes for a lifelong learning process is shared not only by the employers and graduates, but also, with grand centrality, by higher education institutions (HEIs). As cited in Radloff, de la Harpe, Dalton, Thomas & Lawson (2008), the graduates who prove to have relevant attributes are taken into great consideration by the employers and regarded as citizens who generate social rise in value. In this sense, it is quite important to tend to the mutual influence dynamics among the varied agents involved and the structures which they consist of (students, teachers, graduates and employers). Trying to ensure that every student who enters the work market bears a set of personal attributions acknowledged as essential, confronts HEIs with the need to activate new ways to produce and disclosure knowledge. Some authors insist in the idea that it is central to change learning and teaching strategies, in order to develop students' horizontal competences (e.g. Silén & Juhlin, 2008). The arguments involved in such methodologies are multidimensional and diversified.

In the present study we highlight PBL methodologies (either in a perspective of project-based learning or a problem-based learning), based upon the principle of using contextualized problems of a professional nature as a starting point for the acquisition and integration of knowledge (Kolmos, 1996). Throughout this work we reflect upon the need for the HEIs to answer to new ways of knowledge production and dissemination, which value not only the *know-how* and the *do*, but also the *know how to be with others* and the *know how to be*. Against the background of this problematic, the general goal of this project is to try to contribute for the theoretical discussion on the way change movements associated to the PBL methodology produce implications at the level of the higher education students. We did, however, limit our field of study to the context of personal competences, trying to render more viable the control of the existing complexity and diversity in the PBL methodology paradigm. Specifically, we will centre our analysis on the set of perceptions and positions assumed by the main groups involved and with particular interests in the learning processes: students, teachers, graduates and employers. Based on the pointed outlines, and more specifically, we intend to: (1) inquire about the role which the PBL methodology plays in the development of the students' personal competences; (2) find out if the methodology improves the personal competences of the PBL graduates when compared to others; and (3) perspective the role of the PBL methodology at the level of personal competences, in the construction of a graduate profile for the third millennium.

This article is organized into five key points. After the introduction we try to contextualize PBL methodologies within the changing learning and teaching paradigm in vocational higher education. The next section focuses on the methodological

aspects of the study, including the context of the case study used in the research and techniques for collecting and processing data. The fourth section is devoted to presenting and discussing the results obtained from students, graduates, academics and employers. The paper ends with the main conclusions of the study.

## PBL Methodologies and the Changing Paradigm in Vocational Education

In the Report made for UNESCO by the International Commission on Education for the Twenty-first Century (International Commission on Education for the Twenty-first Century, 1996) a complementary mission for education is immediately referred: that of fructifying the creative talents and potentialities of all individuals. In that very same report, the need for a lifelong learning process is strengthened, as one of the keys to access education. The idea conveyed by the group of rapporteurs sustains that, in order to be able to answer its set of assignments, education must be built upon the symbiosis of four basilar learning processes: learning to know (acquiring not only a set of codified knowledge, but also, and most importantly, the domain of those instruments), learning to do (adjusting training to the future professional activity, in such a way as to apply the knowledge obtained), learning to live together (cooperating with others in the resolution of common projects) and learning to be (allowing for the full development of the person, rendering him/her apt to create autonomous and critical thoughts, capable to judge different circumstances in life). However, if traditional teaching (which is understood as a model of transmission of both knowledge and values, in the unequivocal direction teacher to student) is primarily oriented by the learning of how to know and, especially in the field of higher vocational training, by the learning of how to do, according to the authors of the above mentioned report, it will be necessary to provide education with structured methodological ways, capable to involve both the learning of how to live together and the learning to be. In such a perspective, it is possible to sustain the idea of focusing on learning, thus realizing that the latter can not occur without people or a reference to its subjectivities and personal and social contexts (Fyrenius *et al*, 2007).

All together, the adequacy of the higher education system to the teaching-learning model sustained by the Bologna Process, did also jeopardize a profound change of paradigm: in order to confront the European student profile, the HEIs should emphasize horizontal competences which render students responsible for their learning processes, thus leaving the teachers with the task to facilitate and orient those processes. The implementation of these guidelines does inevitably create the need to re-evaluate the pedagogical activities at the level of goal definition and assessment, as well as, particularly, at the level of execution and follow-up of the methodological processes. In the Portuguese case, the higher education network is developed upon a binary system, accentuating the distinctly professional prominence of the polytechnic higher education, as opposed to more conceptual and theoretical features of the university education. Hence we find two distinctive logics: in the university education and in sequential periods of time, we may distinguish *knowledge* and *know-how*, whereas in the polytechnic education, at the same time, *knowledge*, *know-how* and *do* coincide. So, and particularly in polytechnic education it is possible to understand the importance to rethink the training of its students adjusting it, as far as possible, to the professional needs demanded by employers. In order to strengthen such a position, new pedagogies centred in the relation between pedagogical practices and professional practices have been revealing themselves as an important methodological paradigm (e.g. Musal, Taskiran & Kelson, 2003).

A possibility to establish the transition between educational practice and professional practice is that of fostering the change of a traditional teaching system to a PBL model. Developed by Howard Barrows and Robyn Tamblyn as of the late sixties and initially associated to medical schools, the PBL methodology has been used in various professional areas and programs, already gathering 40 years of experience (Nel, *at al.*, 2008). The PBL methodology is based upon the principle of using contextualized problems of a professional nature as a starting point for the acquisition and integration of knowledge (Barrows & Tamblyn, 1980). So being, and ontologically speaking, the use of professional problems works, simultaneously, as a learning incentive and a focus. In PBL methodology, students work in small groups, analysing the problem they are presented with, identifying the necessary information for its solution, directing their learning activities according to the knowledge needed to process the problem presented and, finally, formulating possible solutions. Throughout this process and by means of self-learning mechanisms, one may assume students develop competences which allow them not only to achieve the desired professional results, but also to work different personal and social features (Papinczack, 2009). In this way, it is supposed for the profile of a graduate who recurred to a PBL methodology to include not only basic knowledge, which will allow him to research, understand and critically explain the existing literature on a certain matter, but also the aptitude to communicate with others or the ability to solve problems which his professional experience enables him with, both as a person and a technician. On the other hand, and accepting the perspective of several authors (e.g. Tate & Grein, 2009) that learning has its place when there is an active and committed participation of the learner, it becomes fundamental for him to reconstruct knowledge, adjusting it to his needs and image. PBL methodology conceptually predicates an active construction of meanings for those who learn it, promoting, as a result, a more lasting internalization of the learning experiences. In such a perspective, this custom made concept stimulates, on the one hand, personal and social competences of intellectual growth and, on the other, it makes those competences more effective ones. Following the PBL methodology, the students who are looking for the answers to the questions they asked themselves, will select which may in fact answer their doubts and justify the solutions d«found. As a result, it is possible to refer the acquisition of competences at three different levels: technical (referring to the quality of the service rendered), social (associated to the nature of interpersonal relations) and self-developing (regarding questions of organization, argumentation and communication) (e.g. Albanese & Mitchell, 1993; Musal, Taskiran & Kelson, 2003). In particular, some studies of PBL in the accounting area can be consulted. According to the analysis of the state of the art about accounting and education, Rebele *et al.* (1998), Apostolou *et al.* (2001) and Watson *et al.* (2003, 2007), reveal that that between 1991 and 2005 only three articles refer to PBL. Nevertheless, some other studies may be point out. More recently, Tate and Grein (2009) or Xu and Yang (2010) have done some work on it. So, it is precisely the condition of the existence of

few readings about PBL methodologies in accounting that instigates us to consider the paradigm of the effects on the students' personal competences of the usage of PBL methodologies in professional reality simulation environments.

## Method

Within the problematic discussed, the main objective of our work is to contribute to the theoretical discussion of how changes related with PBL methodologies produce implications on personal competences in vocational higher education. Supported on the several authors that frame the conceptualizing of our study, it is possible to sustain the thesis that PBL methodologies develop and reinforce students' personal competences (*e.g.* Tate & Grein, 2009). In more specific terms, we intend to inquire about the role which the PBL methodology plays in the development of the students' personal competences. Simultaneously, we want to find out if the methodology improves the personal competences of the PBL graduates when compared to others. Finally, we want to perspective the role of the PBL methodology at the level of personal competences, in the construction of a graduate profile for the third millennium.

### 3.1 The Case Study: Business Simulation

As previously referred, the case study which shapes this work is based upon the curricular unit of Business Simulation (running since 1997), included in the last semester of the last year of the study plan of the first cycle of studies of the accounting course available at the ISCA-UA. The origin of the idea to create a subject which aims to present a new teaching solution which brings the later closer to the business reality derived, mainly, from the conjugation of two primordial factors: a first factor which results from the difficulty to introduce a curricular training period in the course (which meant professionally placing about 160 students per year) and a second factor which resulted from the need to place upon the market accountants who were potentially more apt and advantageously competitive for the exercise of their profession, facing the growing offer of graduates qualified to exercise it.

Methodologically, the need to build bridges between the theoretical knowledge and its practical applications, among the conceptions teachers had on the professional needs and the competencies required by employers, motivated the use of a contextual learning process, integrated in a reality which mirrored the professional environment of the future graduates, following an ideological line of learning by doing. Parallel to this, there is the idea to simulate, within the school, the business reality which tried to offer a greater follow-up to the passage from a purely academic life to an active professional one and, at the same time, complement the initial training of the future graduates, by means of a holistic integration of the knowledge achieved during previous academic years. Such a context revealed itself a window of opportunity for the structuring of a systemic model inspired in PBL methodologies. The structure of the model chosen for the subject of Business Simulation completely unfolds around projects which imply themes from different subject areas, thus fostering learning by the resolution of problems that emerge during the formulation or implementation of those very projects. Based on teamwork, the model privileges self-learning and comprises, in its logical structure, the figure of the group's tutor who has a role of guidance.

The Business Simulation method consists of a simulated market of virtual companies, which small groups of students must manage and administer. The number of groups created annually is, roughly, 75, comprising the most varied fields of activity, with special attention to the fact that the interconnection among them demands for the existence of supplier and consumer companies, as well as competitive companies, just like it occurs in the real market. The subject takes place in 15 real weeks, which correspond to a virtual year, thus allowing students to perform the accounting simulation of the beginning and the end of the exercise. In order to maximize the real character which the Business Simulation is intended to have, the subject has similar goals to those established for analogous situations in the real world, with the delivery being the only true fictional aspect. The approximation to the professional activity is also ensured by the collaboration of three centrals which simulate the products and services necessary for the full operation of the business network: public, financial and commercial. While the public central emulates the role of different public entities, the financial central focus on assuring a set of diversified financial products and services. Finally, the commercial central has the role to promote the necessary dynamic to the functioning of the various sectors of business activity represented in the simulated market.

The importance granted to the subject is acknowledged by the Chartered Accountants Association Council (OTOC), which means that ISCA-UA is one of the schools which is exempt of the training period requested by the OTOC in order to have access to the enrolment as a chartered accountant. As that training period has the triple goal supplying professional experience, complementing social and professional competences and enabling a stronger articulation between the school and the world of work, the Business Simulation fulfils, according to the OTOC's perspective, the goals established for a training period. So being, it brings an added value to the profession of the future graduates.

### 3.2 The research design

After the definition of the main objective and the investigation questions that circumscribe this investigation, we elected a case study methodology. As a means of research, the methodology of case study enables, as far as Bell (1998) is concerned, to broaden the limitations of the existing knowledge and enable future researchers to confront their decisions with those referred to on the study. Yin (1994) also refers the fact that the most important aspect of a case study is not the statistical generalization of the phenomenon, but rather the analytical generalization in itself. So, our option derives from the belief that it can confirm and complete conceptual knowledge and from the opportunity of interest it represents, namely at a vocational level in accounting courses. More, we add the fact that a single case study can be a pilot case in future studies of multiple cases. On the other hand, we considerer important to elect the main groups involved and with particular interests in the learning processes: students, teachers, graduates and employers. In the empirical study we developed, we used the technique of interviews with the teachers and employing entities and that of questionnaire with the remaining participants. When observing the data collected



we also resorted to varied strategies: the qualitative approach elects content analysis techniques to deal with the information gathered, whereas the quantitative approach chooses a statistical treatment of the inquiries performed.

The scripts for the semi-structured interviews made to teachers and employers were basically outlined according to the literature review and to the specific object and goals defined for the research. It must be properly highlighted that during the qualitative collection of information, all the interviews transferred a role of informer, rather than that of respondent, on to the interviewees, as they were free to express facts and convictions in their own language (Lessard-Hébert, Goyette & Boutin, 1997). All interviews were recorded with the proper consent of the authors and their answers were studied with the QSR NUD\*IST software (*Non-numerical Unstructured Data Index Searching and Theorizing*). The questionnaires proposed to the students and graduates were conceived similarly to the interviews, as of the revised theoretical setting and the specific object and goals established. In each question, it was explored whether the PBL methodology of Business Simulation did or did not originate the changes in the students' personal competences. The answers were pre-oriented on a Likert scale with 5 points, with a neutral possibility, and the respondent had to mark that which was closer to the way he/she perceives things. All questionnaires were prepared for an optical reading and the answers were examined following descriptive statistics. The software used was the SPSS (*Statistical Package for Social Sciences*).

While selecting the teachers, we choose to include all those who had at least four years of experience in the subject, admitting that punctual collaborations dispersed throughout several years would result in less limited perspectives on the methodological functioning of the curricular unit. 14 interviews were made. In order to confirm the diversification principles and in such a way as to ensure the most broaden overview possible of the problems and situations which take place within the group of the employing entities, we choose to only retain entities with graduates from ISCA-UA who were carrying out duties related to the accounting area, but spread out in several departments. Such a choice returned five entities, which corresponded to thirty-two graduates (twenty-three of which had attended Business Simulation as opposed to nine who hadn't). In this study we also involved all the students enrolled in the subject when the empirical part of the project was developed, which meant a total of 138 students. The return rate achieved was of 96%. Given that it was quite relevant to streamline the questionnaires to all the graduates from ISCA-UA who had attended Business Simulation, the 881 graduates present in the process since its beginning were taken into account. In this group, the return rate was of 84%.

Finally, it is also very important to mention that the adoption of a PBL methodology within Business Simulation presented itself as a challenge accrued both for students and for teachers. In fact, with the total development of the curricular units of the accounting degree running according to traditional teaching methodologies (identified, as previously mentioned, as a uniform model for the transmission of knowledge in the univocal direction teacher to student), the methodological organization of the Business Simulation suddenly supervenes as a model which opposes to the traditional one. This factual situation rises, namely by students and teachers, an inevitable comparison between the methodological philosophies inherent to the two models. In terms of this study, the fact that students, graduates and teachers tend to compare their traditional methodological experiences with the PBL experience of the Business Simulation, presents itself as a unique opportunity which adds up to the research the possibility to understand every opinion reported on the empirical part, as considered under the light of the PBL methodology *versus* the traditional teaching methodologies.

## Results and discussion

As formerly referred, the sudden introduction of a PBL methodology in a course formatted according traditional teaching moulds, constitutes, *per se*, a fundamental element for the comparison of the learning experiences reported by students and by teachers of the institution. Methodologically and within the scope of this work, we resorted to the possibility to confront the two teaching methods (traditional and PBL) by the intervening elements (students, teachers and graduates) was a way to conceptualize the same study group and control group. So being, we argued that, although it is possible to introduce external variables in the analysis, such a fact allows for the reduction of the latter, as each analysis unit is built in a paired manner: before and after the use of a PBL model. Ergo, and as an aspect prior to the whole discussion, we assumed that each element (student, teacher and graduate) is his/her own control, with each group simultaneously becoming a test and a control group, where the samples gathered concern the records of the same element exposed to different aspects of the situation under study: traditional and PBL methodologies.

In this stage of our analysis, we tried to account for a set of perceptions expressed by the varied elements from the samples under study, who conceptualized the positions of students, teachers, graduates and employing entities regarding the features of the students and graduates' competences at a personal level. We included items relating to written and oral communication, critical analysis, time management, task planning, synthesis capability, creativity, setting of goals, decision reasoning, initiative capability, personal organization, dynamism and work methodology. With the dimension regarding the self-development abilities, we were able to circumscribe a set of assertions in on how the surveyed intervenients interpret the ways how the teaching-learning processes which use the PBL methodologies may eventually interfere in the structuring of the students and graduates' personal competences.

### 4.1 The Students' Perspective

The information presented in Table 1 characterizes the set of answers collected by the inquiry presented to the students, thus allowing us to establish an approximate picture regarding the reflection they make on possible alterations of their personal competences due to the PBL methodology implemented in the Business Simulation.

**Table 1.** Characterization of the percentage results of the group of students

Degree of alteration or non-alteration of the personal competences at the level of	Tendency to decrease	Unaltered	Tendency to increase
written communication	5.3	31.1	63.6
oral communication	3.8	35.6	60.6
critical analysis	6.8	15.9	77.3
time management	12.1	7.6	80.3
task planning	7.6	12.1	80.3
synthesis capability	3.1	26.5	70.4
creativity	4.6	25.8	69.6
setting of goals	6.1	26.7	67.2
decision reasoning	4.6	20.6	74.8
initiative capability	4.5	21.4	74.1
personal organization	9.1	31.1	59.8
dynamism	2.3	23.1	74.6
work methodology	3.0	22.0	75.0

Focusing on the students' answers in positive positions regarding the question of the influence of learning in the development of their personal competences, some items seem to reveal a stronger convergence of positions. Therefore, at a first level of analysis, it is possible to find an accentuated positive influence of the methodologies implemented in two terms: that of the planning and organization (time management and task planning); and that of knowledge construction (critical analysis, synthesis capability, creativity, decision reasoning, initiative capability, dynamism and work methodology). At a second level of analysis, the empirical study points to the development, although slightly less accentuated, of competences referring to communication (oral and written), personal organization and setting of goals. Although the results need to be carefully processed, an hypothetical interpretation of the values gathered (especially for the first three items) may refer to the fact that the competences regarding communication and personal organization transit, in a more direct manner than the others, from the traditional learning methodologies previously used by students. In fact, the whole traditional path run by the student during his/her schooling process, had always, generally speaking, relied on written and (probably less, but also) oral communication. On the other hand, the personal organization, in turn, had always been a present element in the student's traditional schooling.

#### 4.2 The Teachers' Perspective

It was also of great interest for us to study, from the teachers' point of view, if the PBL methodology in Business Simulation did have any impact in the personal competences of the students. In this category, we included the following items: oral and written communication, critical analysis, synthesis capability, creativity, initiative capability, personal organization, dynamism, work methodology, reflection and self-esteem and self-confidence. By means of the detailed exhibition of the results gathered, we tried to understand how teachers perceive the effective possibility of changes at the level of the student's personal competences.

As far as the critical analysis is concerned, almost all the interviewees state that the methodology applied allows students to develop their critical reasoning in a constructive perspective. Another perspective referred by two teachers, presents us with the idea that the varied opinion presented by them is not a weak point, but rather an asset which is capable of adding analytical capability to the students' activity. Regarding the decision reasoning there are unanimous positions by the teachers: the PBL methodology enables them to develop, within the student, the ability to consolidate the resolutions he/she chooses to take. Also regarding personal organization aspects, the interviewees state that the methodology followed in the subject provides for mechanisms which go beyond life at school. Prolonging the aspect of personal organization, teachers refer to the urgency of a work methodology motivated by the PBL process, that forces students to have a constant and permanent flow of work. Based upon the answers intentions which were presented, it seemed to us beyond the shadow of a doubt, that there are, throughout the course of the subject, several moments which promote oral and written communication. Exactly as described in literature (e.g. Kirschner, Vilsteren, Hummel & Wigman, 1997) the interviewed teachers state that the methodology crates, in fact, synthesis mechanisms upon students, in such a way as to enable them to manipulate much information with which it is daily confronted. Within the self-development area, the interviewed teachers refer it is possible for students to collect, form the methodology, competences referring to creativity, initiative capability and dynamism. Such an active participation of the students in the construction of their learning processes is, equally, accompanied by a reflexive potential. In fact, teachers are unanimous when underlying the fact that the methodology is an important instrument for the process. In the perspective of one of the teachers, there is also an extra fact, which is the fact that Business Simulation provides the student with self-esteem and self-confidence competencies, capable of rendering him/her more apt to take on a Professional career. Particularly interesting to us seems to be the suggestion by the same teacher in the sense of assessing the number of graduates who choose to start off their career on their own. This choice referred by the teachers seems to understand the methodology as a dynamic process capable of encouraging business opportunities among associates.

### 4.3 The Graduates' Perspective

The statistical analysis performed on the matter of the data collected by this group, aim at analysing the perspective of those as far as the alteration degree of their personal competences is concerned, my means of the methodology followed in the subject. The data presented on table 2, characterizes the set of answers collected.

**Table 2.** Characterization of the percentage results of the group of graduates

Degree of alteration or non-alteration of the personal competences at the level of	Tendency to decrease	Unaltered	Tendency to increase
written communication	2.4	46.0	51.6
oral communication	1.2	36.7	62.1
critical analysis	1.4	18.8	79.8
time management	3.1	14.7	82.2
task planning	2.6	14.0	83.4
synthesis capability	2.4	32.5	65.1
creativity	2.1	34.5	63.4
setting of goals	1.7	22.4	75.9
decision reasoning	1.9	19.1	79.0
initiative capability	2.1	25.4	72.5
personal organization	1.4	33.4	65.2
dynamism	1.7	30.6	67.7
work methodology	1.6	20.6	77.8

The analysis of the set of items which comprise the personal competences block allows us to, broadly, underline the positive tendency evidenced by the graduates on the possibility to register alterations, caused by the PBL methodology followed in the Business Simulation. The statistical treatment described, besides allowing the identification of some more relevant themes in terms of the results gathered, does also induce hypothetical interpretations in terms of the configuration of the subjects' answers. Despite certain optimism, it soon becomes quite obvious that there are different valorisations of the items under study, somehow allowing the creation of a hierarchy of two distinctive answer profiles. The analysis of the table allows the verification of a markedly positive profile, which comprises critical analysis, time management, task planning, setting of goals, decision reasoning, initiative capability and work methodology. However, there is also another shade in the opinions of the graduates. According to this second profile, it is possible to detect more moderate positions which, surely, continue to express the perception that there is a positive trend which promotes oral and written communication, synthesis capability, creativity, personal organization and dynamism. One must particularly highlight the graduates' judgement, as far as the written communication item is concerned, where opinions are divided between a neutral assessment and weak positive evaluation.

### 4.4 The Employers' Perspective

With the interviews made to the employers we intend to perspective a set of questions referring to the personal competences of the graduates. In order to better circumscribe changes at this level, we now describe the results extracted from the meaning units associated to the items approached by entities, being that they only referred the items decision reasoning, personal organization, self-esteem and self-confidence.

According to all the employers interviewed, the Business Simulation enables graduates to develop their ability to reason decisions, limited not only by theoretical concepts, but also by practical aspects which have already been experienced. Upon such a basis, the graduates who attended the curricular unit of Business Simulation present themselves, this way, more valued and professionally acknowledged, while achieving certain levels of the profession, when compared to other colleagues who choose not to attend the subject. When observing the sense of the answers, generally speaking, employers do not acknowledge personal organization as a competence which benefits from the attendance of the Business Simulation subject. As far as self-esteem and self-confidence are concerned, only one of the employers approached the subject, assuring that the experience acquired during the Business Simulation subject, while granting them with more preparation, renders graduates more confident and secure of their actions. The very same employing entity meets the opinions presented by some teachers, referring that attending the subject is an asset in terms of ability to assume a positive attitude. An element worthy of mentioning has to do with the fact that all employers who were interviewed were aware of the existence of the subject of Business Simulation at ISCA-UA, a fact which seems to reveal the attentions schools who train graduates within the scope of companies' needs deserve.

## Conclusions

This work investigates the expression modes of the use of PBL methodologies at the level of personal competences by students and graduates at a higher education level. It is not our intention to generalize results. In fact, the data we processed does not allow for it. Nevertheless, based upon the indicators we examined it is, already, possible to conclude that the teaching-learning methodologies grounded on PBL models, validate some conceptual propositions of the already existing theoretical production on this theme. Still, there are others which do not seem to be corroborated by the practical results collected. Based upon some reflections we have been establishing, it is possible to ponder new perspectives, capable of contributing for the activation of a debate around the dynamics of self-development competences, associated to the use of PBL methodologies. Hence, despite the fact that, theoretically, the research reveals methodologies under study tend to affect the students' personal profile, it is not



clearly evident how such alterations are perceived by the various agents involved in the educational process (students, teachers, graduates and employers). Such as it was observed, we identified two trends in the perceptions evidenced by the interviewees and the respondents.

On the one hand, the results collected with the group which comprised students, graduates and teachers leads us to sustain that the methodologies under study contribute to the development of personal competences, mainly at the level of resources' usage (management, planning and work methodology) and knowledge construction (critical analysis, decision reasoning and initiative capability). Such specificities are eventually identified with the characteristics of the profile of the graduate who used a PBL methodology on his training process, as Albanese (1993) and Kolmos (1996) refer. Another conclusion of the study is the fact that the communication skills (oral and written) appear far less valued, when compared to the remaining items for self-development. One may perhaps find a justification in the fact that traditional methodologies already explore these aspects. Another possible perspective refers to the circumstance that teachers may not present uniform solutions, which, likewise, encourages debate among the students. In this sense, it seems that the discussion of ideas which often occurs bears an underlying methodology which significantly increases the argumentative power of students, though they appear to develop more comfortable attitudes in more traditional environments. One must also underline that teachers have been questioning the choice on the possibility to establish a professional career on their own (entrepreneurship). To some extent, this aspect acknowledges that methodologies have the ability to foster self-esteem, and self-confidence in students, also being able to, together with several other factors, contribute for the assumption of the idea to create companies in the field. As literature does not approach this matter, it seems possible to us to sustain the possibility of inserting the entrepreneurship logic, motivated by the new methodologies under study in this work, in the existing theories.

On the other hand, the perception manifested by the group of employing entities seems, however, not to acknowledge, at least not so noticeably, the impact of those methodologies at the level of the trainees' personal development. Following a certain path, we find a tone of speech which values methodology as a potentiating force for more consistent groundings, enhanced by the practical experiences the students have already gathered. The same positive tone is evidenced in the items referring to attitudes of a more confident posture and greater security. It is, however, possible to find a persistent tendency for employers not to acknowledge PBL methodology as responsible, at least not directly, for the improvement of the graduates' personal competences. These facts lead us to conclude that the methodological models which sustain alterations in the students at a personal level are rather simplistic rendering it, in our opinion, unreasonable to generalize this problem, at least as far as employers are concerned.

The results achieved with the analysis of the data collected also require some lateral reflections. A possible consideration has to do with the understanding of a strategy which potentially favours the development of personal competences, but which does not have the same effect on every student or context. Another pertinent reflection: if, as the European Centre for the Development of Vocational Training refers, the forecasts for employability for Europe in 2020 point at eighty million jobs, the bottom question which arises is the need to understand what kind of competences will be necessary to fulfil these vacant jobs, according to the employers' needs. On this page, a potential uneasiness refers to the need to know how we may be able to assure the early identification of competences which will secure the needs of a multifaceted market.

Simultaneously, we reflected on the need to open the worlds of education and training, namely at a higher level, making them more reactive to the needs of learners and employers, by means of the development of relevant competences, centred on tangible studies and results. Nonetheless, and according to the HEIs role while cultural diffuser, it is important to carefully analyse the equilibrium aspect between theoretical conceptualization and its practical applicability. We are, therefore, before the pressure of a flexibility exercise at the level of competence management, not only professionally, but, more intensely, at a non-cognitive level and, particularly, at a personal one. This because modernizing in order to meet new challenges places a considerable pressure on the current education and training systems, especially in developing countries.

## References

- Albanese, M. A., & Mitchell, S. (1993). Problem-based learning: a review of literature on its outcomes and implementation issues. *Journal of the Association of American Medical Colleges*, 68(1), 52-81.
- Apostolou, B.A., Watson, S.F., Hassell, J.M. e Webber, S.A. (2001). Accounting education literature review (1997 – 1999). *Journal of Accounting Education*, 19, 1-61.
- Barrows, H. S., & Tamblyn, R. M. (1980). *Problem-based learning. An approach to medical education*. New York: Springer.
- Bell, J. (2010). *Doing your research project: a guide for the first-time researchers in education, health and social science*. Berkshire: Open University Press.
- Fyrenius, A., Wirell, S., & Silén, C. (2007). Student approaches to achieve understanding - approaches to learning revisited. *Studies in Higher Education*, 32(2), 149-165.
- International Commission on Education for the Twenty-first Century. (1996). *Learning: the treasure within*. Paris: UNESCO.
- Kirschner, P., Vilsteren, P., Hummel, H., & Wigman, M. (1997). The design of a study environment for acquiring academic and professional competence. *Studies in Higher Education*, 22(2), 151-171.
- Kolmos, A. (1996). Reflections on project work and problem-based learning. *European Journal of Engineering Education*, 21(2), 141-148.
- Lessard-Hébert, M., Goyette, G., & Boutin, G. (1997). *Recherche qualitative: fondements et pratiques*. Montréal: DeBoeck Université.
- Musal, B., Taskiran, C., & Kelson, A. (2003). Opinions of tutors and students about the effectiveness of PBL in Dokuz Eylul University School of Medicine. *Medical Education Online*, 8. Retrieved November 23, 2009, from <http://www.med-ed-online.org/pdf/f0000073.pdf>

- Nel, P., Keville, S., Ford, D., McCarney, R., Jeffrey, S., Adams, S., & Uprichard, S. (2008). Close encounters of the uncertain kind: reflections on doing problem-based learning (PBL) for the first time. *Reflective Practice*, 9(2), 197-206.
- Papinczack, T. (2009). Are deep strategic learners better suited to PBL? A preliminary study. *Advances in Health Sciences Education*, 14, 337-353.
- Radloff, A., de la Harpe, B., Dalton, H., Thomas, J., & Lawson, A. (2008). *Assessing graduate attributes: Engaging academic staff and their students*. Paper presented at the 2009 ATN Assessment Conference, Adelaide, Australia.
- Rebele, J.E., Apostolou, B.A., Buckless, F.A., Hassell, J.M., Paquette, L.R. & Stout, D.E. (1998). Accounting education literature review (1991 – 1997) part II: students, educational technology, assessment and faculty issues. *Journal of Accounting Education*, 16(2), 179-245.
- Silén, C., & Juhlin, L. (2008). Self-directed learning - a learning issue for students and faculty. *Teaching in Higher Education*, 13(4), 461-475.
- Tate, S. L., & Grein, B. M. (2009). That's the way the cookie crumbles: an attribute sampling application. *Accounting Education*, 18(2), 159-181.
- Watson, S.F., Apostolou, B.A., Hassell, J.M. e Webber, S.A. (2003). Accounting education literature review (2000-2002). *Journal of Accounting Education*, 21, 267-325.
- Watson, S.F., Apostolou, B.A., Hassell, J.M. e Webber, S.A. (2007). Accounting education literature review (2003-2005). *Journal of Accounting Education*, 25, 1-58.
- Xu, Y. e Yang, Y. (2010). Student learning in business simulation: an empirical investigation. *Journal of Education for Business*, 85(4), 223-228.
- Yin, R. (2009). *Case study research. Design and methods* (4th ed.). Thousand Oaks: Sage Publications.

# Expert Idea on Liquid Limit and Plastic Limit Estimation with Soil Resistivity Profile

Zamri Chik<sup>\*1</sup>, S.M. Taohidul Islam<sup>1</sup>, Hilmi Sanusi<sup>2</sup>, Mohd. Marzuki Mustafa<sup>3</sup>

<sup>1</sup>Department of Civil and Structural Engineering, Universiti Kebangsaan Malaysia, Bangi 43600, Selangor, Malaysia

<sup>2</sup>Universiti Kebangsaan Malaysia, Bangi 43600, Selangor, Malaysia,

<sup>3</sup>Electrical, Electronics and System Eng. Dept., University Kebangsaan Malaysia, Bangi, 43600, Malaysia

irzamri@yahoo.com

**Abstract**-This paper presents the idea on determination of liquid limit and plastic limit with soil electrical resistivity in geotechnical investigations. Depending on the moisture contents, the soil behavior is revealed as solid, semisolid, plastic and liquid states in geotechnical engineering and other division of civil engineering. Determination of liquid limit and plastic limit of soil in conventional laboratory test is very tedious, slower and costly for the laboratory testing example as fall cone testing with a lot of collected soil sample. In this work, a method of soil liquid limit and plastic limit determination with electrical resistivity is revealed to define the state of soil as well as the relationship of soil particle distribution in the soil site investigations of geotechnical engineering. In addition, soil resistivity measurements with moisture contents and conventional laboratory test as fall cone test are performed whereas experimental results in laboratory and results from the available literature review are considered. A good correlation of soil electrical resistivity and moisture contents is demonstrated in results to determine the liquid limit, LL and plastic limit, PL in soil behavior. The research is most significant to obtain faster, cost-effective and consistent performance in soil liquid limit and plastic limit determination through electrical signal for a wide range of applications in geotechnical engineering.

**Key words:** Liquid limit, Plastic limit, Fall cone test, Electrical resistivity profile

## Introduction

Observations of soil state behaviors and determinations of soil strength are prerequisite in highway and road engineering including construction of highway embankments, earth dams, geotechnical engineering, and other divisions of civil engineering (Benson and Trast, 1995). The behaviors of soil can be divided into the basic states of solid, semisolid, plastic and liquid depending on the moisture contents. The change from one state to the next is measured with increasing of moisture contents. These smooth transitions are considered for introducing LL, PL in geotechnical investigations. The moisture content between PL and LL is defined as the plasticity index, PI where PI is a measure of the plasticity of soil.

General techniques for the determination of this soil LL and PL were conducted through the laboratory tests, in-situ tests and geophysical methods (Avnimelech et al., 2001; Sridharan and Nagaraj, 2005). The laboratory test is generally conducted to obtain the moisture contents for changing the behaviors of soil states in soil investigations (Elshorbagy and Mohamed, 2000). As an example, in fall cone test, moisture contents are obtained corresponding to the empirical cone penetration to determine LL and PL of soil. Determination of LL and PL in soil is also tedious, slower and costly using conventional laboratory testing based on the procedure of testing. In addition, conventional methods are usually in difficulties during the collecting of dry sample and soil sampling processes, which may change the original value of the testing results.

Determination of soil LL and PL with electrical resistivity shows the important role in the construction of highway embankments, structural engineering and others geotechnical engineering (Osella and Favetto, 2000; Yoon and Park, 2001 ). The electrical resistivity of the soil is manipulated by soil type, degree of saturation, concentration of ions, water contents and temperature of pore water. Transport properties such as electrical conductivity (Friedman, 2005), soil resistivity (Huang and Fraser, 2002), thermal conductivity, and hydraulic conductivity show associations with the porosity, water saturations, composition, salinity of the pore water, grain size distribution, and particle shape and orientation (Samouelian et al., 2005 ).

The fall cone test for determination of liquid limit and plastic limit is performed in this work to get the empirical relationship with soil resistivity profile for the collected sample of different type soil. The resistivity of the collected soil is measured with the high resistance meter for each sample of the estimation of LL and PL. The relationship is shown to determine the soil state behaviors with the measurement of soil resistivity corresponding to the different moisture contents in collected soil. Experimental results and study from the available literature are considered to justify the measurements of LL and PL with electrical properties in geotechnical investigations. Background and objective of this study intends the relationships between electrical resistivity and determination of LL and PL in context of electrical properties of collected soils. The aim of the research is to obtain a set of consistent measurements of LL and PL which is used to yield an equivalent model with the electrical performance in geotechnical investigation system.

## Methodology

The research work on determination of LL and PL of soil through electrical resistivity is conducted at University Kebangsaan Malaysia with the cooperation of Ministry of Science, Technology and Innovation of Malaysia. The fall cone test for the different type of soil sample is done in the geotechnical laboratory of Civil and Structural Department, UKM. The data collection for soil resistivity measurement is carried out using digital precision multimeter, model 8846A, Fluke at construction site of University Kebangsaan Malaysia (UKM) in Bangi, Selangor, Malaysia shown in Fig. 1. The study on the relationship development between soil electrical resistivity and LL, PL of soil is done and the analysis is performed using MATLAB 2009 in Geotechnical Laboratory, Faculty of Engineering and Built Environment, UKM.



**Figure 1.** Soil electrical resistivity measurement for soil state determination

Conventionally, LL and PL estimation of soil is estimated with fall cone test as moisture contents of soil corresponding to the cone penetration in soil considering the specifications of penetration depth and size of cone in the test (Sridharan and Gurtug, 2004). As an example, moisture contents corresponding to the 20 mm cone penetration for 0.75 N cone weight reveals the LL of the soil sample in fall cone test.

In the research, soil resistivity is taken considering the increasing of moisture contents to get the soil state behaviors. Decreasing of the resistivity of surface soil is dependable on the increasing of water contents of soil in geotechnical field. Thus, the relation of soil water content with soil resistivity at the time of measurement clearly is major factors contributing to soil EC surveys. The resistance,  $R$  in unit of Ohm ( $\Omega$ ) of soil sample is defined with fundamental equation of electrical engineering called as Ohm's law.

$$R = \frac{V}{I} \quad (1)$$

Where  $V$  is the potential difference in volt (V) and  $I$  is the supplied current in ampere (A) of electrical measurements. The resistivity,  $\rho$  of compacted soil is defined from the measured resistance including probe space and area of the soil sample.

$$\rho = \frac{R \times A}{l} \quad (2)$$

Where  $R$  is the resistance ( $\Omega$ ) of the material,  $l$  is the length of the conductor (m), and  $A$  is the cross sectional area ( $m^2$ ).

When a constant voltage is applied to one of the two probes placed in the soil, the current that flows between the probes is inversely relative with the resistance of the soil (Doolittle et al., 1994; Kelleners et al., 2005). Electrical resistivity shows indeed strong variations that principally depend on variations of water contents in soil (McNeill, 1980; Saarenketo, 1998). The electric current passed through the soil between two steel probes makes an electric field in surface soil investigations. The voltage difference as well as electric field strength in geo-electric field is obtained for soil resistivity measurements. The analog electrical signal is converted into a digital value for getting robust performances using criteria of Analog to Digital Converter (ADC) in soil resistivity observations.

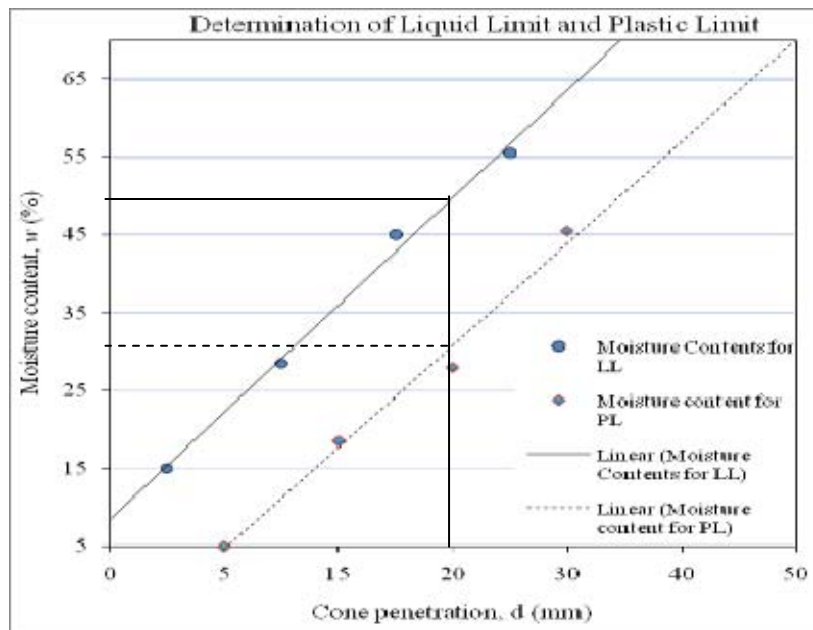
The soil resistivity measurements for determination of LL and PL of soil are done in this work using precision digital multimeter of Fluke Company, model 8846A with accurate measurements and Kilo-Ohm scale for easier reading. The specifications and functions of digital multimeter shown in Table 1 for soil resistivity calculations include 100  $\mu A$  to 10 A current ranges, with up to 100 pA resolutions for the measurements techniques. High resistance meter with digital and analog configurations are used in our research to measure soil resistance with consistency.

**Table 1** Specifications of insulation tester used in soil resistance measurements

	Specifications	Functions
Insulation Resistance Tester-Digital	Test Voltage	1000 V and 600 V
	Measuring ohms Ranges	10 $\Omega$ to 1 G $\Omega$ with up to 10 $\mu\Omega$ resolution
	Measuring current ranges	100 $\mu$ A to 10 A current range, with up to 100 pA resolution
	Measurement technique	2 x 4 ohms 4-wire

## Results and Discussions

Modern research and innovations in geo-electric and system engineering have improved the ability to collect and process data with manifesting reliable subsurface soil properties of near surface soil profile. Usually, soil LL and PL is determined through the laboratory testing with demonstration of soil moisture contents corresponding to the reading of specified tools (Sridharan and Gurtug, 2004) in geotechnical characterizations. As an example, soil moisture contents corresponding to the specified cone penetration depth in millimeter is considered as LL for particular size of cone for the fall cone test method. PL can be estimated with another size of cone considering the moisture contents for specified cone penetration depth in millimeter. The laboratory tests of different soil sample are also costly and tedious to obtain the criteria of estimation of cone penetration, moisture contents in soil for geotechnical investigations (Sridharan and Nagaraj, 2005). The previous soil LL and PL estimation in laboratory is also time consuming system due to the collecting sample with fall cone test as well as obtaining dry sample of soil.

**Figure 2.** Fall cone test for liquid limit and plastic limit

In this research, fall cone test is performed and cone penetration size is obtained with increasing of water contents for determining LL and PL shown in Fig. 2. The LL of soil is observed using with the weight of cone as 0.75 N whereas the PL of soil is determined with 2.35 N as cone weight in the fall cone test. In both cases, the moisture contents are taken as LL and PL at the empirical cone penetration depth of 20mm. Figure 2 shows that about 49.5 % of moisture contents are considered as LL of soil according to the criteria of fall cone test in the investigated soil sample. Hence, PL is shown as about 30.75 percent moisture contents in soil including cone penetration of 20 mm in the convention laboratory test.

In this study, the resistivity of collected soil sample is determined according to the increasing of moisture contents in soil identifications. Figure 3 shows the soil resistivity decreases exponentially with increasing of moisture content in soil sample. Thus, the resistivity of soil sample is shown about 38 Kilo Ohm-meter (k  $\Omega$ -m) for 50 percent water contents in soil resistivity estimation.



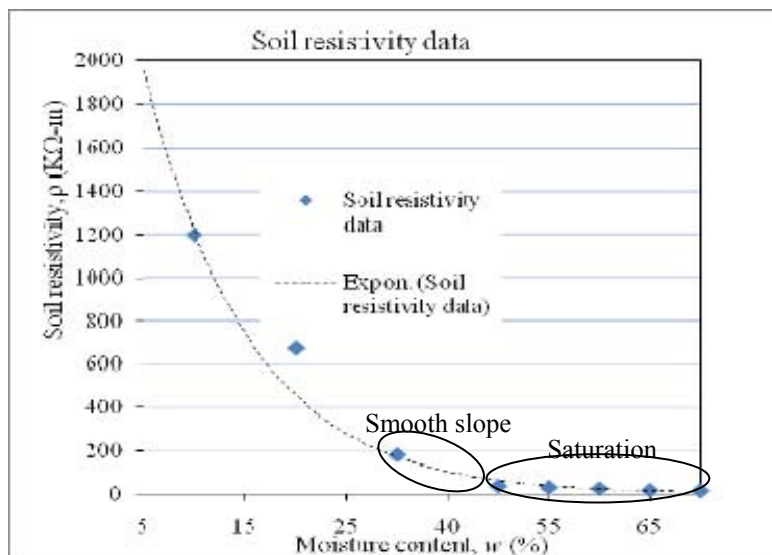


**Figure 3.** Soil resistivity observations with moisture contents

The resistivity of soil goes into the saturation state with increasing the moisture contents after 50 percent in the soil sample. Moreover, the smooth slope of resistivity data is observed in the range of 30 percent to 50 percent water contents shown in Fig. 3. The moisture content of the starting point of the saturation state is revealed as the LL of soil sample in the research criteria with soil resistivity profile. In addition, the initial moisture content of the smooth slope of soil resistivity data is demonstrated as the PL of soil state behavior observations.

The method of soil LL and PL determination through soil resistivity is faster, easier and more cost-effective than the conventional laboratory test in soil investigations. The soil resistivity measurements manifest better and robust performance in geotechnical monitoring systems. There is no criteria of collecting dry sample with certain temperature in geotechnical laboratory which is tedious, time consuming and labor intensive for soil type identification system. In this study, expert idea of soil LL and PL determination are taken from the measured resistivity data of collected soil sample through high resistance meter. Table 2 shows the data of obtaining empirical relationships of LL and PL with soil resistivity in geotechnical characterizations. This system is also consistent for data acquisition and analysis to estimate soil properties with non-destructive performance for roads and highway engineering, geotechnical and many other engineering structures.

**Table 2** Soil LL and PL determination with resistivity profile

Sample No.	Sand (%)	Silt (%)	Clay (%)	Soil LL	Soil PL	Soil resistivity, KΩ-m
A	33.5	38.5	26.0	37.0	20.0	150
B	36.5	58.5	5.0	39.0	26.0	123
C	3.5	56.0	40.5	55.4	31.0	76
D	13.0	35.5	51.5	70.5	35.6	29

## Conclusions

A technique of soil LL and PL determination with electrical resistivity is revealed with the aim of achieving better performance in sensing of soil properties for geotechnical engineering. The empirical relationship is demonstrated to get the soil state behaviors through resistivity measurement in soil profile. The saturated state of resistivity with increasing of soil moisture contents is shown as LL of soil whereas the smooth slope in resistivity data before the saturation state is considered as PL of soil in this research work. The resistivity measurement of collected soil sample is able to obtain the better, faster and cost-effective performance in soil type estimation system. The analysis used in this study incorporates collected data with high resistance meter for soil sample in geotechnical characterizations. In addition, laboratory testing also verifies the idea for obtaining soil condition with soil electrical properties as reliable and consistent investigations in geotechnical profile. There will be future studies including more test data for different type of soil on refining this method to estimate earth parameters in particular applications of geotechnical engineering.

## Acknowledgements

This research is sponsored by Research Project of Science Fund No. 01-01-02-SF0681 from Ministry of Science, Technology and Innovation of Malaysia.

## References

- Avnimelech, Y., Ritvo, G., Meijer, L.E., and Kochba, M. (2001) Water content, organic carbon and dry bulk density in flooded sediments. *Aquacultural Engineering*, 25, 25–33. PII: S0144-8609(01)00068-1
- Sridharan, A., and Nagaraj, H. B. (2005) Plastic limit and compaction characteristics of fine grained soils. *Ground Improvement*, 9 (1), 17–22. DOI: 10.1680/grim.2005.9.1.17
- Doolittle, J.A., Sudduth, K.A., Kitchen, N.R., and Indorante, S.J. (1994) Estimating depths to claypans using electromagnetic induction methods. *J. Soil and Water Conservation*, 49, 572-575. <http://www.jswnonline.org/content/49/6/572.full.pdf>
- Elshorbagy, W.A., and Mohamed, A.M.O. (2000) Evaluation of using municipal solid waste compost in landfill closure caps in arid areas. *Waste Management*, 20, 499-507. DOI: 10.1016/S0956-053X(00)00025-8
- Friedman, S.P. (2005) Soil properties influencing apparent electrical conductivity: a review. *Computers and Electronics in Agriculture*, 46, 45–70. DOI: 10.1016/j.compag.2004.11.001
- Huang, H., and Fraser, D.C. (2002) Dielectric permittivity and resistivity mapping using high-frequency, helicopter-borne EM data. *Geophysics*, 67 (3), 727–738. DOI: 10.1190/1.1484515
- Kelleners, T.J., Robinson, D.A., Shouse, P.J., Ayars, J.E., and Skaggs, T.H. (2005) Frequency dependence of the complex permittivity and its impact on dielectric sensor calibration in soils. *Soil Sci. Soc. Am. J.*, 69, 67–76. <http://ddr.nal.usda.gov/bitstream/10113/4074/1/IND43668307.pdf>.
- McNeill, J.D. (1980) Electromagnetic terrain conductivity measurement at low induction numbers. Technical note TN-6, Geonics Limited, Mississauga, Ontario, 1980.
- Osella, A., and Favetto, A (2000) Effects of soil resistivity on currents induced on pipelines. *Journal of Applied Geophysics*, 44, 303–312. DOI:10.1016/S0926-9851(00)00008-2.
- Saareketo, T. (1998) Electrical properties of water in clay and silty soils. *Journal of Applied Geophysics*, 40, 73–88. DOI:10.1016/S0926-9851(98)00017-2
- Samouelian, A., Cousin, I., Tabbagh, A., Bruand, A., and Richard, G. (2005) Electrical resistivity survey in soil science: a review. *Soil & Tillage Research*, 83, 173–193. DOI: 10.1016/j.still.2004.10.004
- Sridharan, A., and Gurtug, Y. (2004) Swelling behaviour of compacted fine-grained soils. *Engineering Geology*, 72, 9–18. DOI:10.1016/S0013-7952(03)00161-3
- Yoon, G.L., and Park, J.B. (2001) Sensitivity of leachate and fine contents on electrical resistivity variations of sandy soils. *Journal of Hazardous Materials*, 84, 147–161. DOI:10.1016/S0304-3894(01)00197-2
- Benson, C.H., and Trast, J. M. (1995) Hydraulic conductivity of thirteen compacted clays. *Clays and Clay Minerals*, 43(6), 669-681. <http://www.clays.org/journal/archive/volume%2043/43-6-669.pdf>

# Fate of Fluometuron Dissolved in Natural Waters and Exposed to Solar Light

Sabrina HALLADJA<sup>1,2</sup>, Abdelaziz BOULKAMH<sup>2</sup>, Claire RICHARD<sup>3</sup>

<sup>1</sup> Département Sciences de la matière, Université 20 août 1955 – Skikda-Algeria

<sup>2</sup> Laboratoire des Techniques Innovantes de Préservation de l'environnement, Université Mentouri – Algeria.

<sup>3</sup> Laboratoire de Photochimie Moléculaire et Macromoléculaire, Université Blaise Pascal, France

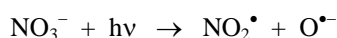
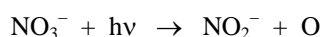
sabrinahalladja@gmail.com

**Abstract** - To predict the fate of pollutants in the aquatic environment and to assess the risk they may pose, it is necessary to improve our knowledge on their chemical reactions under environmental conditions. Photochemical reactions are a route for the attenuation of organic pollutants present in surface waters. This work was devoted to herbicide fluometuron which is used to control weeds in cotton. Phototransformation of fluometuron (1  $\mu$ M) in natural sunlight was investigated in synthetic waters containing either natural organic matter, nitrate ions or both in order to mimic reactions taking place in aquatic environments. Fluometuron underwent photolysis and its degradation was faster in the presence of fulvic acids (10 mg l<sup>-1</sup>, factor 2.5) or nitrates (25 mg l<sup>-1</sup>, factor 15) than in Milli-Q water showing the importance of natural waters constituents. Identification of major photoproducts was conducted under laboratory conditions. Hydroxylation of the aromatic ring with or without hydrolysis of CF<sub>3</sub> into CO<sub>2</sub>H and oxidation of the urea chain leading to demethylation were observed.

**Keywords:** photodegradation, phenylureas herbicides, solar light, naturel waters.

## Introduction

Photochemistry is one of the main abiotic degradation pathway of organic pollutants occurring in surface waters. This is a route for attenuation of organic pollutants. Several types of reactions may occur depending on the medium composition. Direct photolysis is possible if the considered pollutant absorbs solar light. In addition, photoinduced or photosensitized transformations mediated by components of the aquatic medium can also take place. In particular, dissolved natural organic matter (DOM) which absorbs a large portion of photons is a potential photosensitizer. Singlet oxygen, superoxide ion/hydroperoxyl radicals, hydroxyl radicals, excited triplet states and alkylperoxyl radicals were proved or proposed to be generated in natural waters under the influence of sunlight (Vaughan and *al.*, 1998; Canonica and *al.* 1995; Halladja and *al.* 2007). However, a part of these species are trapped by DOM itself. Nitrate ions that are present in surface waters at level varying from 0.2 to 25 mg.L<sup>-1</sup> generate the highly oxidizing hydroxyl radicals under light excitation (Boule and *al.*, 1999).



The percentage of hydroxyl radicals trapped by pollutants is thus strongly dependent on the medium composition. In the present work, we focused on the phototransformation of the phenylurea herbicide fluometuron (FM). This compound is widely used for pre- and post-emergence control of weeds in fields of conventional cotton cultivars. It is persistent (Stoeckel and *al.*, 1997) and may pose some risks to aquatic organisms (Muschal and *al.*, 2003). FM poorly absorbs solar light (*see Fig. 1*) but indeed its direct photolysis in simulated solar light ( $\lambda > 290$  nm) was reported (Lam and *al.*, 2005). The CF<sub>3</sub> group undergoes photohydrolysis into CO<sub>2</sub>H.

The objective of the present work was to investigate the photolysis of FM in conditions approaching real ones. FM in the micromolar range was irradiated in natural solar light. The influence of DOM or/and nitrates on the phototransformation was assessed. In parallel, laboratory experiments were conducted to identify the main photoproducts on the basis of HPLC–ESI–MS analyses.



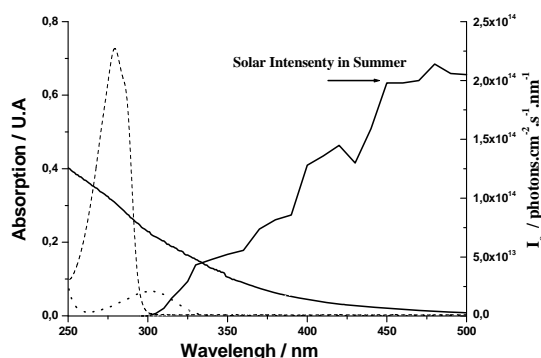


**Fig. 1:** Absorption spectrum of (---) FM at  $3.10^{-4}$  M, (—) FA at  $10 \text{ mg.L}^{-1}$ , (.....) nitrates at  $0.01 \text{ M}$  and solar light emission reaching the earth surface in summer (Zepp and al., 1977)

## Methods and Procedures

### Photoreaction setup

For kinetic purpose, FM ( $1 \mu\text{M}$ ) was irradiated (1) in Milli-Q water, (2) in water containing fulvic acids ( $10 \text{ mg.L}^{-1}$ ) used as a surrogate of DOM, (3) in water containing nitrate ions ( $25 \text{ mg.L}^{-1}$  or  $3.10^{-4} \text{ M}$ ) and (4) in water containing both fulvic acids ( $10 \text{ mg.L}^{-1}$ ) and nitrate ions ( $3.10^{-4} \text{ M}$ ). Irradiation experiments in natural sunlight were performed at Clermont–Ferrand ( $46^\circ \text{ N}$ ,  $3^\circ \text{ E}$ ) in June 2006. Cylindrical quartz glass reactors (14 mm internal diameter) were filled with 14 ml of solutions. Reactors were closed by a septum, attached on a rack inclined by about  $15^\circ$  from horizontal and exposed to solar light. Samples received 13 h of sunshine per day. Aliquots of 0.5 ml were removed simultaneously from all the solutions at selected intervals. Samples were immediately analyzed by HPLC. Irradiations under laboratory conditions were also carried out for photoproducts identification. Irradiations were performed in a device equipped with six TLAD 15W/05 fluorescent tubes emitting within the wavelength range 300–450 nm with a maximum of emission at 365 nm and in a Pyrex glass reactor (14 mm i.d.). The device was cylindrical and equipped with reflecting inner walls. A ventilator was used as a cooling system. The reactor was placed in the centre of the device and was surrounded by the six fluorescent tubes. Light intensity was measured using p-nitroanisole/pyridine as a chemical actinometer. PNA ( $10^{-5} \text{ M}$ ) and pyridine ( $10^{-4} \text{ M}$ ) were irradiated in the same conditions as samples in the polychromatic device and in solar light. In the polychromatic device, PNA loss was 12% after 1 h and 63% after 5 h. In solar light, 56% of PNA had disappeared after 4 h of exposure between 10 am and 2 pm. It can be deduced that the average light intensity delivered by the tubes of the polychromatic device was of the same magnitude order as that of solar light within the wavelength range 300–400 nm (limit of PNA absorption).

### Analytical procedures

Loss of fluometuron and formation of photoproducts were monitored by HPLC–UV using a Waters apparatus equipped with two pumps (model 510), an autosampler, a photodiode array detector (model 996), a detector W2487 and a C18 reverse-phase column (4.6 mm, 250 mm, Spherisorb S5 ODS2, 5  $\mu\text{m}$ , Waters). Eluent was a mixture of water acidified with 0.1% of orthophosphoric acid and methanol (50%/50%) delivered at a constant flow of  $1 \text{ mL.min}^{-1}$ .

The HPLC–UV–MS analyses were performed using a Waters/Micromass LC/QTOF (Micromass, Manchester, UK). For the HPLC conditions, a Waters Alliance 2695 HPLC equipped with a photodiode array detector (DAD) was used. A reversed-phase column (C18 Hypersil ODS, 5  $\mu\text{m}$ , 100 mm, 2.1 mm; Interchim, Montluc, on, France) was used at a flow rate of  $0.3 \text{ mL.min}^{-1}$ . The mobile phase was composed of acetonitrile (solvent A) and acidified water (formic acid, 0.4% v/v; pH 2.6) (solvent B). Gradient: 0–5 min, 5% A; 5–30 min, 5–95% A (linear); 30–34 min, 95% A; 34–35 min, 95–5% A; 35–40 min, 5% B equilibrium period). The injection volume was 30  $\mu\text{l}$ . The LC–ESI–MS worked both in positive and negative mode.

UV spectra were recorded on a Cary 3 (Varian) spectrophotometer. A 1-cm path quartz cell was used for all the experiments. The reference beam blank was always Milli-Q water.

## Results

### Kinetics of phototransformation in solar light

We first compared the profiles of FM loss in various conditions (Fig. 2). In the absence of fulvic acids (FA) and nitrate ions, the consumption of FM ( $1 \mu\text{M}$ ) in solar light was very slow: less than 30% had disappeared after 6.7 d. The addition of fulvic acids ( $10 \text{ mg.L}^{-1}$ ) significantly increased the rate of FM consumption: about 50% of FM had disappeared after 6.7 d. A larger enhancement of the reaction rate was observed in the presence of nitrate ions ( $25 \text{ mg.L}^{-1}$ ): a complete FM loss was obtained after 3.3 d. In the presence of both fulvic acids ( $10 \text{ mg.L}^{-1}$ ) and nitrate ions ( $25 \text{ mg.L}^{-1}$ ), FM disappeared more slowly than in the presence of nitrates alone. To determine rate constants, we plotted  $\ln C_0/C$  vs irradiation time, where

$C_0$  is the initial FM concentration and  $C$  the concentration at  $t$ . In all cases, FM consumption followed pseudo first order kinetics. The rate coefficients,  $k$ , and  $R^2$  values are reported in *Table 1*.

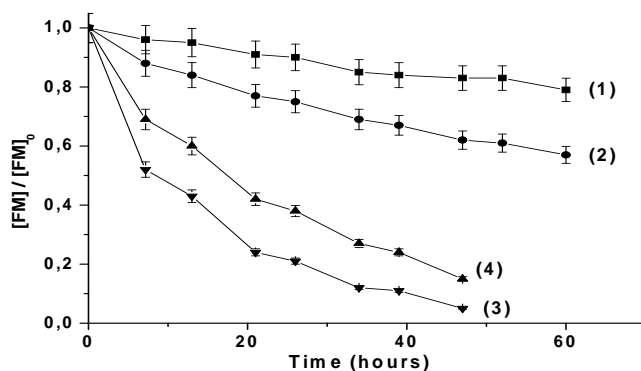


**Fig. 2.** Kinetics of FM ( $10^{-6}$  M) phototransformation in solar light in various aqueous media. (1): in pH 6.5 Milli-Q purified water; (2): in water containing FA ( $10 \text{ mg.L}^{-1}$ ); (3): in water containing FA ( $10 \text{ mg.L}^{-1}$ ) and nitrates ( $3.10^{-4}$  M); (4): in water containing nitrates ( $3.10^{-4}$  M).

**Table 1:** Phototransformation of FM ( $10^{-6}$  M) in solar light

Medium	$k \text{ (s}^{-1}\text{)}$	$R^2$	$t_{1/2} \text{ (days)}$
1	$6.4 \times 10^{-7}$	0.974	12.5
2	$1.6 \times 10^{-6}$	0.964	5.0
3	$9.8 \times 10^{-6}$	0.948	0.82
4	$6.2 \times 10^{-6}$	0.959	1.3

These kinetic results bring insight into the photodegradability of FM in solar light. FM is hardly transformed in pure water due to the poor absorption of solar radiations. Using the rate coefficient given in *Table 1*, one computes a half-life of 175 h. The chromophoric constituents of water (nitrate and fulvic acids) promoted FM phototransformation. The effect of fulvic acids was quite moderate. In the presence of fulvic acids ( $10 \text{ mg.L}^{-1}$ ), the rate coefficient was increased by a factor of 2.5 and the half-life reduced by the same factor. Nitrate ions ( $25 \text{ mg.L}^{-1}$ ) had a more pronounced influence increasing the rate coefficient and reducing the half-life by a factor of 15. In the presence of fulvic acids and nitrate ions, the rate of FM photodegradation was smaller by about 40% than in the presence of nitrate ions alone. At the considered concentrations, the absorbance of nitrates is very small (around 0.002) while that of FA bigger (around 0.22) (*see Fig. 1*). The inhibiting effect of FA on nitrate photolysis through screen effect is difficult to evaluate due to the cylindrical shape of reactors. Based on a mean path-length of 0.7 cm, one would compute a rate reduction between 15% and 20%. It represents 50% of the measured inhibition. The remaining 50% of inhibition are likely to be due to the scavenging of hydroxyl radicals by FA (Brezonik and al., 1998; ter Halle and al. 2006). In an attempt to delineate the role of hydroxyl radicals in the fulvic acids mediated phototransformation of FM, we studied the influence of 2-propanol added as a hydroxyl radical scavenger on the reaction ( $k = 1.9.10^{10} \text{ M}^{-1} \text{ s}^{-1}$ , Buxton and al., 1988). These experiments were undertaken in laboratory conditions. In the absence of fulvic acids, the initial rate of FM phototransformation was equal to  $2.10^{-8} \text{ M.h}^{-1}$ . In the presence of fulvic acids ( $5 \text{ mg.L}^{-1}$ ), it raised to  $5.2. 10^{-8} \text{ M.h}^{-1}$ . The addition of 2-propanol ( $0.015 \text{ M}$ ) reduced the latter rate by a factor comprised between 1.5 and 2, suggesting the involvement of hydroxyl radicals in the phototransformation reaction and showing the ability of FA to produce them under irradiation. We also studied the influence of oxygen on the reaction (*see Fig.3*).

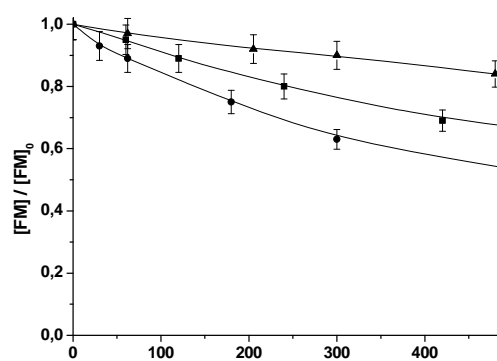


**Fig. 3.** Kinetics of a neutral solution of FM ( $3.10^{-6}$  M) phototransformation containing fulvic acids ( $25 \text{ mg.L}^{-1}$ ) at 365 nm in various aqueous medias: air-saturated medium (■); oxygen-free medium (●); oxygen-saturated medium (▲)

After 5 h of irradiation, FM consumption was twice faster in air-saturated than in oxygen-saturated medium and 3-fold faster in nitrogen-saturated medium than in air-saturated medium. Thus, oxygen clearly inhibited the reaction.

### Photoproducts identification

To achieve photoproducts characterization, we irradiated more highly concentrated FM solutions under laboratory conditions. The photolysis of FM ( $3.10^{-5}$  M) in Milli-Q water yielded the acidic compound resulting from the hydrolysis of  $CF_3$  into  $CO_2H$  as previously reported (Lam and al., 2005). Its UV absorption spectrum differs from that of FM: the far UV absorption band ( $\lambda_{max} = 224$  nm) shows a shoulder and the second maximum of absorption is located at 297 nm instead of 275 nm in the case of FM.

The irradiation of FM ( $3.10^{-5}$  M) in the presence of fulvic acids ( $25 \text{ mg.L}^{-1}$ ) yielded two HPLC–UV detectable photoproducts, **I** and **II** (Fig. 4a).

The UV spectrum of **I** exhibited the same shoulder as that of the acidic product and a second maximum red-shifted by 27 nm ( $\lambda_{max} = 297$  nm). The UV spectrum of **II** resembled that of FM but the second maximum was red-shifted by 20 nm compared to it ( $\lambda_{max} = 295$  nm).

The HPLC–mass analysis of **I** gave a first molecular ion at  $m/z = 223$  in  $ES^-$  mode and at  $m/z = 225$  in  $ES^+$  mode corresponding to the loss of 9 amu that may be explained by the hydrolysis of  $CF_3$  into  $CO_2H$  and the addition of an oxygen atom. Fragments at  $m/z = 179$  [ $M - 44$ ] and at  $m/z = 134$  [ $M - 89$ ] were obtained in  $ES^-$  mode. These data are compatible with the structure proposed in Table 2. The first fragment would correspond to the loss of the carboxylic group and the second to the cleavage of the terminal amine group  $-N(CH_3)_2$  followed by loss of an H atom to yield an isocyanate. Photoproduct **II** gave molecular ions at  $m/z = 247$  and  $249$  in  $ES^-$  and  $ES^+$  modes, respectively, corresponding to the addition of an oxygen atom to FM. A fragment at  $m/z = 202$  corresponding to  $M - 45$  was observed in  $ES^-$  mode. The loss of 45 amu is likely to result from the departure of  $N(CH_3)_2$  by cleavage of the terminal urea C–N bond and the elimination of H to form the isocyanate. It is compatible with structure given in Table 2.

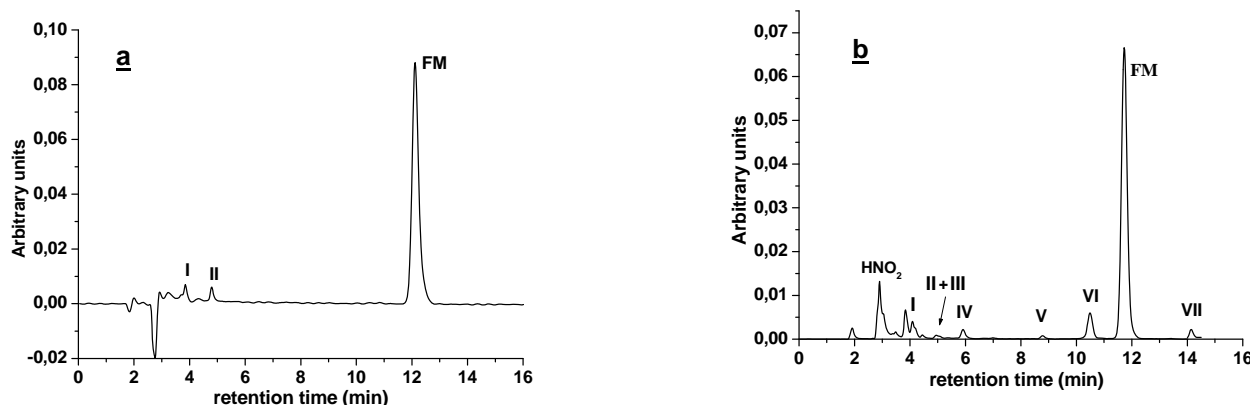


Fig. 4. HPLC chromatogram of (a) a neutral solution of FM ( $3.10^{-5}$  M) containing fulvic acids ( $\text{mg.L}^{-1}$ ) at a conversion extent of 20% and (b) a neutral solution of FM ( $3.10^{-5}$  M) containing nitrate ions ( $25 \text{ mg.L}^{-1}$ ) at a conversion extent of 46%. Both solutions were irradiated in simulated solar light. Photoproducts are numbered as indicated in Table 2.

The irradiation of FM ( $3.10^{-5}$  M) in the presence of nitrate ions ( $25 \text{ mg.L}^{-1}$ ) yielded seven photoproducts detectable by HPLC–UV (see Fig. 4b). Based on HPLC retention times, UV absorption spectra and mass data, we could conclude that photoproducts **I** and **II** were present among the seven photoproducts. Two other compounds **III** and **IV** with a molecular ion at  $m/z = 223$  in  $ES^-$  mode were also detected. As they showed distinct retention times and UV maxima, but similar fragmentation at  $m/z = 179$  and  $134$  with different percentages of fragments, they are likely to be isomers of **I**. Photoproducts **I**, **III** and **IV** should differ from each other in the position of the hydroxyl group on the ring. The photoproducts **V** and **VI** that were eluted just before FM showed similar absorption spectra. One of them, **V**, gave a molecular ion at  $m/z = 203$  in  $ES^-$  mode corresponding to the loss of 28 amu and a fragment at  $m/z = 160$ . The other one, **VI**, gave a molecular ion at  $m/z = 217$  in  $ES^-$  mode and the same fragment at  $m/z = 160$ . These compounds could be assigned to demethylated products; **VI** would be the monodemethylated derivative and **V** the didemethylated derivative (see Table 2).

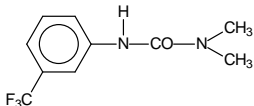
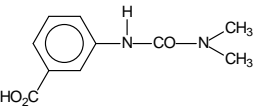
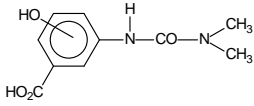
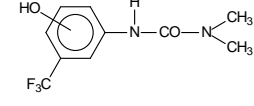
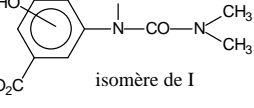
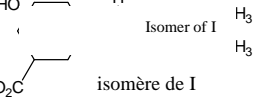
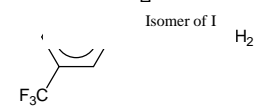
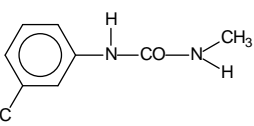
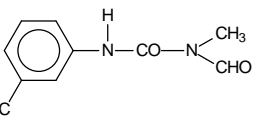
A molecular ion at  $m/z = 245$  in  $ES^-$  mode was also detected at a retention time longer than that of FM. This mass corresponds to the addition of 14 amu. Three fragments were observed at  $m/z = 217$  [ $M - 28$ ],  $188$  [ $M - 28 - 29$ ] and  $160$  [ $M - 28 - 29 - 28$ ]. This fragmentation indicates that the aromatic ring was not altered. It is in favour of photoproduct **VII** that bears a carbonyl group and for which successive losses of CO,  $NCH_3$  and CO are again possible.

Finally, we used the selected peak method to detect some specific photoproducts formation of which was expected. In the case of nitrate ions, we could find nitro derivatives at  $m/z = 276$  in  $ES^-$  mode corresponding to the addition of 45 amu ( $+NO_2 - H$ ). In the case of fulvic acids, careful examination of chromatograms revealed the presence of peaks at  $m/z = 217$  and  $245$  in  $ES^-$  mode and  $m/z = 219$  in  $ES^+$  mode, showing that fulvic acids photosensitized transformation also yielded FM demethylation, but this pathway was very minor.

## Conclusion

Direct photolysis of aqueous FM is slow but photosensitizing processes may promote its transformation in surface waters. In the presence of hydroxyl radicals, both the lateral chain and the ring of FM are oxidized. Photoreactants deriving from fulvic acids privilege oxidation of the aromatic ring. Photoproducts of hydrolysis or hydroxylation of the aromatic ring absorb solar light better than FM itself. They are thus susceptible to undergo photolysis faster than FM. Photoproducts resulting from oxidation of lateral urea chain are more photostable. It would be now necessary to test the toxicity of each individual compound or that of the irradiated mixtures toward reference organisms in order to access the risk that may pose FM.

Table 2: Structure of detected photoproducts, molecular weigh, maxima of absorption, molecular ions and main fragments detected by LC-ESI-MS

Formula	Number	Molecular weigh	Condition Of obtention	$\lambda_{\max}$ (nm)	m/z main fragments
	FM	232		242/275	ESI <sup>+</sup> : 231
	acid	208	Pure water	224/297	ESI <sup>+</sup> : 207
	I	224	FA or nitrates	222/324	ESI <sup>+</sup> : 223 (179, 134) ESI <sup>+</sup> : 225
	II	248	FA or nitrates	242/295	ESI <sup>+</sup> : 247 (202) ES <sup>+</sup> : 249
	III	224	Nitrates	230/311	ESI <sup>+</sup> : 223 (179, 134)
	IV	224	Nitrates	224/315	ESI <sup>+</sup> : 223 (179, 134)
	V	204	Nitrates	241/280	ESI <sup>+</sup> : 203 (160)
	VI	218	Nitrates or FA (minor)	243/279	ESI <sup>+</sup> : 217 (160)
	VII	246	Nitrates or AF (minor)	245 and shoulder at 280	ESI <sup>+</sup> : 245 (217, 188, 160)

## References

- Boule, P., Bolte, M., Richard, C., (1999). *Phototransformations induced in aquatic medium by  $Fe^{III}$ ,  $NO_3^-$ ,  $NO_2^-$  and humic substances*. In: Boule, P. (Ed.), The Handbook of Environmental Chemistry. In: Editor in Chief: O. Hutzinger (Ed.), Environmental Photochemistry, vol. 2. Bayreuth (FRG), part L, pp. 181–215.
- Brezonik, P.L., Fulkerson-Brekken, J., (1998). Nitrate-induced photolysis in natural waters: controls on concentrations of hydroxyl radical photointermediates by natural scavenging agents. *Environ. Sci. Technol.* 32, 3004–3010.
- Buxton, G.V., Greenstock, C.L., Helman, W.P., Ross, A.B., (1988). Review of rate constants for reactions of hydrated electrons, hydrogen atoms and hydroxyl radicals in aqueous solution. *J. Phys. Chem. Ref. Data* 17, 513–886.
- Canonica, S., Jans, U., Stemmler, K., Hoigne, J., (1995). Transformation kinetics of phenols in water: photosensitization by dissolved organic material and aromatic ketones. *Environ. Sci. Technol.* 29, 1822–1831.
- Halladja, S.; Ter Halle, A.; Aguer, J. - P.; Boulkamh, A.; Richard, C., (2007). Inhibition of humic substances mediated photooxygenation of furfuryl alcohol by 2,4,6-trimethylphenol. Evidence for reactivity of the phenol with humic triplet excited states. *Environ.Sci. Technol.* 41, 6066–6073.
- Lam, M.W., Young, C.J., Mabury, S.A., (2005). Aqueous photochemical reaction kinetics and transformations of fluoxetine. *Environ. Sci.Technol.* 39, 513–522.
- Muschal, M., Warne, M.S.J., (2003). Risk posed by pesticides to aquatic organisms in rivers of northern inland New South Wales, Australia. *Hum. Ecol. Risk Assess.* 9, 1765–1787.
- Stoeckel, D.M., Mudd, E.C., Entry, J.A., (1997). Degradation of persistent herbicides in Riparian wetlands. *ACS Symp. Ser.* 664, 114–132.
- ter Halle, A., Richard, C., (2006). Simulated solar light irradiation of mesotrione in natural waters. *Environ. Sci. Technol.* 40, 3842– 3847.
- Vaughan, P., Blough, N., (1998). Photochemical formation of hydroxyl radical by constituents of natural waters. *Environ. Sci. Technol.* 32, 2947–2953.
- Zepp, R.G., Cline, D.M., (1977). Rates of direct photolysis in aquatic environment. *Environ. Sci. Technol.* 11, 359–366.

# Geochemical distribution of heavy metals in soils and stream sediments of Omiyale and environs, Ibadan, southwestern Nigeria

Laniyan, T. A, Omosanya, K.O, Adesanya, O. O

Department of Earth Sciences, Olabisi Onabanjo University, Ago-Iwoye- Nigeria  
kamaloomosanya@yahoo.com

**Abstract:** An assessment of geochemical distribution of heavy metals in soils and sediments of Omiyale was done to elucidate their effect on plants and animals in the study area. Nine (9) soil samples and four (4) stream sediments were randomly collected, sieved with the 63 $\mu$ m sieve and analyzed using the inductive coupled plasma mass spectrometry (ICP-MS) technique. Fe<sub>2</sub>O<sub>3</sub> is dominant in the stream sediment used as waste disposal tanks. Influence of anthropogenic enrichment was noticed from the index of geoaccumulation ( $I_{geo}$ ) Zn (2.40), Pb (4.75); inter-elemental analysis Cu-Pb (0.6), As-Zn (0.7), and quantification of degree of pollution Pb (62.2%) in soil, Pb (44.6%) in stream sediment with an increasing order Zn>Pb>Ba>Cu>As>Cd. The study area is polluted with Pb and Zn attributed to urbanized anthropogenic sources, which are mostly vehicular emission, and domestic sewage. Public effect of these elements could include lung cancer and cardiovascular diseases. Based on the above evaluation, a recommendation in respect of public awareness program on sanitizations and contamination of quality control of soil and sediments are encouraged.

**Key words:** Anthropogenic, disposal tank, contamination, sanitization, urbanization

## Introduction

Soils are produced from the breakdown of pre-existing rocks of Precambrian basement complex and are transported from one place to another by different media (Aweto, 1994). The chemistry of a soil is the cumulative reflection of its geology regionally, and locally, with the type and genesis of the weathered regolith (Zhang et al, 2002, Price & Velbel, 2003, Mitchell, 1974; Sharma & Rajamani, 2003), these factors will be responsible for the chemistry of loose sediment. Contaminants of surface drainage systems are mostly related to the consequences of population growth, urbanization, agricultural activities and development of new industrial zones (Olade 1987, Paul & Piilai, 1983), while uncontrolled direct dumping of domestic wastes and discharge of sewage into the urban drainage systems, inadequate land-use planning and improper waste disposal and management systems are critical components of heavy metals contamination (Ajayi & Mombeshora, 1990). However, the release of trace metals associated with such soil processes could have both positive and negative impacts on the environment (Fergusson 1990, Tiller 1989). The type of bedrock beneath the soil in an area can determine the kinds of trace elements present in vegetation, water and sediments in such an area; investigation of heavy metals in soil and sediment is therefore, essential since a slight change in the concentration above the acceptable level, whether due to geogenic (natural) or anthropogenic (man-made) sources like inadequate sewage facilities, road constructions, mining activities, traffic emissions, landfills, agro-chemicals, industrial effluents can result in serious environmental and subsequent health problems (Cobelo-Garcia et al, 2003, Figueiro et al, 2002, Sandroni & Smith, 2002). Trace metal contaminated soil and sediments, therefore, represent a significant environmental concern which has been demonstrated to be toxic to soil/sediment-dwelling organisms, human health, and fishes resulting in decreased survival, reduced growth, or impaired reproduction, and lower species diversity (La Pointe & Hudson, 1985). In Nigeria, rapid population increase due to rural – urban migration in the last few decades, characterizes most of the big cities and urban centers. Unfortunately,



poor sanitary and wastes/ sewage disposal facility had led to gradual degradation of the environment (Tijani et al, 2004).

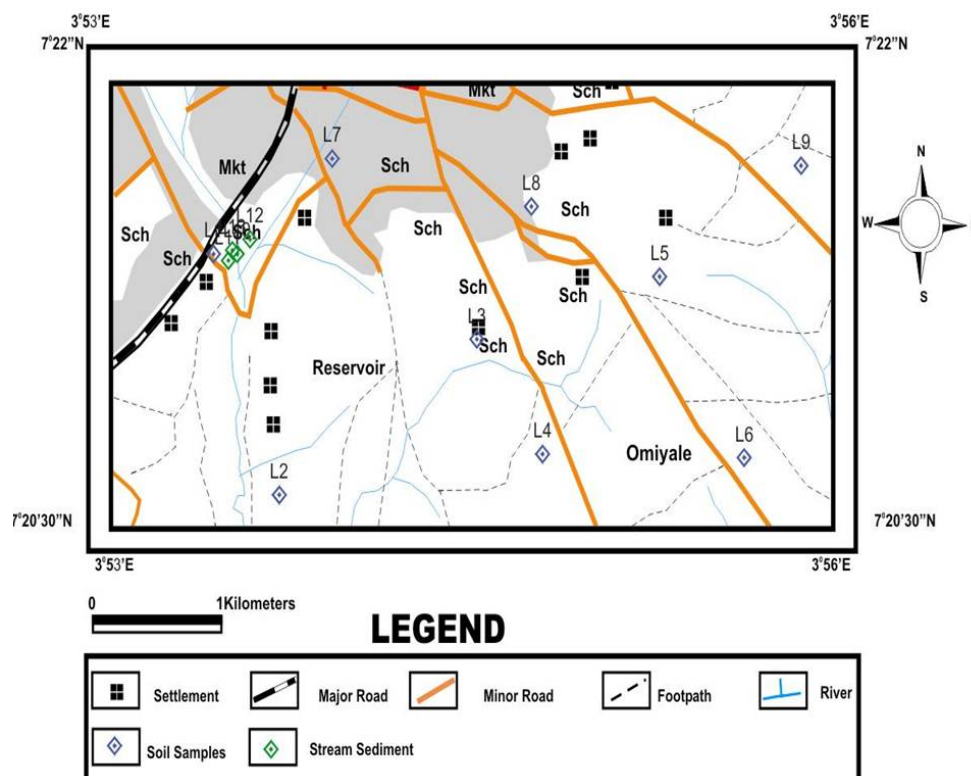


**Fig.1:** Map of the study area and location of sample points

Based on the above background, these study focuses on the contamination of heavy metals in the soil and sediments of the densely populated areas of Ibadan metropolis (Fig. 1), with the aim of assessing the implication of this contamination to the public health, and in addition examining the possible sources of contamination of the environment.

## Materials and method

Nine (9) soil and four (4) stream sediment samples were taken at locations close to the groundwater samples (See fig.1); the soil and stream sediments were decanted and immediately bagged to avoid contamination; they were then air dried for seven days to reduce the rate of fungi growth contamination, and subsequently sieved with the 63 $\mu$ m mesh. The samples were analyzed using the inductive coupled plasma mass spectrometry (ICP-MS) technique.

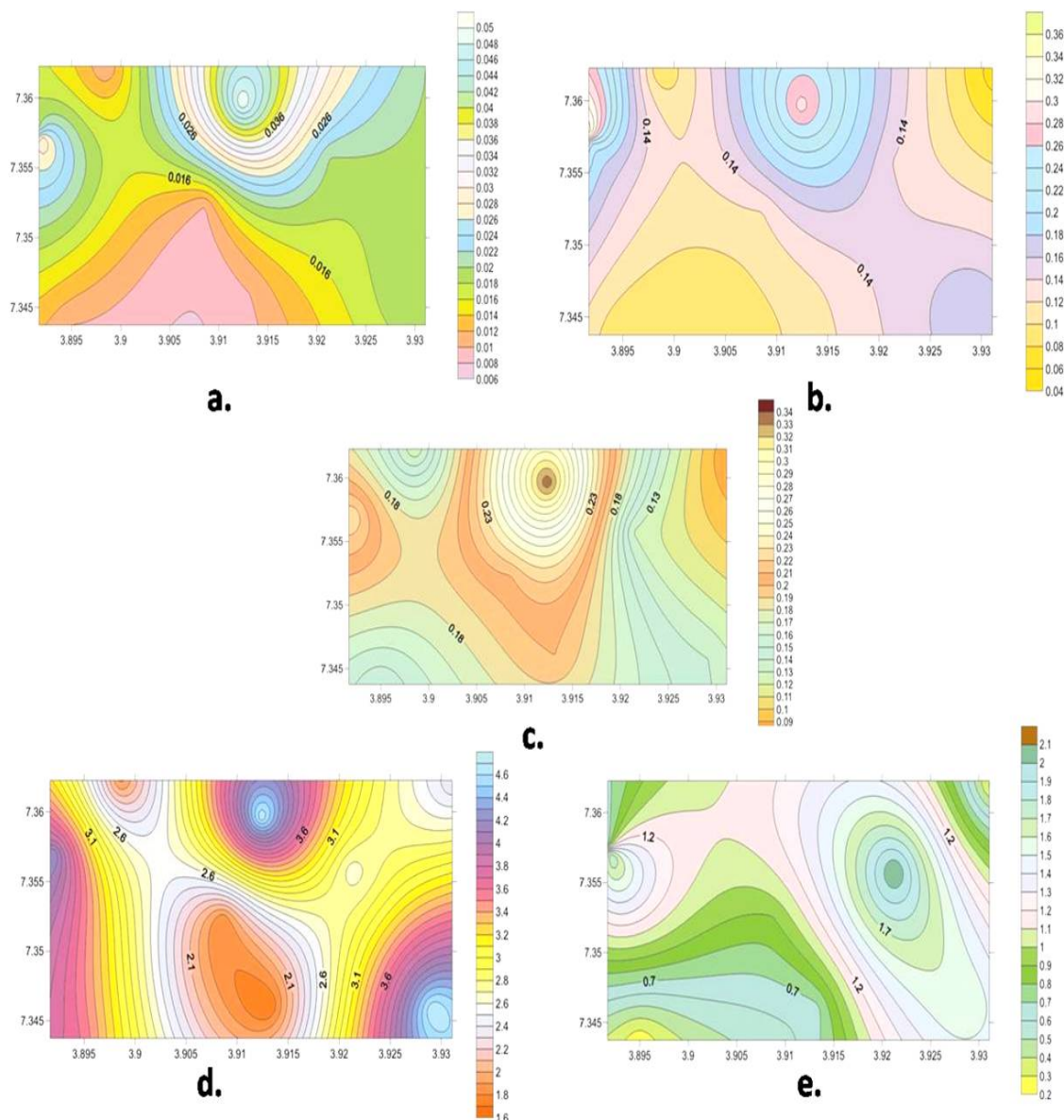


**Fig.2:** Geochemical map for concentration of (a)Na<sub>2</sub>O, (b)MgO, (c) K<sub>2</sub>O, (d) CaO and (e) Fe<sub>2</sub>O<sub>3</sub> in the study area.

## Result and Discussion

### Soil chemistry

**Major Oxides:** Concentrations of the major oxides Table 1.0 of soil and sediments in the study area showed that Fe<sub>2</sub>O<sub>3</sub> ranges from 3.30- 7.15% with mean of 5.23 in the sediment; 2.17-6.06% with mean of 4.04 in the soil; CaO ranges from 0.74-0.99% with mean of 0.84 in the sediment; 0.31-2.97% with mean of 1.48 in the soil; MgO ranges from 0.22-0.98% with mean of 0.41 in the sediment; 0.08-0.48% with mean of 0.27 in the soil; Na<sub>2</sub>O ranges from 0.01-0.02% with mean of 0.02 in the sediment; 0.01-0.07% with mean of 0.03 in the soil; K<sub>2</sub>O ranges from 0.17-0.36% with mean of 0.22 in the poor sanitary and waste/sewage disposal facilities in the study area where their stream channel is used extremely as the waste-disposal tank, sediment; 0.10-0.41% with mean



of 0.22 in the soil. There is dominance of  $\text{Fe}_2\text{O}_3$  in the sediments when compared to the soil (Fig. 2 & 3), in addition, the dominance of the other oxides ( $\text{CaO}$ ,  $\text{MgO}$ ,  $\text{Na}_2\text{O}$ ,  $\text{K}_2\text{O}$ ) in the soils was found in all the areas showed the oxides had been majorly contributed from the weathering of aluminosilicates, Ferromagnesian and aplite rich minerals of the rocks on the soil, Fig. 2 & 3 showed the geochemical maps of the oxides, and this reveals the impact of each oxide on the environment. A significant correlation also confirms the above revelation Table 2.0. Factor analysis, Table 3.0 of the soil and stream used to explain the underlying controlling variables (Hakanson, 1980) showed that the variables in factor 1 consist of all the major oxides, which shows that they are those controlling the chemical character of the soil and stream sediments, and they account for 57% of the total variance of the variables with Eigen value of 2.8; furthermore, the relatively high positive correlation is a reflection of the influence of community on the soil and stream sediment chemistry which affirms that the indiscriminate dumping of industrial and market sewage waste in the soils and sediments of the study area. Factor 2 consists of all the oxides except  $\text{Fe}_2\text{O}_3$ ,  $\text{K}_2\text{O}$  suggests a natural environment for the oxides, but it still shows the influence of  $\text{CaO}$  on the chemistry. Factor 3, also affirms the same controlling environment for the oxides except for  $\text{CaO}$  and  $\text{Fe}_2\text{O}_3$ . This can be concluded that the chemical character of the soil and sediment is mostly the major oxides analyzed, but it is dominated by  $\text{CaO}$  and  $\text{Fe}_2\text{O}_3$ .

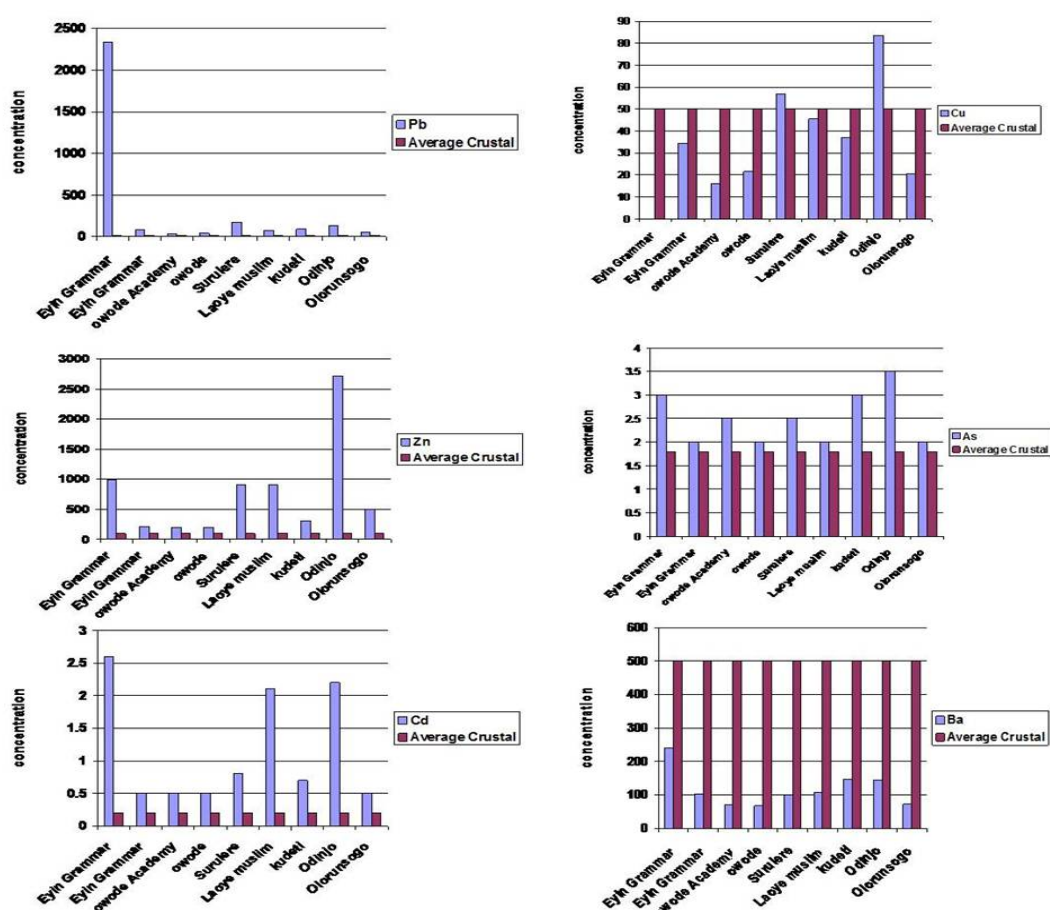
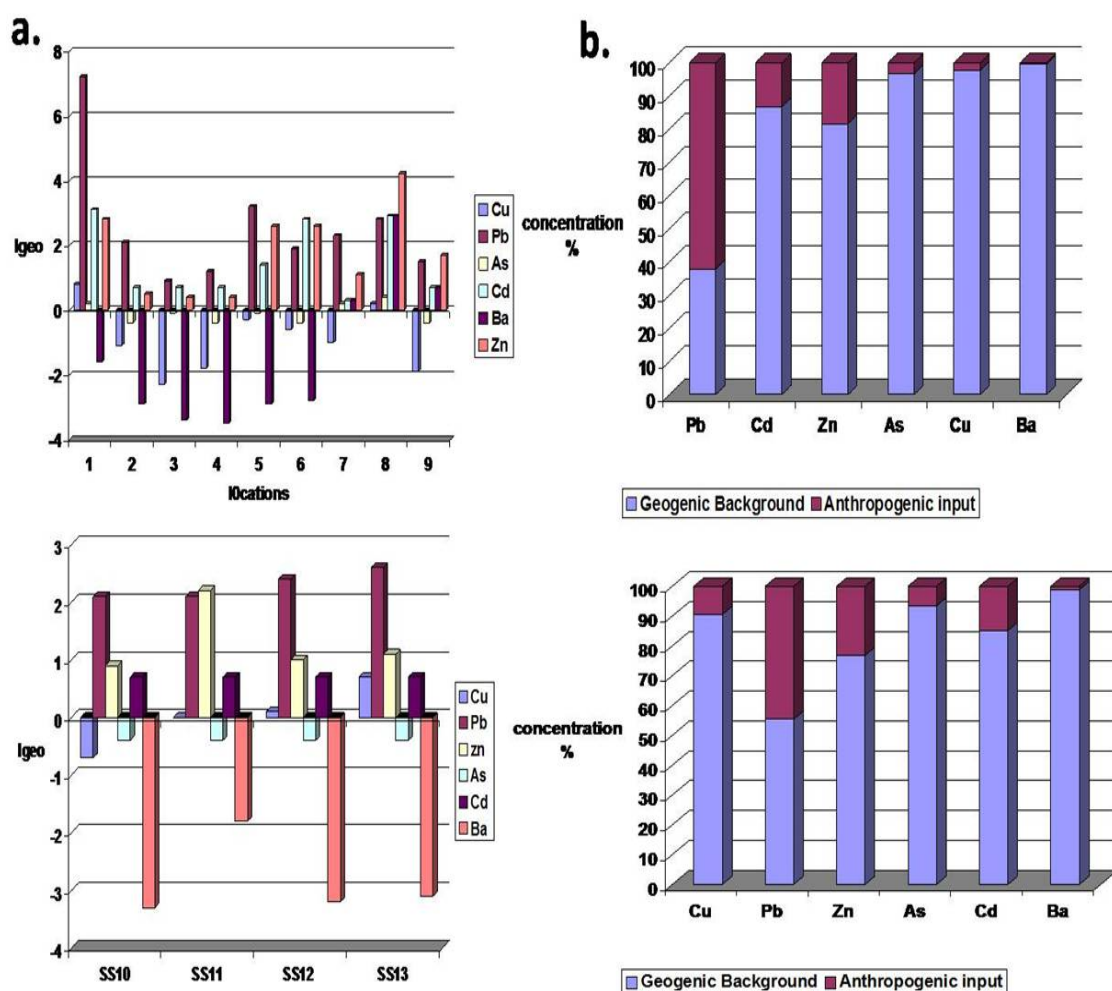


Fig 3: Bar chart concentration of Pb, Cu, Zn, As, Cd and Ba in the study area compared with crustal averages.

**Trace Elements:** mean concentrations for all the elements in both soil and stream sediment showed an increasing order of  $Zn > Pb > Cu > As > Cd$ . However, the concentration of trace elements in soil samples is quite higher compare to stream sediments. The highest concentrations were found in Elere River (LC13), Eyin Grammar (LC1) and Surulere (LC5) due to sewage sludge, steel and irons works and refuse incineration activities found within the area. The concentration of the metals when compared with their respective crustal average (Taylor, 1964) are higher than the recommended except for Ba (Table 4); since the samples taken are from areas that are densely populated, it, therefore, implies the metals are the product of human activities consequent upon supply from mini - industries such as soap making, plastic factory, battery making, steel and iron work industries. Fig.7. & 8 shows the comparison of the element with the crustal averages. There is strong and positive correlation (Table 5) among the metals Cu-Pb (0.6), Cu-Ba (0.6), As-Zn (0.7), Cd-As (0.6), Zn-Cd (0.7); these results thus buttress the anthropogenic and homogeneous nature of the source area. Fig.3 shows the comparison of each of the metals with the crustal average.



**Fig.4a:** Bar chart for the  $I_{geo}$  concentrations of trace elements for the samples. (b) Distribution of in-input sources of the trace elements in (a) Soil and (b) Stream sediments

### Data Evaluation

For the assessment and quantification of the level of contamination in the various media studied, some quantitative contamination indices were used to describe the concentration trends, it and also allows for ease comparison between the determined parameters. These indices used include;

- Anthropogenic Factor (A.F)
- index of geoaccumulation ( $I_{geo}$ ) and
- risk index. ( $K_o$ )

### Anthropogenic Factor (AF)

The anthropogenic factor for soil (Table 6) showed that Ba (0.2) has low contamination; Cu (1.0) and As (1.4) and Cd (5.7) moderately contamination and Zn (7.9) and Pb (26.7) are high contamination

**Table 1:** Descriptive statistics of major oxides for the soil and stream sediment

Element	N	Range%	Minimum	Maximum	Mean
Fe <sub>2</sub> O <sub>3</sub>	s	2.17-6.06	2.17	6.06	4.04
	ss	3.30-7.15	3.3	7.15	5.23
CaO	s	0.31-2.97	0.31	2.97	1.48
	ss	0.74-0.99	0.74	0.99	0.84
MgO	s	0.08-0.48	0.08	0.48	0.27
	ss	0.22-0.98	0.22	0.98	0.41
Na <sub>2</sub> O	s	0.01-0.07	0.01	0.07	0.03
	ss	0.01-0.03	0.01	0.03	0.02
K <sub>2</sub> O	s	0.10-0.41	0.1	0.41	0.22
	ss	0.17-0.36	0.17	0.36	0.22

ss- stream sediments, s- soil

**Table 2:** Correlation Coefficient of major oxides for the soil and stream sediment

	Na <sub>2</sub> O	K <sub>2</sub> O	Fe <sub>2</sub> O <sub>3</sub>	CaO	MgO	
Na <sub>2</sub> O	1					
K <sub>2</sub> O	.623*	1				
Fe <sub>2</sub> O <sub>3</sub>	.453	.454	1			
CaO	.521	.221	.159	1		
MgO	.479	.786**	.628*	.165	1	

level (2-tailed).

\* Correlation is significant at the 0.05 level (2-tailed).  
\*\* Correlation is significant at the 0.01 level (2-tailed).

**Table 3:** Factor Analysis of major oxides for the soil and stream sediment

	Component		
	1	2	3
Na <sub>2</sub> O	.810	.353	-
K <sub>2</sub> O	.860	-	-.411
Fe <sub>2</sub> O <sub>3</sub>	.730	-	.609
CaO	.464	.825	-
MgO	.854	-.356	-
Eigen vales	2.872	1.048	0.567
Percentage of variance	57.448	20.964	11.345
Cummulative percentage	57.448	78.412	89.757

**Table 4:** Descriptive statistics of trace elements of soils and sediments of the study area

NO	Description	Cu	Pb	Zn	As	Cd	Ba
S1	Eyin Grammar	137	2333	992	3	2.6	240
S2	Eyin Grammar	34.5	79	211	2	0.5	102
S3	Owode Academy	16	36	198	2.5	0.5	70
S4	Owode	21.5	41.5	197	2	0.5	67
S5	Surulere	57	170.5	906	2.5	0.8	101
S6	Laoye Muslim	45.5	74.5	912	2	2.1	107
S7	Kudeti	37	90.5	312	3	0.7	147
S8	Odinjo	83.5	127	2716	3.5	2.2	145
S9	Olorunsogo	20.5	53	493	2	0.5	72
	mean	50.28	333.89	770.78	2.50	1.16	116.78
	Stan dev	38.74	750.88	800.73	0.56	0.87	54.92
	Range	16-137	36-2333	197-2716	2-3.5	0.5-2.6	67-240
SS10	Ogunpa River	46	78	267	2	0.5	77
SS11	Ogunpa River	75	82	657	2	0.5	217
SS12	Elere River	77	99	285	2	0.5	81
SS13	Elere River	121	114	307	2	0.5	88
	mean	79.75	93.25	379.00	2.00	0.50	115.75
	starndev	30.93	16.56	186.05	0.00	0.00	67.65
	Range	46-121	78-114	267-657	02-Feb	0.5-0.5	77-217
	Crustal Average	50	12.5	97.9	1.8	0.2	500

**Table 5:** Correlation Coefficient of trace elements for the soil and stream sediment

	Cu	Pb	Zn	As	Cd	Ba
Cu	1					
Pb	<b>.643(*)</b>	1				
Zn	.355	.177	1			
As	.292	.401	<b>.707(**)</b>	1		
Cd	.497	<b>.645(*)</b>	<b>.724(**)</b>	<b>.612(*)</b>	1	
Ba	<b>.604(*)</b>	<b>.672(*)</b>	.388	.477	<b>.559(*)</b>	1

\* Correlation is significant at the 0.05 level (2-tailed).

\*\* Correlation is significant at the 0.01 level (2-tailed).

#### *Index of Geo-Accumulation for soil and stream sediment*

Geo-accumulation classification index ( $I_{geo}$ ) for soil (Table 7) revealed Ba (-2.7), Cu (-0.6) and As (-0.11) with  $I_{geo} < 0$  (practically uncontaminated), Cd (1.93) and Zn (2.4) (moderately contaminated), and Pb with the highest  $I_{geo}$  of 4.75 indicating high to very high contamination. The geo-accumulation classification index ( $I_{geo}$ ) for stream sediment revealed practically uncontaminated Ba (-2.7), As (-0.4), Cu (0.1) and Cd (0.7); and moderately contaminated Zn (1.4) and Pb (2.3) in all the elements (Fig. 6). Possible sources of Pb may include leaded gasoline, tyre wears and automobile emissions, batteries and municipal waste effluents/sewage sludge. Excessive concentration of the element in areas can cause lung cancer in human.

**Table 6:** Anthropogenic Factor of the trace elements in Soil and Stream sediments

Elements	Cu	Pb	As	Cd	Ba	Zn
S <sub>1</sub>	2.7	186.6	1.7	13	0.5	10.1
S <sub>2</sub>	0.7	6.3	1.1	2.5	0.2	2.2
S <sub>3</sub>	0.3	2.9	1.4	2.5	0.1	2.0
S <sub>4</sub>	0.4	3.3	1.1	2.5	0.1	2.0
S <sub>5</sub>	1.1	13.6	1.4	4.0	0.2	9.3
S <sub>6</sub>	0.9	6.0	1.1	10.3	0.2	9.3
S <sub>7</sub>	0.7	7.2	1.7	3.3	0.3	3.2
S <sub>8</sub>	1.7	10.2	1.9	1.1	0.3	27.7
S <sub>9</sub>	0.4	4.2	1.1	2.5	0.1	5.0
SS10	0.9	6.2	1.1	2.5	0.2	2.7
SS11	1.5	6.6	1.1	2.5	0.4	6.7
SS12	1.5	7.9	1.1	2.5	0.2	2.9
SS13	2.4	9.1	1.1	2.5	0.2	3.2

**Table 7:** Geo-accumulation index ( $I_{geo}$ ) of the trace elements in soil and stream sediment

Elements	Cu	Pb	As	Cd	Ba	Zn
S <sub>1</sub>	0.8	7.2	0.2	3.1	-1.6	2.8
S <sub>2</sub>	-1.1	2.1	-0.4	0.7	-2.9	0.5
S <sub>3</sub>	-2.3	0.9	-0.1	0.7	-3.4	0.4
S <sub>4</sub>	-1.8	1.2	-0.4	0.7	-3.5	0.4
S <sub>5</sub>	-0.3	3.2	-0.1	1.4	-2.9	2.6
S <sub>6</sub>	-0.6	1.9	-0.4	2.8	-2.8	2.6
S <sub>7</sub>	-1.0	2.3	0.2	0.3	0.3	1.1
S <sub>8</sub>	0.2	2.8	0.4	2.9	2.9	4.2
S <sub>9</sub>	-1.9	1.5	-0.4	0.7	0.7	1.7
SS10	-0.7	2.1	-0.4	0.7	-3.3	0.9
SS11	0	2.1	-0.4	0.7	-1.8	2.2
SS12	0.1	2.4	-0.4	0.7	-3.2	1.0
SS13	0.7	2.6	-0.4	0.7	-3.1	1.1

#### *Quantification of Degree of Pollution*

In table 8a&b, the degree of pollution of the soils revealed high anthropogenic contribution of Pb (62.2%), Zn, Cd, As, Cu and Ba with 18.4%, 13.3%, 3.3%, 2.3% and 0.47% respectively. The summation of the respective single metal contamination indices shows a contamination degree (Cdeg) of 42.9 similar contamination degree (Cdeg) of >32 (Hakanson, 1980) associated with high metal contamination within the study area. In stream

sediments high anthropogenic contribution of the elements include Pb, Zn, Cd, Cu, As, and Ba with 44.6%, 23.2%, 14.9%, 9.5%, 6.6% and 1.2% respectively (see fig.7). The respective single metal contamination indices revealed considerable degree of metal contamination in the study area (Hakanson, 1980). Therefore, the order of degree of anthropogenic factor contamination or enrichment in both soil and stream sediments is  $Pb > Zn > Cd > Cu > As > Ba$ .

**Table 8a:** Summary of quantitative indices with respect to metal contamination in soil samples

Trace elements	A.F		$I_{geo}$		Summary of overall contamination level
	RANGE	MEAN	RANGE	MEAN	
<b>Cu</b>	0.32-2.74	1.0	-2.3-0.8	-0.6	<i>Very low/No contamination</i>
<b>Ba</b>	0.13-0.48	0.2	-3.4 to -1.6	0.16	<i>Very low/no contamination</i>
<b>As</b>	1.1-1.9	1.4	-0.4-0.4	-0.11	<i>Very low/no contamination</i>
<b>Cd</b>	2.5-13	5.7	0.7-3.1	1.93	<i>Moderate to high contamination</i>
<b>Zn</b>	2.02-10.13	7.9	0.4-4.2	2.40	<i>Moderate to heavily contamination</i>
<b>Pb</b>	2.88-186.6	26.7	0.9- 7.2	4.75	<i>Heavily contaminated</i>

*A.F=Anthropogenic Factor*

*I<sub>geo</sub>=Index of geoaccumulation*

**Table 8b:** Summary of quantitative indices with respect to metal contamination in stream sediments

Trace elements	A.F		$I_{geo}$		Summary of overall contamination level
	RANGE	MEAN	RANGE	MEAN	
<b>Cu</b>	0.92-2.42	1.60	-0.71-0.69	0.1	<i>Very low/no contamination</i>
<b>Ba</b>	0.15-0.4	0.23	-3.3 -1.8	-2.71	<i>No contamination</i>
<b>As</b>	1.1-1.1	1.0	-0.4 --0.4	-0.4	<i>No contamination</i>
<b>Cd</b>	2.5-2.5	2.5	0.7-0.7	0.74	<i>Very low contamination</i>
<b>Zn</b>	2.73-6.71	3.9	0.9-2.17	1.4	<i>Moderate contamination</i>
<b>Pb</b>	0.24-9.12	7.5	2.1- 2.61	2.3	<i>Moderate to high Contamination</i>

*A.F=Anthropogenic Factor*

*I<sub>geo</sub>=Index of geoaccumulation*

### Risk Index

The risk index of soil is shown in table 9; Ba, As and Cu are within the permissible index of  $K_o < 1$ , Cu is medium dangerous with  $K_o$  of 1-3, Cd and Zn are dangerous and Pb is extremely dangerous with  $K_o > 10$ . Similarly, Zn (3.9) and Pb (7.5) dangerous in stream sediment though with values are lower than the soil.

Quantitative indices with respect to metal contamination in soil and sediment phase (Table 9& 10) revealed the trend of anthropogenic contamination to be consistent with the estimated index of geo-accumulation values and anthropogenic factor, though higher in soils than sediment samples. Environmental contamination arose from urban degradation triggered by improper land-use plans, poor sanitary and waste/sewage disposal facilities, and inadequate public awareness of environmental health issues. This had resulted into systematic degradation of the environment in Ibadan metropolis. Notable aspect of this degradation that is of serious health concern is the contamination of ground water and drainage by the heavy metals.

**Table 9:** Risk index ( $K_o$ ) for trace elements in soil and stream sediment.

Elements	Cu	Pb	As	Cd	Ba	Zn
S <sub>1</sub>	2.8	186.6	1.7	13	0.5	10.1
S <sub>2</sub>	0.7	6.3	1.1	2.5	0.2	2.2
S <sub>3</sub>	0.3	2.9	1.4	2.5	0.1	2.0
S <sub>4</sub>	0.4	3.3	1.1	2.5	0.1	2.0
S <sub>5</sub>	1.1	13.6	1.4	4.0	0.2	9.3
S <sub>6</sub>	0.9	6.0	1.1	10.3	0.2	9.3
S <sub>7</sub>	0.7	7.2	1.7	3.3	0.3	3.2
S <sub>8</sub>	1.7	10.2	1.9	1.1	0.3	27.7
S <sub>9</sub>	0.4	4.2	1.1	2.5	0.1	5.0
SS <sub>10</sub>	0.9	6.2	1.1	2.5	0.2	2.7
SS <sub>11</sub>	1.5	6.6	1.1	2.5	0.4	6.7
SS <sub>12</sub>	1.5	7.9	1.1	2.5	0.2	2.9
SS <sub>13</sub>	2.4	9.1	1.1	2.5	0.2	3.2

## Conclusion

The result showed effect of urbanization coupled with poor sanitization that occurs in many cities in the study area. The dominance of Fe<sub>2</sub>O<sub>3</sub> in the sediments when compared with the soil confirmed poor sanitary and waste/sewage disposal facilities in the study area where the stream channel is used majorly as the waste disposal tank, high pollution of Pb, Zn, Cd found in the study area could also be attributed to anthropogenic impacts that could be from vehicular emission, related repair products, domestic sewages, market and industrial effluents.

## References

- Ajayi, S.O., & Mombeshora, C. (1990). Sedimentary trace metals in Lakes in Ibadan, Nigeria, *Science Total Environmental*, 87/88, 1-18.
- Aweto, A.O. (1994). Soils of Ibadan region. In: Filani, M.O., Ikporukpo, & F.O., Areola, C.O. (Eds.). *Ibadan Region. Rex Charles Publ.* (pp. 45-57.)
- Cobelo-Garcia, A., Prego, R., & Labandiera, A (2003). *Water Research*, 38, 1753.
- Fangueiro, D., Bermond, A., Santos-Carapura, H., & Duarte, A (2002). *Anal. Chim. Acta*, 459:245.
- Fergusson, J.E. (1990). *The heavy Element Chemistry*. Environment.
- Hakanson, L.(1980). "An ecological risk index for aquatic pollution control—A sedimentological approach, "Water Res, 14, 975-1001.



- La Pointe, P.R., & J. Hudson, (1985). Characterization and interpretation of Rock Joint Patterns. GSA Special Paper 199. GSA, Denver.
- Mitchell, R. L.(1974). Trace element problems in Scottish soils. *Neth. J. Agr. Sci.* 22, 295-304.
- Olade, M.A. (1987). Heavy metal pollution and the need for monitoring; illustrated for developing countries in West Africa. In: T. Hutchinson and K. Meema (eds). Lead, Mercury, Cadmium and Arsenic in the environment, SCOPE, John Wiley and Sons. 335-341.
- Paul, P.C.& Piilai, K.C. (1983). Trace metals in a tropical river environment distribution water, Air, soil pollution, 19, 63-73.
- Price, J. R., & Velbel., M. A., (2003). Chemical weathering indices applied to weathering profiles developed on heterogeneous felsic metamorphic parent rock. *Chemical Geo.* 202, 397-486.
- Sandroni, V., & Smith, C.M. (2002). *Anal. Chim. Acta.* 468:335.
- Sharma, A. & Rajamani, V., (2003). Weathering of gneissic rocks in the upper reaches of Cauvery River, South Indian; implications to neotectonics of the region. *Chem. Geol.* 166, 203-223.
- Taylor, S.R. (1964). Abundance of chemical elements in the continental crust: anew table. *Geochim Cosmo him Acta*; 28, 1273-1285.
- Tijani, M.N., Jinno, K., & Hiroshiro, Y. (2004). Environmental impacts of Heavy metal distribution in water and stream sediments of Ogunpa River Ibadan, SW Nigeria. *J. Min. Geol.* 40 (1), 73-83.
- Tijani, M.N., Olatunji, A. S., Sangolade, O. O., & Chukwurah, B. N., (2005). Hydrochemical evaluation of sea water influence on on water quality in metropolitan Lagos, Nigeria. *African Geoscience Review*, 12(3), 225-240.
- Tiller, K.G.(1989). Heavy metals in soils and their environmental; significance. In; Stewart, B.A. (Ed.), *Advances in soils Sciences*, 9,113-142.
- Zhang, N. P., Deng, W., & Yang, X. M., (2002). The background concentrations of 13 soil-trace elements and their relationship to parent materials and vegetations in Xiang (Tiber) China. *J Asian Earth Sci.* 21,167-174.

# Global Stability and Settlement of Segmental Retaining Walls Reinforced with Geogrid

Anuar Kasa, Zamri Chik, Mohd Raihan Taha

<sup>1</sup>Department of Civil & Structural Engineering, Faculty of Engineering & Built Environment, The National University of Malaysia, 43600 Bangi, Selangor, Malaysia  
anuar@eng.ukm.my

**Abstract:** Most of segmental retaining wall design procedures such as NCMA, BS8006, AASHTO and NCHRP do not take into account global stability and foundation settlement in their design calculation. A system to solve the problem and to predict the stability of the wall quickly and accurately by using simple input was planned to be developed. This study used a residual soil that was classified as SC-SM according to the Unified Soil Classification System (USCS). Geogrid used in this study had a characteristic strength of 40 kN/m while concrete blocks had a minimum strength of 35 MPa. Simulations were performed using two-dimensional FEM to calculate maximum deflection, maximum foundation settlement and maximum surface settlement. In addition, global stability was calculated by using phi/chi reduction method for each design. Prediction was done by using Response Surface Methodology. Mathematical models used for the RSM were MLR (Multiple Linear Regression), Pure Quadratic, Interactions and Full Quadratic. Among all the mathematical models in RSM, output of Full Quadratic was the closest to the target value.

**Key words:** Prediction, Segmental retaining wall, Geogrid, FEM, RSM

## Introduction

In Malaysia, the first reinforced retaining structure was built in 1982 and since then has expanded its use (Chiu 1987). Geogrid reinforced segmental retaining walls are used extensively throughout the world because of its low cost, simple construction and its ability to accommodate the deformation (Yoo and Kim 2008; Zhang et al. 2008). However, studies of this type of walls, especially on the mode of failure and the bonding mechanism of reinforcement are still at the level of exploration (Skinner and Rowe 2005; Al and Muhunthan 2006).

Reinforced retaining walls offer competitive solutions to the problems associated with lack of space caused by the phenomenal growth in the infrastructure at present. Research on the retaining wall is reported in many papers since its introduction e.g. Edgar et al. (1989), Faisal (1993), Wong et al. (1994), Ho and Rowe (1996), Kasa (1997), Bathurst et al. (2005) and Skinner and Rowe (2005). In the design of reinforced concrete, bond between the bar and the concrete provides sufficient tensile stress to the concrete. While the principles of reinforced soil, the tensile stress is caused by friction between the soil and buried layers of reinforcement (Ingold 1982).

Normally, backfill material used in the construction of the wall is granular soil such as river sand and mining sand. However, the price of sand is high at present. Another alternative is to use quarry dust or residual soil. Economically, residual soil has many advantages because it is easy to find in Malaysia at relatively low cost. By using residual soil, contractors can reduce construction costs and overall time since no transportation of backfill is needed (Kasa 1998).

Reinforced retaining walls can be constructed using various types of reinforcement and wall systems. Reinforcement may consist of metal strips or polymer products such as geotextiles, geogrid and geomembrane. Wall system may consist of a wall wrap (wrap facing), fully rigid wall, segmented block and modular block (Holtz 2001). Most widely used reinforcement in Malaysia is steel strip. Although it is well-received, there is still uncertainty about its durability, especially under wet soil conditions such as residual soil. A practical reinforcement for the work under the residual soil is geogrid which is durable and suitable for the environment. In addition, the geogrid is easier to handle, carry and install than steel strip (Kasa 1998).

The main objective of this study is (i) to predict the stability of geogrid reinforced segmental retaining wall in terms of global factor of safety, surface and foundation settlement and wall deflection, (ii) to compare the accuracy of statistical methods of MLR (Multiple Linear Regression), Pure Quadratic, Interactions and Full Quadratic to predict the stability of the wall, (iii) to observe the actual performance of segmental retaining walls by comparing results of field monitoring with the

results of FEM calculations, and (iv) to produce a computer system that can predict the stability of walls quickly and accurately by using simple input such as slope angle, surcharge and height of wall.

Among the motivations for this study has to do with the problems faced by some local engineers who refused to recommend the construction of segmental retaining walls as an alternative to customers on the grounds that the design calculations received from the supplier do not take into account the global stability and foundation settlement. This is clearly stated in the design calculations. In other words, the supplier shall not be liable for if the occurrence of failure caused by the global stability or foundation settlement.

## Methodology

Backfill material used in this study was classified as SC-SM (a mixture of sand and clay and inorganic clay) according to USCS (Unified Soil Classification System). Plasticity index value of this soil was between four and seven ( $4 \leq PI \leq 7$ ). According to the Design Manual Naval Facilities Engineering Command, 7.01 version published in September 1986, a typical value for the wet unit weight was  $20.4 \text{ kN/m}^3$  and internal friction angle 33 degrees. These values were used in all the segmental retaining wall designs. The geogrid had characteristic tensile strength of  $40 \text{ kN/m}$  and long-term design strength of  $21 \text{ kN/m}$ . The concrete block had a dimension of  $305 \text{ mm} \times 200 \text{ mm} \times 150 \text{ mm}$  with minimum strength about  $35 \text{ MPa}$ .

For predictions, RSM (Response Surface Methodology) was used. Four mathematical models of MLR, Pure Quadratic, Interactions and Full Quadratic were used to predict the stability of the wall. RSM was a technique used to model and analyze problems in which a response was influenced by several independent variables and the main objective was to optimize the response (Montgomery 2005). RSM was useful to develop, improve and optimize the response or responses. Most of the problems in the RSM, the response function,  $f$  was not known. The first order model was known as linear regression model. When there were more than two independent variables such as  $x_1$ ,  $x_2$  and  $x_3$ , the model was called MLR. In general, the equation was as follows

### Multiple Linear Regression

$$y_i = \beta_0 + \beta_1 x_1 + \beta_2 x_2 + \beta_3 x_3 + \varepsilon \quad (2.1)$$

The second order model was used when there was a curve in the first order model. The second order model was more flexible and had several functions such as Pure Quadratic, Interactions and Full Quadratic. The general equations were as follows

### Pure Quadratic

$$y_i = \beta_0 + \beta_1 x_1 + \beta_2 x_2 + \beta_3 x_3 + \beta_4 x_1^2 + \beta_5 x_2^2 + \beta_6 x_3^2 + \varepsilon \quad (2.2)$$

### Interactions

$$y_i = \beta_0 + \beta_1 x_1 + \beta_2 x_2 + \beta_3 x_3 + \beta_4 x_1 x_2 + \beta_5 x_1 x_3 + \beta_6 x_2 x_3 + \varepsilon \quad (2.3)$$

### Full Quadratic

$$y_i = \beta_0 + \beta_1 x_1 + \beta_2 x_2 + \beta_3 x_3 + \beta_4 x_1 x_2 + \beta_5 x_1 x_3 + \beta_6 x_2 x_3 + \beta_7 x_1^2 + \beta_8 x_2^2 + \beta_9 x_3^2 + \varepsilon \quad (2.4)$$

where  $y_i$  was the predicted value,  $x_1$  was slope angle (degree),  $x_2$  was surcharge ( $\text{kN/m}^2$ ),  $x_3$  was height of slope (m) and  $\varepsilon$  was error.  $y_i$  and  $x_1$ ,  $x_2$ ,  $x_3$  were input values while  $\beta_0$  until  $\beta_9$  were output values obtained from analysis using the equations.

For the purpose of obtaining data, analysis of deflection, surface and foundation settlement and global FOS (factor of safety) were performed by using Plaxis ver. 8 while MATLAB ver. 2009 was used to make the statistical analysis. All software was working under Microsoft Windows XP system with Intel® Core™ 2 Duo, 2.80 GHz and 1.99 GB of RAM. FEM simulation of the retaining walls was carried out by using two dimensional analysis. A triangular-shaped element with 15 nodes was used since the weakness of using the element of six nodes was over prediction of bearing capacity and some calculations using phi/chi reduction method (Plaxis 2008).

Model of the retaining wall is shown in Figure 2.1. The height of wall was 5.5 m, the length of geogrid was 3.5 m and the depth of soil below foundation level was 6.0 m. Dimension of modular block was 30 cm long, 15 cm high and 20 cm wide. The width of drainage using granular materials was 30 cm. Interface elements were used to model the interaction between the geogrid and soil.

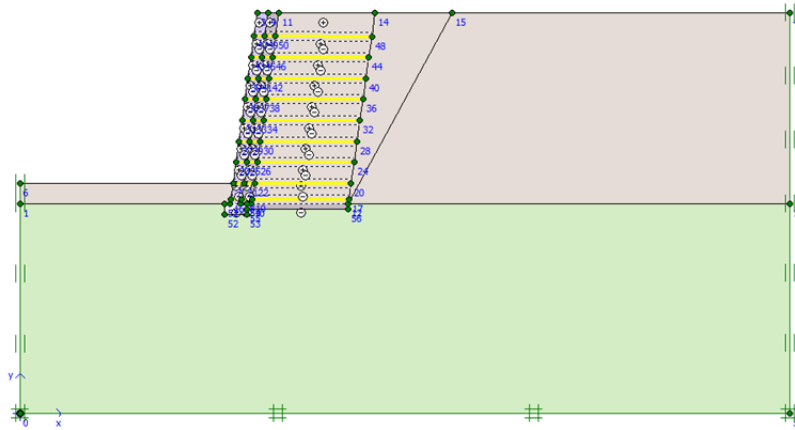


**Figure 2.1** Geometry of retaining wall used in FE analysis

The input values for FEM simulation such as unit weight, cohesion and friction angle of the foundation, concrete blocks, drainage and residual soil were similar to the input values used in the NCMA design while other input values such as Young's modulus, Poisson's ratio and hydraulic conductivity which were not considered in the NCMA design were obtained from literature. To avoid any failure on the concrete blocks and drainage, a high value of strength ( $c = 200 \text{ kN/m}^2$ ) was used. High value of elasticity ( $EA = 1,200 \text{ kN/m}$ ) was also used for geogrid since the strength of geogrid did not affect the failure because soil would fail sooner in the event of excessive strain (Guler and Hamderi 2002). The output obtained from FEM analysis used for prediction using RSM was the value of (i) max. deflection, (ii) max. foundation settlement, (iii) max. surface settlement and (iv) global FOS.

To observe the actual performance of the wall and accuracy of FEM calculations, a full-scale wall was built. This five-meter high wall was installed with various instruments such as strain gauges, horizontal and vertical pressure cells, inclinometer, stand pipe and pneumatic piezometer and surface settlement markers at specified location as shown in Figure 2.2.

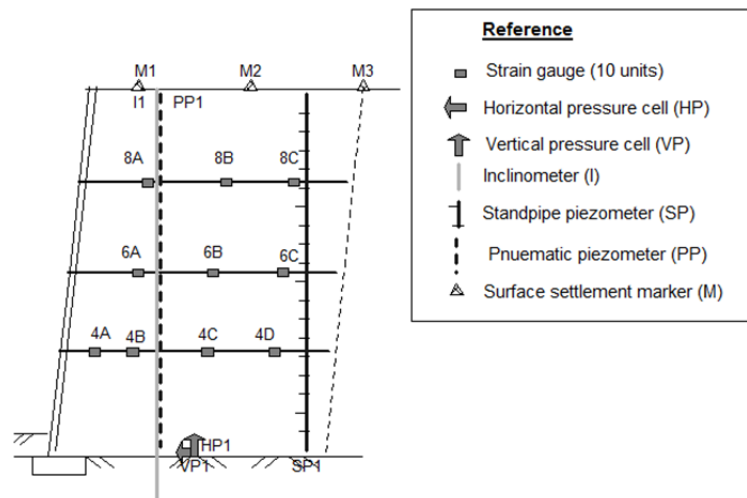


**Figure 2.2** Location of various type of instrument

The purpose of strain gauges installed on the geogrid was to determine the tensile force distribution along the geogrid layers. Strain gauge type 5 YFLA applied in this study uses the principle of electrical resistance of a conductor. The conductivity changes when the material was strained. So, strain and tension can be calculated from the change in electrical resistance. Strain changes were measured by using a digital strain meter, TC-1K model.

Horizontal deflection of the whole wall was measured by using inclinometer. An inclinometer casing was installed behind the wall and readings were taken at every 0.5 m depth by means of inserting a sensor into the casing. Vertical and horizontal earth pressures including effective stress and pore water pressure were measured by using a pair of total pressure cell. Effectiveness of drainage system and water pressure in soil was measured by using a pneumatic piezometer installed at the base of the wall. In addition, a standpipe piezometer was used to measure water level by inserting a sensor up to the water level. To measure settlement, three surface settlement markers were installed after end of construction.

## Results and Discussion

Actual performance of the segmental retaining walls could be observed by comparing the results of field monitoring with the results of FEM calculation. According to the original design, this wall was with a surcharge of  $5.0 \text{ kN/m}^2$ , but during the monitoring, no load was applied in the field. FEM calculation results discussed here was based on the original design as the effect of the surcharge on the results of FEM calculations was too small. For example, the max. deflection of the wall without surcharge and with surcharge was 12.67 mm and 12.77 mm respectively, as well as the value of the max. foundation settlement, 15.86 mm and 15.87 mm respectively. Based on FEM calculations for the instrumented wall, it was found that the max. deformation was 27.82 mm. The max. effective stress was  $167.48 \text{ kN/m}^2$  and based on the analysis of phi/chi reduction method, the global FOS was 2.29.

Changes in the measurement of inclinometer over 203 days showed that the max. deflection of the wall was 13.0 mm at the height of 4.0 m from the base of the wall (See Figure 3.1). FEM results showed clear similarities with the value of 12.77 mm, a difference of only 0.33 mm. Location of the max. deflection was also similar, i.e. 4.0 m high. However, there were significant differences in shape of the distribution because the value of the measured deflection at the base of the wall was only 1.0 mm. This happened because the base of inclinometer casing was fixed to the concrete mix. In FEM simulation, there was no fixity considered. Based on the results, it could be concluded that the FEM simulation of the retaining wall could estimate the value of max. deflection accurately.

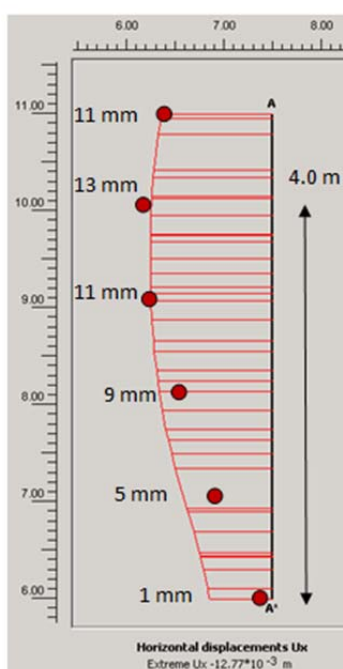


**Figure 3.1** Horizontal deflection of the wall

The value of the max. surface settlement measured in the field was 17 mm. This value was different from the values obtained by FEM (24.55 mm) with a difference of 7.5 mm. In engineering practice, this difference could be considered small for a five meter high wall because the wall of this type could accommodate large deformation (BS8006 1995). Besides, if we looked at the distribution of the surface settlement, the location of the max. settlement for both cases was similar, i.e. at the center of the reinforced zone. No measurements were taken for foundation settlement in the field for comparison. The max. value calculated by FEM was 15.87 mm. The distribution of foundation settlement was shown in Figure 3.3.

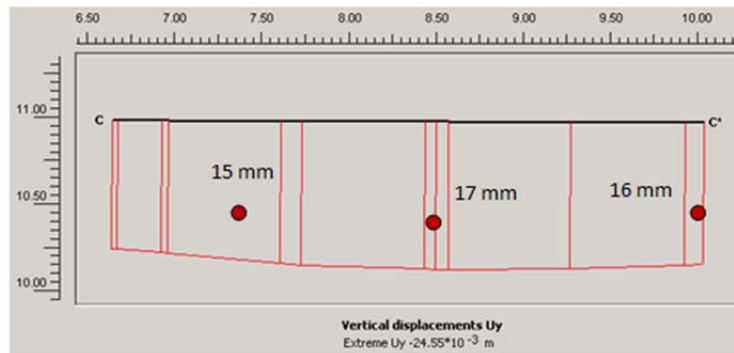


**Figure 3.2** Surface settlement of the wall

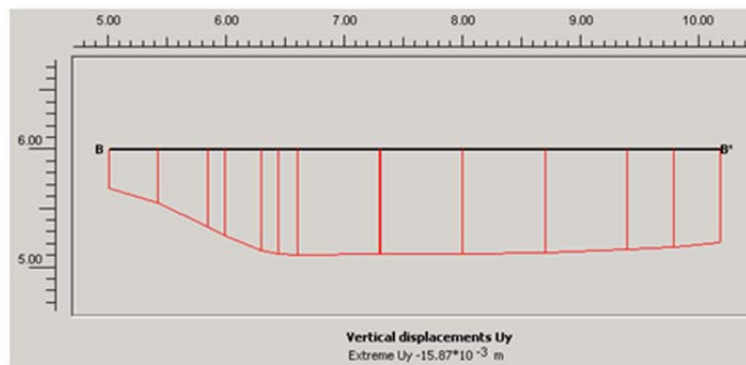


**Figure 3.3** Foundation settlement of the wall

Value of RMSE (Root Mean Square Error) based on 232 data for each mathematical model was shown in Figure 3.4 while value of  $R^2$  was shown in Figure 3.5. From Figure 3.4, it was obvious that Full Quadratic was the best model for RSM since the value of RMSE for each output parameter, i.e. global FOS, surface settlement, foundation settlement, location of max. deflection and deflection was the lowest or closest to zero. Similarly, from Figure 3.5, it was obvious that Full Quadratic was the best model because the value of  $R^2$  for each output parameter was the highest or closest to one. Thus, equation of Full Quadratic was selected to be used in developing a computer system to predict the stability of the segmental retaining wall.

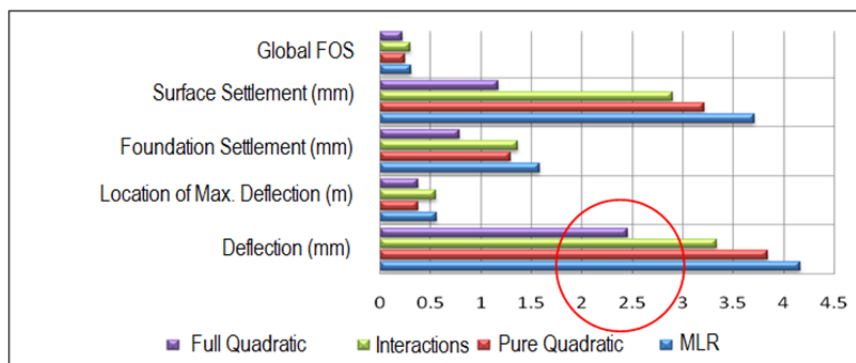


**Figure 3.4** Value of RMSE for each mathematical model

## Conclusion

In conclusion, this study has successfully predicted the stability of geogrid reinforced segmental retaining wall in terms of global FOS, surface and foundation settlement and wall deflection, compared the accuracy of statistical methods of MLR, Quadratic Pure, Interaction and Quadratic Full, observed the actual performance of the retaining wall by comparing the results of field monitoring with the results of FEM calculations and produced a system that can predict the stability of walls quickly and accurately. Since Full Quadratic is the best mathematical model to predict global FOS, surface settlement, foundation settlement, location of max. deflection and deflection, it has been used to develop a computer system.



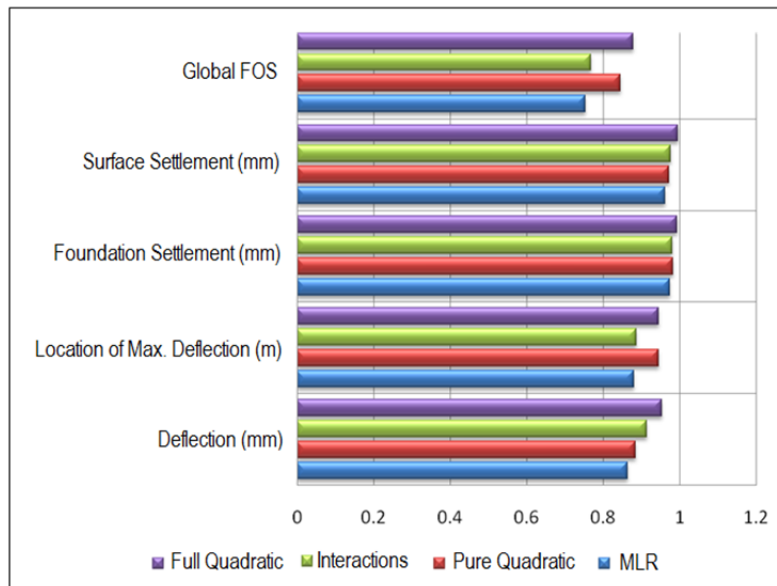


**Figure 3.5** Value of  $R^2$  for each mathematical model

## Acknowledgement

The authors would like to thank the National University of Malaysia and Ministry of Higher Education, Malaysia for their financial support through research grant UKM-OUP-NBT-28-130/2011 and ERGS/1/2011/TK/UKM/02/19.

## References

- Chiu, H.K. (1987). Reinforced Earth Wall in Malaysia, *9th Southeast Asian Geotechnical Conference*, Bangkok, pp 8/121 - 8/138.
- Yoo, C. & Kim, S.B. (2008). Performance of a two-tier geosynthetic reinforced segmental retaining wall under a surcharge load: full-scale load test and 3D finite element analysis. *Geotextiles and Geomembranes* 26 (6): 460–472.
- Zhang, M.X., Zhou, H., Javadi, A.A. & Wang, Z.W. (2008). Experimental and theoretical investigation of strength of soil reinforced with multi-layer horizontal-vertical orthogonal elements. *Geotextiles and Geomembranes* 26 (1): 1–13.
- Skinner, G.D. & Rowe, R.K., (2005). Design and behaviour of a geosynthetic reinforced retaining wall and bridge abutment on a yielding foundation. *Geotextiles and Geomembranes* 23 (3): 234–260.
- Al, H.O. & Muhunthan, B. (2006). Numerical procedures for deformation calculations in the reinforced soil walls. *Geotextiles and Geomembranes* 24 (1): 52–57.
- Edgar, T.V., Puckett, J.A. & D'Spain, R.B. (1989). Effects of geotextiles on lateral pressure and deformation in highway embankments. *Geotextiles and Geomembranes* 8: 275–292.
- Faisal, H.A. 1993. Field Behaviour of a Geogrid-Reinforced Slope. *Journal of Geotextiles and Geomembranes*. 12: 53-72.
- Wong, K.S., Broms, B.B. & Chandrasekaran, B. (1994). Failure modes at model tests of a geotextile reinforced wall. *Geotextiles and Geomembranes* 13 (6–7), 475–493.
- Ho, S.K. & Rowe, R.K. (1996). Effect of wall geometry on the behavior of reinforced soil walls. *Geotextiles and Geomembranes* 14 (10): 521–541.
- Kasa, A. & Ali, F. (1997). Reinforced Modular Block Wall with Residual Soil as Backfill Material. *Geotropika '97*, Johor Bahru, Malaysia, pp 425 - 431.
- Bathurst, R.J., Allen, T.M. & Walters, D.L. (2005). Reinforcement loads in geosynthetic walls and the case for a new working stress design method. *Geotextiles and Geomembranes* 23 (4): 287–322.
- Ingold, T.S. (1982). *Reinforced earth*. London: Thomas Telford Ltd.
- Kasa, A. (1998). Field behaviour of a reinforced modular block wall with a residual soil as backfill. Msc. Thesis. University of Malaya, Kuala Lumpur.
- Holtz, R.D. (2001). Geosynthetics for soil reinforcement. Ninth Spencer J. Buchanan Lecture, College Station, TX, 9 November, p. 20.
- Montgomery, D.C. (2005). *Design and Analysis of Experiments: Response surface method and designs*. New Jersey: John Wiley and Sons, Inc.
- Plaxis, (2008). *Reference Manual*. Delft, The Netherlands.
- Guler, E & Hamderi, M. (2002). FEM analysis of reinforced segmental retaining walls with cohesive and granular backfills. *Geosynthetics*, 103-106
- BS8006 (1995). *Code of Practice for Strengthened/Reinforced Soils and Other Fills*, British Standards Institution, London.



# Influence of Process Conditions on Glycerol Esterification Catalyzed by Tetra-N-Butylammonium-Modified Montmorillonite Catalyst

Iman Hashemizadeh, Ahmad Zuhairi Abdullah

School of Chemical Engineering, University Sains Malaysia, Engineering Campus, 14300 Nibong Tebal, Penang, Malaysia.

chzuhairi@eng.usm.my

**Abstract** - Selective synthesis of glycerol monolaurate from glycerol and lauric acid was investigated. Loading of tetra-n-butylammonium modified montmorillonite catalyst (1-5 wt. %), reaction temperature (110-140 °C) and glycerol to lauric acid ratio (4:1 to 8:1) were used as variables and the performance was based on lauric acid conversion and glycerol monolaurate yield. Geometrical constraint in the pores retarded the formation of higher glycerides. Increasing catalyst loading improved the monolaurate yield. Fast reaction occurred within the first 8 h and 3 wt. % was deemed the optimum catalyst loading. No further benefit was achieved above 130 °C and 6:1 for the reactant ratio. Impressive lauric acid conversion of about 80 % with corresponding glycerol monolaurate yield of 70 % were achieved in 8 h at 130 °C, using a reactant ratio 6:1 and 3 wt. % of catalyst. The modified montmorillonite was therefore active and highly selective for the production of monolaurate.

**Key words:** Esterification ; Monolaurate, montmorillonite, tetra-n-butylammonium; selectivity.

## Introduction

The development and commercial use of biodiesel has been rapidly expanding over the last 10 years. In biodiesel production process, glycerol is produced at a rate of about 10 wt. % of total biodiesel produced and presently, its production creates a glut in the market (Bossaert et al., 1996). It plays a very important role as a major by-product toward the price trend of biodiesel (Abdullah et al., 2007). Several factors including its low price, availability and functionality make glycerol very attractive for many industrial processes. Glycerol is expected to become a major chemical platform for future biorefineries since it has emerged as an important organic building block (Hermida et al., 2011). As such, research attempts for the conversion of glycerol into value-added substances seem to worthwhile efforts.

Monoglycerides or more correctly known as monoacylglycerols, are glycerides consisting of one fatty acid chain covalently bonded to a glycerol molecule through an ester linkage. Monoglycerides consist of a hydrophilic head and a hydrophobic tail, which give them detergency characteristics. Therefore, monoglycerides and their derivatives have a wide application as emulsifiers in food, pharmaceutical and cosmetic industries (McClements, 2005 ; Bossaert et al., 1996). The global production of emulsifier is estimated at approximately 200,000-250,000 metric tons per year (Moonen and Bas, 2004) and expected to further increase in the future. These substances have various applications in different fields such as in cosmetics, pharmaceutical formulations, drug delivery systems, oil well drilling, textile, packaging, plastic processing and construction materials (Hermida et al., 2011). The conversion of glycerol to monoglycerides could provide interesting solution to improve the overall economy of biodiesel industry worldwide.

There are two major industrial routes to produce monoglycerides. They are usually manufactured through glycerolysis, a base-catalyzed transesterification of triglycerides with glycerol at elevated temperature. Secondly, monoglycerides may be produced through a direct, single esterification of glycerol with fatty acids catalyzed by acids (Wilson et al., 2000). As the three hydroxyl groups in glycerol do not strongly differ in reactivity, the current industrial processes for mono ester production both lead to mixtures of mono- (40-60 %), di- (35-45 %), and even triglycerides (Gupta, 1996). Techniques for purification of monoglycerides are expensive and involve the use of high temperature leading to the development of unwanted flavors and side products. Therefore, it is highly desirable to improve the monoester yield by choosing favorable reaction conditions and designing an appropriate selective solid catalyst.

Solid catalysts are reported to be sufficiently active catalysts for esterification of fatty acid with glycerol (Bossaert et al., 1999 ; Hermida et al., 2011). However, active catalysts could also promote the formation of di- and triglycerides to result in poor selectivity to monoglyceride. As such, solutions to selective monoglyceride production could stem from unique pore characteristics of the catalyst to consequently allow shape selective catalysis. Recently, there has been considerable interest to use clays to catalyze organic reactions (Bokade and Yadav, 2009). Montmorillonite, a natural smectite, has been found to be a useful catalyst in a variety of organic reactions due to its strong acidity, inexpensive compared to ion exchange resin, noncorrosive, reusability and non-polluting (Bahulayan et al., 2003 ; Abdullah et al., 2011). Reactions catalyzed by montmorillonite clays are usually carried out at relatively mild conditions with high yield and selectivity towards the desired products (Abdullah et al., 2011).

The use of montmorillonite in conjunction with phase transfer catalyst (PTC) provides potential synergical effects of their properties and catalytic activity. When mixed with organic molecules, this clay mineral presents a proton rich environment to theoretically affect the reaction. On the other hand, the catalytic abilities can also be improved by incorporating the organic cations in the interlamellar space which enables better accessibility of reactants. This study addresses the behavioral study of tetra-n-butyl ammonium montmorillonite in catalyzing selective synthesis of glycerol monolaurate from glycerol and lauric acid.

## Materials and Methods

### Materials

Na-montmorillonite (Na-MMT) clay with a cation exchange capacity (CEC) of 119 meq/100 g was supplied by Kunimine Industry Co., Japan. The surfactant used in this study was tetra-n-butylammonium bromide (TBAB,  $C_{16}H_{36}BrN$ , FW: 322.368) from Sigma Aldrich. Lauric acid (Fisher) and glycerol (Fisher) with a purity of 99% were used without further purification.

### Catalyst Preparation and Characterization

A method as reported by He et al. (2009) and Wibowo et al. (2009) was used to prepare the modified clay catalyst. A stoichiometric amount of TBAB was first dispersed in 400 mL of distilled water at 80 °C under stirring at about 600 rpm. Then, 5.0 g of Na-MMT which was pre-dried at 105 °C for 1 h was added slowly and the stirring was continued for another 3 h. The organoclay product was then thoroughly washed until it was completely free of bromide anions as determined by the use of  $AgNO_3$ . It was then dried at room temperature, ground in an agate mortar, screened with a 200-mesh sieve and stored in a dry cabinet before use. The parent (NaMMT) and the modified montmorillonite catalyst (TBMMT) were characterized using XRD and surface analysis methods by means of a Siemens 2000X system and Micromeritics ASAP 2020 systems, respectively.

### Esterification of Glycerol with Fatty Acid

The esterification of glycerol with lauric acid was performed in a 250 mL stirred flask heated in an oil bath under atmospheric pressure. Variable amounts of catalyst between 1 wt. % to 5 wt. %, previously dried at 100 °C overnight were used in a reaction temperature range of between 110 °C and 140 °C for up to 12 h. The lauric acid to glycerol molar ratio was varied between 4:1 and 8:1. For product analysis, samples from the reaction vessel were withdrawn at various intervals to be analyzed for their composition. For the analysis of the product mixture, 100  $\mu$ L of the sample withdrawn from reaction vessel was first added into 100  $\mu$ L of water and 100  $\mu$ L of methyl acetate. The solution was then vortexed and the organic phase containing acylglycerols and fatty acid was separated by means of centrifugation. The composition was then analyzed using a Hewlett Packard HP 5800 gas chromatograph equipped with an FID.

## Results and discussion

### Characteristics of the Catalyst

The calculated basal spacing from the Bragg equation and the results of surface analysis on the catalysts are shown in Table 1. The basal spacing was found to increase from 1.1 to 1.7 nm when the TBAB was intercalated into the parent montmorillonite. The basal spacing of montmorillonite could reach about 2.0 nm was reported when a larger molecule octadecyltrimethylammonium bromide ( $C_{21}H_{46}NBr$ ) was exchanged into montmorillonite (Xi et al., 2004). As such, changes in the basal spacing could be influenced by the size of intercalated molecules in the clay inter layers.

Table 1. Basal spacing and surface characteristics of NaMMT and TBMMT.

Sample	Basal spacing (nm)	$S_{BET}$ ( $m^2/g$ )	$d_{pore}$ (nm)	$V_{pore}$ ( $cm^3/g$ )
NaMMT	1.1	24	4.1	0.04
TBMMT	1.7	11	14.0	0.05

Significant enlargement of basal spacing could be of significant contribution when dealing with catalytic conversions involving large molecules such as fatty acid. Surface analysis showed that clay was a low surface area material with a surface area of 24  $m^2/g$  and the mean pore size was in mesoporous size range. As theoretically expected, the exchange of native sodium ions with the surfactants resulted in significant drops in the surface area and correspondingly, significant enlargement of the pores occurred. The effect on the pore diameter was indeed consistent with the basal spacing increase as noted in the XRD results.

### Effect of Catalyst Loading

The variations in lauric acid conversion and monoglyceride yield were demonstrated by keeping other variables constant in order to study the effects of catalyst loading on the esterification process. As noted in Figures 1(a), significant conversions took place without the use of any catalyst. This was attributed to autocatalysis by lauric acid which acted as a

catalyst besides being a reactant. However, the use of TBMMT clearly improved the glycerol monolaurate yield, suggesting some degree of shape-selective catalysis might have taken place. This was attributed to the higher number of active sites and pore characteristics to suppress the formation of by-products.

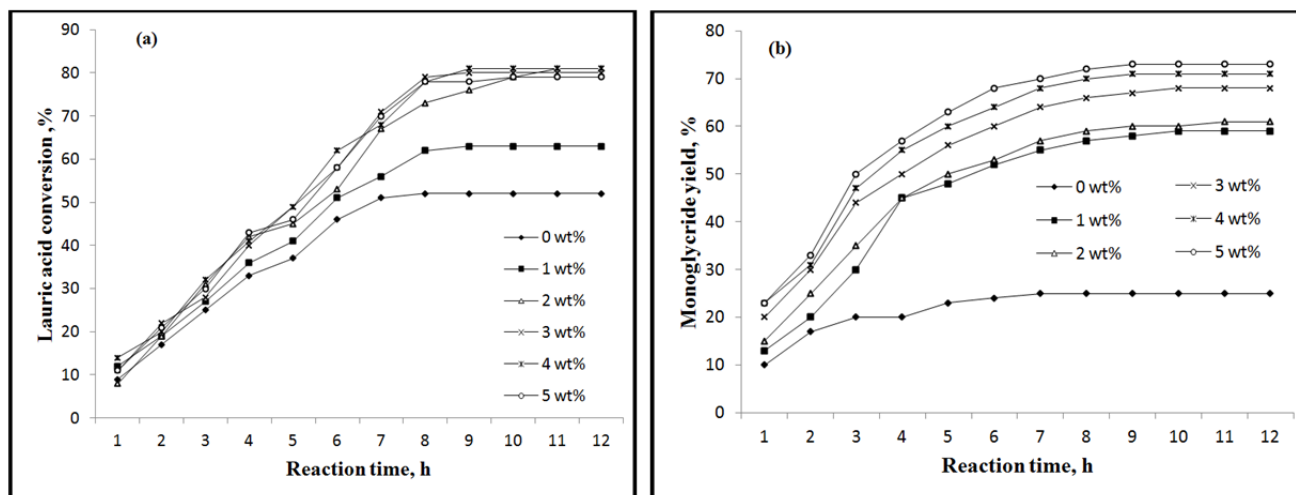


**Figure 1.** Effect of various catalyst loadings on a) lauric acid conversion and b) monoglyceride yield in the glycerol esterification with lauric acid (Glycerol:lauric acid molar ratio 6:1, 130 °C).

After relatively sharp increases in the first 8 h, the conversions leveled off for all catalyst loadings. Therefore, the reaction reached its equilibrium after about 8 h due to low reactant concentration and high concentration of products to shift the equilibrium towards the reactants side. The reaction time to reach equilibrium was not significantly influenced by the catalyst amount. However, increasing catalyst loading clearly resulted in higher conversion until about 3 wt. %. At higher loading, liquid phenomena between the glycerol and lauric acid which are mutually immiscible could play significant role in controlling the overall rate of reaction. Similar behavior was reported by Hermida et al. (2011) in a similar catalytic system using an acid functionalized SBA-15 catalyst.

Without the use of the catalyst, the monoglyceride yield reached in the esterification was only about 25 % and it was due to the co-formation of di- and triglyceride in the homogeneous reaction. This observation clearly showed the disadvantage of the homogeneous system. In the presence of a solid catalyst, the formation of di- and triglyceride with significantly larger molecule sizes was retarded due to geometric constraint in the catalyst pores. As such, the formation of monoglyceride was favored to give better yield. However, the formation of higher glycerides was still possible at larger pores, especially those at the interstices between catalyst particles. Unlike the trend in the lauric acid conversion, increasing catalyst loading to 5 wt. % led to a gradual increase in the yield.

Bossaert et al. (1999) comparatively studied the effect of variable loading of MCM-41-SO<sub>3</sub>H and SBA-15-SO<sub>3</sub>H catalysts between 0 and 5 % in the synthesis of monoglyceride performed under similar reaction conditions. Similar to this result, they observed a monotonous increase of the conversion and monoglyceride yield to imply that transfer of reactants from one liquid phase to another was not rate-limiting. This observation suggested the higher catalytic activity of TBMMT compared to those MCM-41-SO<sub>3</sub>H and SBA-15-SO<sub>3</sub>H. This conclusion was based on the effect that the overall reaction rate is governed by the rate-limiting step (Bokade and Yadav, 2009).

### Effect of Reaction Temperature

Figures 2(a) and 2(b) respectively illustrate the enhancement observed in lauric acid conversion and monoglyceride yield in the reaction carried out at 4 different temperature increase in the reaction temperature. At a temperature of 110 °C, the lauric acid reached a plateau after 5 h of reaction which could be attributed to a shift in the reaction direction. This observation led to a conclusion that the equilibrium in this reaction was influenced by the reaction temperature.

In order to carry out the esterification reaction to completion, appropriate temperature with efficient removal of water was required as water (by-product) could promote the reverse reaction. Monoglyceride yield of 70 % with corresponding lauric acid conversion of 80 % was achieved in 8 h at 130 °C. Higher temperature neither significantly improve the conversion nor the yield. It could be explained on the basis of increasing mass transfer of the fatty phase with the increase in temperature. As the reaction generally occurs in the fatty phase, glycerol molecules have to be transferred into this phase prior to the reaction. Then, glycerides (mono-, di- and triglyceride) were formed and an increase in the lauric acid conversion was observed (Wilson et al., 2000).

No significant improvement in the fatty acid conversion and glycerol monolaurate yield was observed by increasing the temperature beyond 130 °C. At lower temperatures, more reaction took place with increasing temperature as the system was kinetic-controlling. However, when the reaction was sufficiently fast at 140 °C, liquid phenomena such as diffusion rate of fatty acid in the excess glycerol could have compensated the beneficial effects of higher reaction temperature.

Sanchez et al. (1997), Bossaert (1999), Diaz et al. (2001) and Machado et al. (2000) investigated temperature effects in direct esterification of glycerol by fatty acid. The range of reaction temperature studied was 90–160 °C. At high fatty acid conversions, the selectivity to monoglycerides decreased due to the production of diglycerides and also triglyceride on the external surface of the catalyst. In this respect, TBMMT catalyst used in this study offered a particular advantage as

corresponding increase in the yield with increasing fatty acid conversion was obtained. The interlayer spacing within meso size range was deemed the responsible factor to the suppression of di- and triglyceride formations.

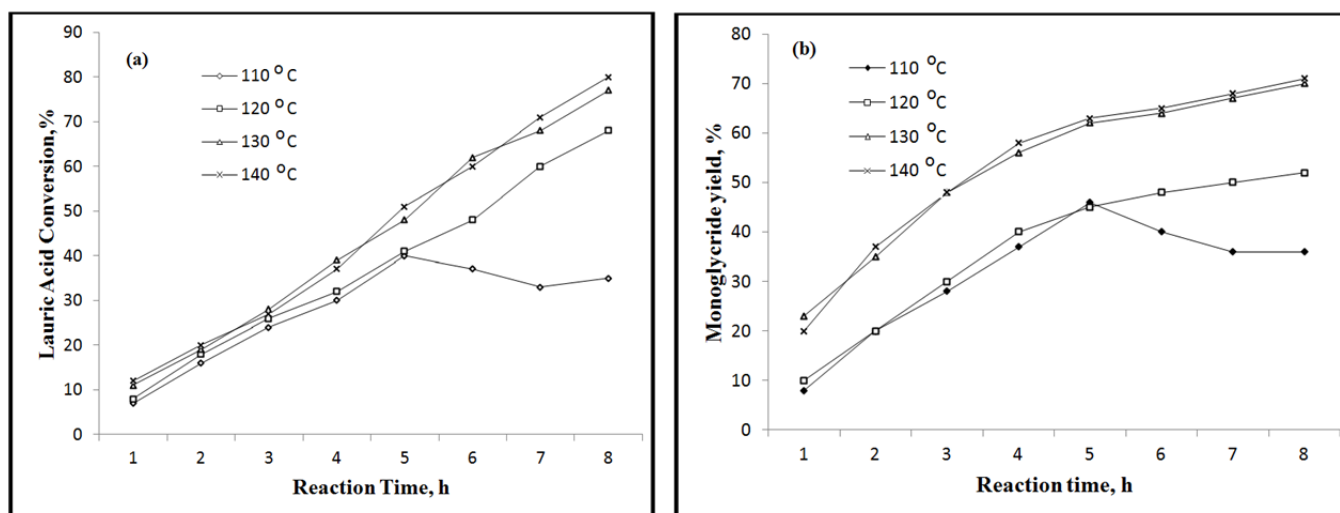


**Figure 2.** Effect of reaction temperature on a) lauric acid conversion and b) monoglyceride yield in the glycerol esterification reaction. (Glycerol:lauric acid molar ratio 6:1, catalyst loading 3 wt. %).

### Effect of Glycerol/Lauric Acid Molar Ratio

Esterification of glycerol with fatty acid to produce monoglyceride is a reversible reaction. Based on stoichiometry, the esterification reaction requires glycerol/fatty acid molar ratio of 1:1 to produce monoglyceride. In reality, di- and triglyceride could also form in the reaction so that excess glycerol is needed. In order to investigate the effect of glycerol/lauric acid molar ratio on the esterification reaction, catalytic tests were performed with different glycerol/lauric acid molar ratios, i.e. 4:1, 6:1 and 8:1.

As can be seen in the Figures 3(a) and 3(b), the effect of glycerol/lauric acid molar ratio on the lauric acid conversion was insignificant beyond a ratio of 6:1. At lower ratio, significant improvement was achieved as more glycerol was available for effective contact with the relatively more viscous lauric acid. As a result, increases in the lauric acid and glycerol monolaurate yield were observed. Further increase to 8:1 meant significant dilution to the limiting reactant to bring about adverse effect to the reaction. However, it worth noting that the fatty acid conversion steadily increased with time with corresponding increase in glycerol monolaurate yield. In this respect, TBMMT catalyst offered an advantage over  $\text{HO}_3\text{S-SBA-15}$  mesoporous catalyst (Hermida et al., 2011).

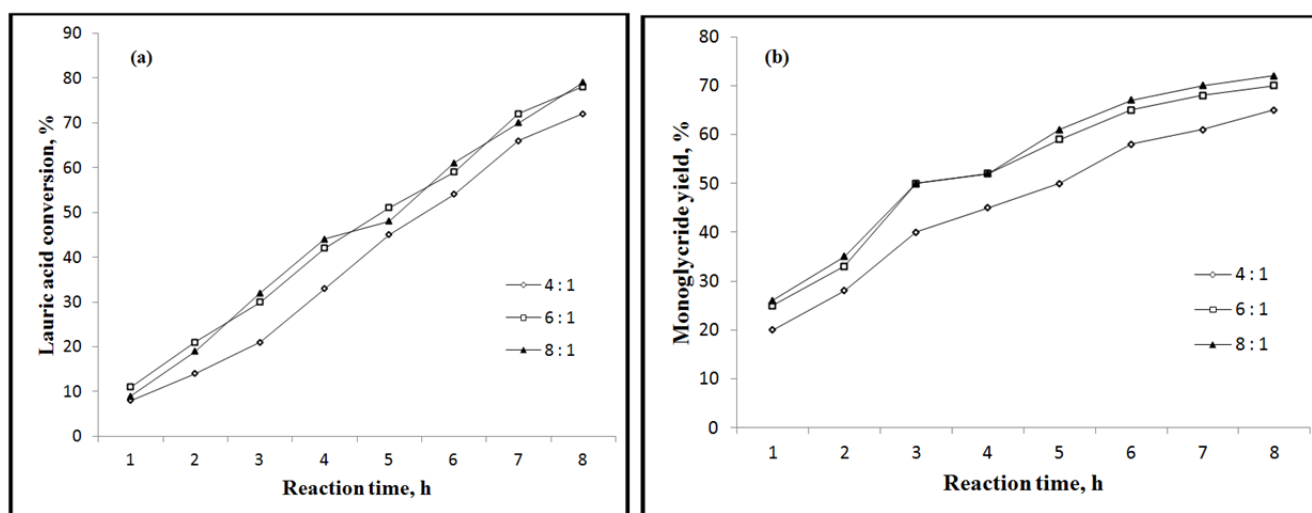


**Figure 3.** Effect of glycerol/lauric acid molar ratio on a) lauric acid conversion and b) monoglyceride yield in the glycerol esterification reaction. (Catalyst loading 3 wt. %, 130 °C).

Selectively to monoglyceride has been reported to be significantly influenced by the increase in glycerol/lauric acid molar ratio. Bossaert et al. (1999) observed the effect of glycerol/fatty acid ratio in their study between 1:1 to 6:1. They reported that the increase in glycerol/fatty acid ratios would increase the monoglyceride selectivity. The effect of glycerol/fatty acid ratios was somehow similar to that reported by Sanchez et al. (1997) using glycerol/fatty acid ratios from 1:3 to 3:1. This was because there was a larger chance for a fatty acid to react with glycerol to consequently result in an increase in

monoglyceride selectivity. As the fatty acid conversion also increased, corresponding increase in the monoglyceride yield was observed.

## Conclusions

Geometrical constraint in the pores retarded the formation of higher glycerides. Fast reaction occurred within the first 8 h decreasing reactant concentration resulted in low rate of reaction after that. No further benefit was achieved above 3 wt. % of TBMMT catalyst loading due to liquid phenomena between the reactants and a reaction temperature of 130 °C and 6:1 for the reactant ratio were the optimum levels. Increasing catalyst loading improved glycerol monolaurate yield. Monoglyceride yield of about 70 % at corresponding lauric acid conversion of 80 % were achieved in 8 h at 130 °C using a glycerol/lauric acid molar ratio 6:1 and 3 wt.% of catalyst.. The modified montmorillonite catalyst show high catalytic activity and good selectivity to monolaurate. The behaviors were successfully correlated with the surface characteristic of the catalyst. Thus, TBMMT catalyst was an active catalyst to selectively produce glycerol monolaurate in the esterification reaction.

## Acknowledgement

A short Term Research Grant from Universiti Sains Malaysia and a Fundamental Research Grant Scheme from Ministry of Higher Education of Malaysia are gratefully acknowledged.

## References

- Abdullah, A.Z., Razali, N., Mootabadi, H., & Salamatinia, B. (2007). Critical technical areas for improvement in biodiesel technologies. *Environmental Research Letters*, 2, 1-6.
- Abdullah, A. Z., Wibowo, T. Y., & Zakaria, R. (2011). Effect of tetramethyl ammonium hydroxide on the activity of LiOH-intercalated montmorillonite catalyst in the transesterification of methyl laurate with glycerol. *Chemical Engineering Journal*, 167 (1), 328-34.
- Bahulayan, D., Das, S.K., & Iqbal, J. (2003). Montmorillonite K10 clay: An efficient catalyst for the one-pot stereoselective synthesis of beta-acetamido ketones. *Journal of Organic Chemistry*, 68, 5735-38.
- Bokade, V.V., & Yadav, G.D. (2009). Transesterification of edible and nonedible vegetable oils with alcohols over heteropolyacids supported on acid-treated clay. *Industrial & Engineering Chemistry Research*, 48, 9408-15.
- Bossaert, W. D., Vos, D.E.D., Rhijn, W.M.V., Bullen, J., Grobet, P.J., & Jacobs, P.A. (1999). Mesoporous sulfonic acids as selective heterogeneous catalysts for the synthesis of monoglycerides. *Journal of Catalysis*, 182, 156-64.
- Diaz, I., Mohino, F., Pérez-Pariente, J., & Satre, E. (2001). Synthesis, characterization and catalytic activity of MCM-41-type mesoporous silicas functionalized with sulfonic acid. *Applied Catalysis A: General*, 205, 19-30.
- Gupta, M., in: Hui, Y.H. (Ed). (1996). Manufacturing Processes for Emulsifiers. In Bailey's Industrial Oil & Fat Products, John Wiley & Sons, Inc. New York.
- He, H., Ma, Y., Zhu, J., Yuan, P., & Qing, Y. (2009). Organoclays prepared from montmorillonites with different cation exchange capacity and surfactant configuration. *Applied Clay Science*, 48, 67-72.
- Hermida, L., Abdullah, A.Z., & Mohamed, A. R. (2011). Synthesis of monoglyceride through glycerol esterification with lauric acid over propyl sulfonic acid post-synthesis functionalized SBA-15 mesoporous catalyst. *Chemical Engineering Journal*, 174, 668-76.
- Machado, M. D. S., Cardoso, D., Perez-Pariente, J., & Sastre, E. (2000). Esterification of lauric acid using modified zeolite beta as catalyst. *Studies in Surface Science and Catalysis*, 130, 3417-22.
- McClements, D. J. (2005). Food Emulsions: Principles, Practice, and Techniques, Second Ed. CRC Press, Boca Raton.
- Moonen, H., & H. Bas. (2004). Mono- and Diglycerides, Emulsifiers in Food Technology, Oxford Blackwell, Oxford.
- Sanchez, N., Martinez, M., & Aracil, J. (1997). Selective esterification of glycerine to 1-glycerol monooleate. 1. Kinetic modeling. *Industrial & Engineering Chemistry Research*. 36, 1524-8.
- Wibowo, T. Y., Abdullah, A.Z., & Zakaria, R. (2009). Cationic surfactant-modified clay catalysts for selective synthesis of glycerol monolaurate through glycerol esterification with lauric acid. *Applied Clay Science*, 50, 280-1.
- Wilson, K., Shorrock, K., Renson, J., Hoyer, A. W., Gosselin, B., Macquarrie, et al. (2000). Novel supported solid acid catalysts for environmentally friendly organic synthesis. *Studies in Surface Science and Catalysis*, 130, 3429-34.
- Xi, Y., Ding, Z., He, H., & Frost, R.L. (2004). Structure of organoclays-An X-ray diffraction and thermogravimetric analysis study. *Journal of Colloid and Interface Science*, 277, 116-20.



# Isolation and Characterization of Antiviral Protein From *Salsola Longifolia* Leaves Expressing Polynucleotide Adenosine Glycoside Activity

Zenab Aly Torky

Department of Microbiology, Faculty of Science, Ain Shams University, Cairo, Egypt

ZenabAly72@yahoo.com

**Abstract:** Disease control of economically important crops using non-costly and environmentally non-harmful methods is a necessity. Due to their wide antimicrobial activities in general and their antiviral activities in particular, ribosome-inactivating proteins (RIPs) have a very strong potential in plant defense. A new type -1 single chain RIP named SLP was purified from the leaves of *Salsola longifolia* by ammonium sulphate fractionation, anion exchange on DE-cellulose chromatography and cation exchange chromatography on CM-cellulose. This new RIP's molecular mass was 32 KDa with homology to single-chain ribosome inactivating protein. Reverse transcriptase polymerase chain reaction detected the ribonuclease activity of SLP from the examined species showing SLP to be a broad spectrum RIP that depurinates not only its own ribosomes but also other heterologous plant ribosomes (*Phaseolus vulgaris*). SLP also showed deoxyribonuclease activity against pBlue Script SK<sup>+</sup> plasmid DNA at moderate SLP concentration which led to nick super coiled DNA and then to nicked circular form. By increasing RIP concentration, it transformed the nicked DNA into a linear form. SLP also showed to possess a powerful antiviral activity.

**Keywords:** Isolation, Antiviral protection, *Salsola longifolia* leave

## Introduction

RIPs are plant proteins capable of inactivating ribosomes. Due to their biological activities toward animal and human cells, RIPs are very important in biological and biomedical research. Some RIPs also have a big role in plant defense (Peumans et al., 2001; Kim et al., 2003; and Vepachedu et al., 2005), and hence can be used in plant protection against different pathogens. Those RIPs are known as antiviral proteins (Stirpe et al., 1992; Van Damme et al., 2001; Girbes et al., 2004; and Corrado et al., 2005).

Most RIP-catalytic ribonuclease activity, via the single depurination of the large rRNA upon treatment with acidic aniline, releases the RIP diagnostic fragment (Barbieri et al., 1993). Although a few studies in the literature state that some RIPs show both DNase and RNase enzymatic activity, many studies show that RIPs' enzymatic activities are mostly DNase activities (Hudak et al., 2000 and Choudhary et al., 2008) and depurination of capped mRNAs (Hudak et al., 2002). Recent studies on the other hand, show that RIPs may also induce cell death by apoptosis (Sikriwal et al., 2008).

Although, It is a broad belief that RIPs have characteristic N-glycosidase activity and that this activity inactivates the ribosomes, and inhibits protein synthesis irreversibly (Van Damme et al., 2001), it is still kind of vague how these antiviral proteins operate to inhibit virus infection (Gu et al., 2000; Park et al., 2004; and Stripe, 2004). Those antiviral / RIPs genes are therefore resistant genes, which can be isolated and transferred to crops that have economic value to develop virus resistant plants (Moon, et al., 1997; Zoubenko et al., 2000; and Vandenbussche et al., 2004).

Searching the available literature, it is clear that many type-1 RIPs have been isolated and characterized in details and the search for novel type-1 RIPs with interesting properties is still a very active research topic. Since, the majority of type-1 RIPs at the current time are isolated from dicotyledons plants of families like *Cucurbitaceae*, *Chenopodiaceae*, *Caryophyllaceae*, *Euphorbiaceae*, *Nectaginaceae* and *Phytolaccaceae*, the isolation and characterization of novel type-1 RIPs from other dicots is again a very hot research topic to stress and confirm the biological activities of type-1 RIPs. It is well known that RIPs represent a family of isoenzymes and consequently a family of multigenes that can be expressed in different plant species. Highest activity was found in the mature seeds, 1-fold more than that in the root, and 5-fold more than that in the leaves of *Saponaria officinalis* (Stirpe et al., 1983). Developmental and environmental statuses as well as the plant tissue are the various factors that each RIP gene can express its own pattern accordingly. This study has been performed to determine the structure analysis of RIP gene(s), on the DNA level, for *S. longifolia*. The direct PCR amplification has been undertaken in order to achieve that. In this study, a type-1 RIP from *Salsola longifolia* Forssk (*Chenopodiaceae*) is isolated and its enzymatic and molecular characterization and antiviral activity are studied.



## Materials and Methods

### Virus inoculum

Two viruses were used; TNV and BYMV for testing the virus inhibitory activities of leaf extract and purified preparation of *S.longifolia*. The viruses were maintained on the local lesion host (*Phaseolus vulgaris*) and systemic host (*Vicia faba*), respectively. The plants were grown in small plastic pots containing soil, and sand mixture. The pots were kept in an insect free glass house. Virus inocula were prepared by homogenizing the infected leaves with 20mM sodium-potassium phosphate buffer, pH 7.0, with a sterilized pestle and mortar. The contents were squeezed through two layers of muslin cloth and the filtrate was centrifuged at 12,000g for 10mins. The clear supernatant was used as virus inoculum after suitable dilution with distilled water.

### Plant viral bioassay

Seeds of *P.vulgaris* were grown in 15cm plastic pots; each pot containing 8 seeds, and kept in the green house under natural conditions. Those plants were used as local lesion host to quantitatively measure the activity of TNV-D. Ten primary leaves of 10-13 days old french bean plants were inoculated with TNV. *Vicia faba* plants were used as the systemic host for BYMV, and the inoculation was done on the fourteenth day stage. Inoculation was done under green house conditions at  $25 \pm 5$  °C, by dusting virus inoculum with Carborandum (600 mesh). Ten replicates were made for each virus inoculation.

The antiviral bioassay of the purified SLP-32 was done on the test plants with same height, and age. For each treatment, ten replicates of equal size were used. The purified 32kD protein from *S.longifolia* leaves was applied on the test plant leaves. For controls, test plant leaves were treated with only buffer and virus inoculum. After one hour, the protein treated leaves were washed with distilled water and gently blotted dry. The leaves were then sprinkled very lightly with 600mesh carborundum powder and inoculated gently and uniformly with virus inoculum. After inoculation, leaves were washed with distilled water. In case of TNV infection, plants were observed for the development of lesions for 3-5 days. The inhibitory activity of the proteins was calculated in terms of percentage inhibition using the following formula: %inhibition = (Cont-Treat)/Cont x 100% , where, Cont is average number of lesions in control plants, and Treat is the average number of lesions in treated plants.

As for the BYMV infection, plants were observed for the development of systemic symptoms for 14 days. The inhibitory activity of the proteins was calculated according to the ratio between obviously infected plants (showing systemic symptoms) to the total inoculated plants.

### Protein extraction and purification from *S.Longifolia* leaves

Plant materials from fresh and dry leaves (100g) were ground in liquid nitrogen, homogenized in three volumes of extraction buffer (25mM NaPO<sub>4</sub>, pH 7.0, with 250mM NaCl, 10mM EDTA, 5mM dithiothreitol, 1mM phenylmethylsulfonyl fluoride, and 1.5% [w/v] polyvinylpolypyrrolidone), and then centrifuged for 30mins at 10,000g. The supernatant was brought to 20% (w/v) ammonium sulfate by continues stirring. The mixture was chilled for one hour and then centrifuged again for 30mins at 10,000g. The supernatant was precipitated with 90% (w/v) ammonium sulfate and centrifuged at 14,000g for 30mins. The pellet was suspended in 10mM sodium phosphate buffer, pH 7.8, and dialyzed against the same buffer. After dialysis, the clear supernatant was applied to DE-52 cellulose column (2.2 cm x 10cm) pre-equilibrated with the buffer. The flow-through fractions were collected and applied to a CM-52 cellulose column (2.2 cm x 10cm) pre-equilibrated with 10mM sodium acetate buffer, pH 5. The column was eluted with a linear gradient of 0-0.3 M NaCl in the same buffer. Fractions with inhibitory activity towards virus infection were pooled, dialyzed extensively against water and freeze-dried.

### Estimation of soluble proteins

Protein content of leaf extract at each step of purification was estimated by the method described by Lowry et al., (1951).

### SDS-polyacrylamide gel electrophoresis

Discontinuous SDS-PAGE was carried out in 12% separating gel with a 5% stacking gel according to Laemmli (1970). The proteins were visualized by staining with 0.1% Coomassie brilliant blue R-250.

### Effect of actinomycin D on antiviral activity

Actinomycin D (ActD 20µg ml<sup>-1</sup>) was applied at different time intervals (0, 6, and 10h, respectively) following treatment with purified antiviral protein on the same leaves of *P.vulgaris*. An equal number of leaves in control sets were treated with ActD alone, antiviral protein alone and buffer alone. After 24h, all the leaves were inoculated with TNV and observed for lesion development.

### Assay for N-glycosidase activity

Total RNA was isolated from the leaves of *Phaseolus* and *Salsola* using the RNeasy Plant Mini Kit (Qiagen USA) according to manufacturer's instructions. RT-PCR was performed to detect diagnostic depurinated rRNA fragment which is specific for the enzymatic action of RIPs. RT-PCR was carried out using the Titan One Tube RT-PCR system (Roche, cat. No. 1888382) PCR product (about 250 bp) represents the depurinated RNA using two specific primers (Sense Primer I: 5' AACGTAGTACGAGAGGAAC 3', AntiSense Primer II: 5' AAGTCGTCTGCAAAGGATT 3') as described by Kataoka *et al.*, (1992).

### DNase activity

The alkaline hydrolysis mini-preparation method of Ahn et al., (2000) was used to isolate pBlueScript SK<sup>+</sup> plasmid DNA. To gain information like the size, quantity and quality of the isolated plasmid DNA, the agarose (1%), gel electrophoresis was conducted. To conduct the gel electrophoresis, 1 µg of plasmid DNA was incubated with increasing amount of purified SLP in a final volume of 25 µl. The reaction mixture was then incubated at 37°C for 4 h. After those 4 hours on incubation, 5µl loading solution (30% Ficoll, 200mM EDTA, 0.25% bromophenol blue, and 0.25% xylene caynole FF) was added. Electrophoresis was conducted under non-denaturing condition in a 1% agarose gel. Ethidium bromide was used to stain the gel in order to visualize the DNA bands.

## Results and Discussion

Fresh and dry *S.longifolia* leaves were both used in preparing the extracts that inhibited the formation of local lesions by Tobacco Necrosis Virus (TNV) on *P.vulgaris* plants. The antiviral protein was purified from the leaves of *S.longifolia*. Purification of antiviral protein from *S.longifolia* leaves

After collecting the leaves of *S.longifolia*, they were washed with tap water and dried at room temperature. Those leaves were then used to extract the antiviral activity. Around, 2600mg of soluble proteins was obtained from 100g of leaves. Bioassay of crude extracts against TNV, on *p.vulgaris*, showed a very high activity (97.3% inhibition). *S.longifolia* protein was then purified to homogeneity in two steps. The first step of purification resulted in one major peak of DE-52 cellulose chromatography showing the antiviral inhibitory activity against TNV (figure 1A). In this fraction a combination of a major protein of 32KD and minor proteins were present, as revealed by SDS/PAGE analysis. The second purification step removed the minor proteins by CM-52 cellulose chromatography (figure 1B), resulting in a homogeneity and a protein fraction (the first peak) with a molecular mass of 32KD as revealed by SDS/PAGE analysis (figure 2). That protein was then characterized and designated as SLP-32. The inhibitory activity and relative outputs in the various steps of purification are summarized in table 1.

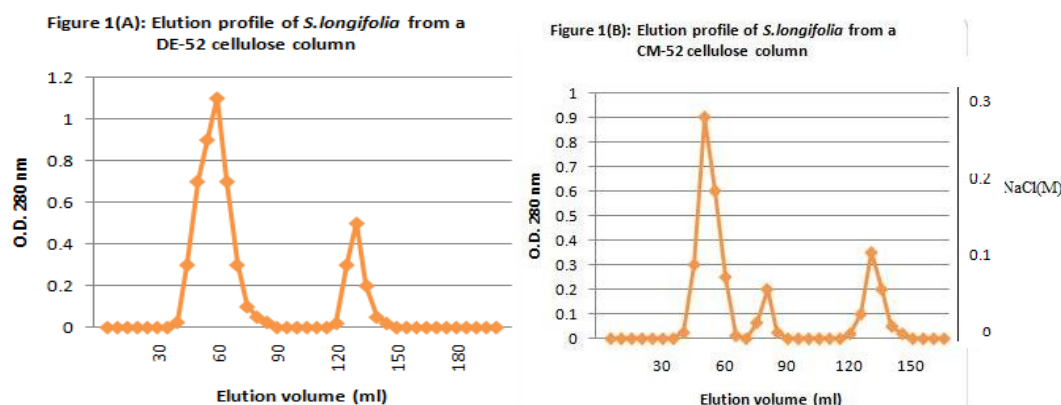


**Table 1:** Purification of antiviral protein (SLP-32) from the leaf extract of *Salsola longifolia*

Protein fraction	Total protein (mg) from 100g of fresh and dried leaves	Percent inhibition
Crude extract	61.34	97.3
Ammonium sulphate fraction 70-90%	50.29	95.8
DE-cellulose chromatography		
Unadsorbed fraction peak1	25.74	96.2
Unadsorbed fraction peak2	8.23	15
CM-cellulose chromatography		
Peak1	7.82	95.3
Peak2	3.06	9.4
Peak3	4.9	7.53

### Molecular weight of SLP-32

SDS-PAGE [12.5% (w/v) gel] was used to determine the molecular weight (Mr) of the purified *S.longifolia* as described by Laemmli(1970). It came out to be 32 KDa (figure 2). This purified salsola antiviral protein has been designated as SLP-32.

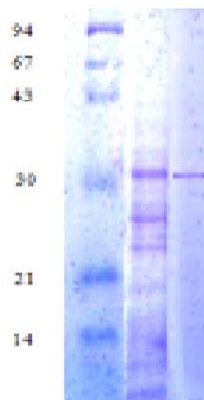


**Figure 2:** SDS-PAGE of purified SLP-32 isolated from *Salsola longifolia* leaves. Lane 1, from the left, is the molecular mass markers; Lane 2, is the crude extract; Lane 3, is the purified fraction of SLP-32. The gel was stained with Coomassie Brilliant Blue R-250. The positions of molecular mass standards (in kDa) are shown at the left.

### Effect of actinomycin-D on antiviral activity

SLP-32 made *P.vulgaris* resistant to TNV. This resistance was inhibited when actinomycin-D (Act-D, 20 µg/ml) was applied immediately after treating the plant with SLP-32 treatment. actinomycin-D however, failed to inhibit the resistance response to a greater extent when applied 6 and 10 hours respectively, after SLP-32 treatment (table 2). Act-D inhibits DNA-directed rRNA synthesis because it binds to double helical DNA by intercalating between the bases. Since, *P.vulgaris* resistance to TNV was inhibited as a result of immediate application of Act-D, following the SLP-32 treatment, then this protein might have induced the synthesis of new substances interfering with the virus or enhance the production of already existent ones, thereby altering the susceptibility of the host plant. The antiviral property of SLP-32 is not reversed however, if Act-D is applied from 6 to 10 hours after protein treatment due to the fact that the substances involved in antiviral effect are already present and the late application of Act-D doesn't interfere in their synthesis. This property is similar to that shown by *C.inerne*, *C.aculeatum* and *C.cristata* antiviral proteins (Verma et al., 1996) and by *A.tricolor* leaves antiviral protein (Sribash et al., 2006).

**Table 2:** Effect of Actinomycin D (ActD) on the antiviral activity of SLP-32 against TNV infection

Treatment	Average lesion number	% Inhibition
Buffer control	89.3	
ActD (20µg/ml)	84.6	
SLP-32 (+ve control)	4.6	94.8
(SLP-32)+ActD after 0h	77.8	12.8
(SLP-32)+ActD after 6h	4.19	95.3
(SLP-32)+ActD after 10h	5.3	94.1

Control sets were treated with buffer alone or with ActD solution alone (20µg/ml), purified SLP-32 was applied on leaves of *P.vulgaris*. In one set, actinomycin (ActD 20µg/ml) was applied immediately, and in other sets ActD treatment was given after 6 and 12 h of SLP-32 application.

### Assay for N-glycosidase activity

Reverse transcriptase polymerase chain reaction (RT-PCR) and specific primers designed from the universally conserved region of 12 nucleotides in rRNA of both eukaryotes and prokaryotes (Kataoka et al., 1992) were then used for the assay of rRNA depurinating activity for SLP-32 on *S.longifolia* and *P.vulgaris* leaf ribosomes through detection of RIP diagnostic fragment. Amplifications of cDNA from 25S rRNA, isolated from *S.longifolia* and *P.vulgaris* by RT-PCR, revealed amplified product about 250 bases (figure 3), which corresponds to RIP diagnostic fragment of target ribosomes. Since RIPs inhibit protein synthesis by deglycosylating rRNA through cleaving the sugar-phosphate back bone at depurination sites (Tumer et al., 1997), these results indicate that SLP-32 is a broad spectrum RIP that depurinates its own ribosomes. These results resemble those reported by Kurinov (1999) on the pokeweed antiviral protein (PAP), and the heterologous ribosomes from other plant species (*P.vulgaris* ribosomes) as well. This is also in accordance with the results of Taylor and Irvin (1990) on *Phytolacca americana*, Park et al., (2004) on *Chenopodium album*. These ribosomes inactivation and consequently cell death is the major cause of viral inhibition of RIP- associated activity (Taylor et al., 1994; Hao et al., 2001; Desmyter, 2002; Sawasaki et al., 2008; and Sikriwal et al., 2008).

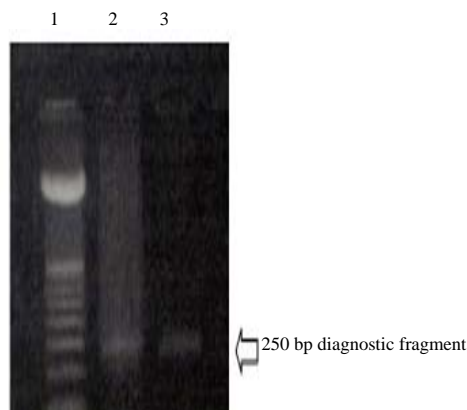


**Figure 3:** 1.2% Agarose gel electrophoresis of RT-PCR amplified product of RIP diagnostic fragment isolated from the leaves of *Phaseolus* (lane 2) and *Salsola* (lane 3) treated with SLP-32. Lane 1 represents the DNA molecular weight marker (100, 200, 300, 400) bp.

### DNase activity

pBlueScript SK<sup>+</sup> DNA has three forms, namely supercoiled, nicked, and linear. Upon incubation of pBlueScript SK<sup>+</sup> DNA with different amounts of SLP-32, it was clear that the degree of supercoiling was altered. Upon incubation of the supercoiled form of pBlueScript SK<sup>+</sup> DNA with 10 and 20 µg of SLP-32, it first nicked giving a nicked circular form. This nicked circular form moved slower than the supercoiled DNA form through the agarose gel. The SLP-32 concentration was then increased to 30 µg causing the emergence of the third form of DNA namely, the linear form. This linear form of DNA migrated faster than nicked circular form and slower than the supercoiled form. Since RIPs cleave only the supercoiled DNA by nicking before linearizing the strand cleavage, the above results implies that the DNase activity of the SLP-32 was conformation specific (Lau et al., 1998, Barbieri et al., 2000 and Choudhary et al., 2008). To confirm that the band shift was not caused by the binding of SLP-32 onto pBlueScript SK<sup>+</sup> DNA, the two species were separated before electrophoresis by digestion with proteinase K, after the DNA was incubated with SLP-32. Afterwards, the DNA was extracted with an equal ration of phenol and chloroform and precipitated with ethanol. Same changes in the bands pattern were confirmed by the electrophoretic analysis (figure 4).

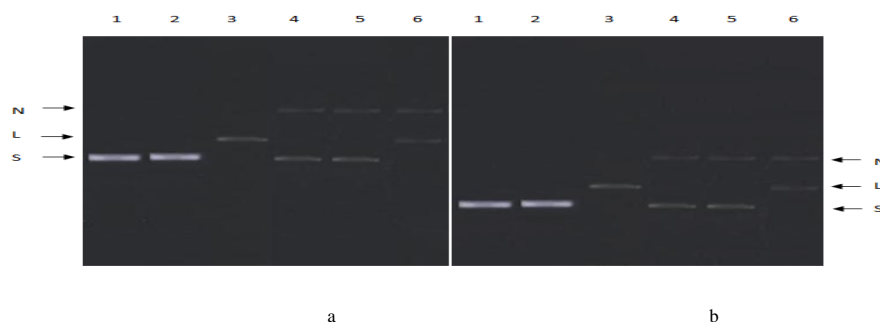


**Figure 4:** a) DNase activity test. Incubating with 10 or 20 µg of SLP-32, pBlueScript SK<sup>+</sup> DNA supercoiled form (S) shows nicked form (N) (lanes 4 and 5) and with 30 µg of SLP-32 shows linear form (L) (lane 6). Lanes: 1) plasmid; 2) control; 3) plasmid restricted with *Eco* RI. b) DNase activity test after proteinase K treatment. Same changes in banding patterns indicating that band shifting was not because of the binding of the protein with the plasmid DNA.

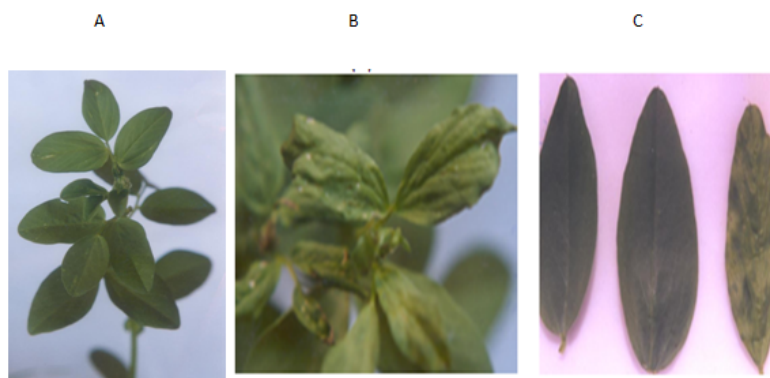
### Antiviral bioassay for SLP-32

Antiviral activity of plant extracts was always used to determine the potential of identifying new RIPs. Isolation of RIPs helps studying their biological activities as well as determining the mechanism of action of these RIPs on the infection process produced by several plant viruses. The results indicated that SLP-32 significantly inhibited local lesion formation by TNV on *P. vulgaris* causing 95-97% inhibition, as in table (1). Effects of different RIP concentrations, from *S. longifolia* against bean yellow mosaic virus (BYMV) systemically infected *V. faba* plants, was also studied to determine the concentration causing the highest percent inhibition. Results in table (2) show that the higher the concentration of RIP the higher the percent of inhibition showing 94.1% inhibition at 100 µg/ml of RIP concentration. These results were consistent with those reported by Watanabe et al. (1997), Zoubenko et al., (2000), Nielsen and Boston (2001), and Iglesias et al., (2005). There are many possibilities to explain the antiviral activity of RIPs against plant viruses. RIPs can act on the viral nucleic acids through their PAG activity, or can act on the host by selectively killing the infected cells, thus preventing the virus from replicating and propagating to neighbor cells. RIPs can also act indirectly by activating the plant defense system (Peumans et al., 2001; Gholizadeh et al., 2004; and Sikriwal et al., 2008). Figure (5) below show the healthy *vicia faba* plants, the plant inoculated with SLP-32 and BYMV, and the plant inoculated with the virus.

**Table 2:** Effects of different RIP concentrations extracted from *S.longifolia* on *Vicia faba* plants inoculated with BYMV

Concentration of <i>S.longifolia</i> RIP µg/ml	% Inhibition of
5	29.0
10	34.1
30	38.0
40	42.3
50	66.7
60	69.5
70	76.3
80	89.3
90	93.75
100	94.1

Figure (5): (A) Healthy *Vicia faba* plants (control); (B) *Vicia faba* plants systemically infected with Bean Yellow Mosaic Virus (BYMV); (C) Left is *Vicia faba* plants inoculated with SLP-32 and the virus; middle is the healthy *Vicia faba* plants (control); right is the systemically infected *Vicia faba* plants with BYMV.



## References

- Ahn, S.C., Back, B.S., Oh, T., Song, C.S., and Chatterjee, B. (2000). Biotechniques, 29, 466-468.
- Barbieri, L., Battelli, M.G., Stirpe, F., (1993). Ribosome inactivating proteins from plants. Biochemica and Biophysica Acta 1154, 237-282.
- Barbieri, L., Valbonesi, P., Righi, F., Zuiccheri, G., Monti, F., Gorini, P., Samori, B., and Stirpe, F., (2000). Polynucleotide: Adenosine glycosidase is the sole activity of ribosome-inactivating proteins on DNA. J. Biochem. 128(5):883-9.
- Barbieri, L., Valbonesi, P., Govoni, M., Pession, A., and Stirpe, F. (2000). Polynucleotide: adenosine glycosidase activity of saporine L1: effect on various forms of mammalian DNA. Biochem. Biophys. Acta 1480, 258-266.
- Choudhary, N.L., Yadav, O.P., and Lodha, M.L., (2008). Ribonuclease, deoxyribonuclease, and antiviral activity of Escherichia coli- expressed Bougainvillea xbuttiana antiviral protein 1. Biochemistry (Mosc), 73(3):273-7.
- Corrado, G., Bovi, P., and Ciliento, R., (2005). Inducible Expression of a Phytolacca heterotepala Ribosome-Inactivating Protein Leads to Enhanced Resistance Against Major Fungal Pathogens in Tobacco. Phytopathology, Feb;95(2):206-15.
- Desmyter, S.(2002). Study of the antiviral activity of Iris RIP, a type 1 ribosome inactivating protein from *Iris hallandica*. PhD thesis, Katholieke Universiteit Leuven, Belgium.
- Gholizadeh, A., Kumar, M., Balasubrahmanyam, A., Kumar, S., Narewal, s., Lodha, M.L., and Kapoor, H.C., (2004). Antioxidant activity of antiviral proteins from Celosia cristata. J. plant Biochem. Biotechnol. 13, 13-18.
- Girbes, T., Ferreras, J.M., Arias, F.J., and Stripe, F.(2004). Description, distribution, activity and phylogenetic relationship of ribosome-inactivating proteins in plants, fungi, and bacteria. Mini Rev. Med Chem., 4, 461-476.
- Gu, Y., Chen, W., Xia, Z.(2000) . Molecular modeling of the interactions of trichosanthin with four substrate analogs. J.Protein Chem. 19(4) :291-7.
- Hao, Q., VanDamme, E.J.M., Hause, B., Barre, A., Chen, Y., Rouge, P. and Peumans, w.J. (2001). Iris bulbs express type 1 and type 2 ribosome-inactivating proteins with unusual properties plant physiol. 125, 866-876.
- Hudak, K.A., Bauman, J.D., and Tumer, N.E., (2002). Pokeweed antiviral protein binds to the cap structure of eukaryotic mRNA and depurinates the mRNA downstream of the cap. RNA 8, 1148-1159.



- Hudak, K.A., Wang, P., and Tumer, N.E., (2000). A novel mechanism for inhibition of translation by pokeweed antiviral protein; depurination of the capped RNA template. *RNA* 6, 369-380.
- Iglesias, R., Perez, Y., Torre, C., Ferreras, JM., Antolin, P., Jimenez, P., Rojo, MA., Mendez, E., and Gribes, T., (2005). Molecular characterization and systemic induction of single-chain ribosome-inactivating proteins (RIPs) in sugar beet (*Beta vulgaris*) leaves. *J.Exp.Bot.* 56(416):1675-84.
- Kataoka, J., Habuka, N., Miyano, M., Masuta, C., and Koiwai, A. (1992). Adenine depurination and inactivation of plant ribosomes by an antiviral protein of *Mirabilis jalapa*, *Plant Molecular Biology*, 20; 1111-1119.
- Kim, J.K., Jang, I. C., Wu, R., Zuo, W.N., Boston, R.S., Lee, Y.H., Ahn, IP., and Nahm, B.H., (2003). Co-expression of a modified maize ribosome-inactivating protein and a rice basic chitinase gene in transgenic rice plants confers enhanced resistance to sheath blight. *Transgenic Research* 12, 475-484.
- Kurinov, IV., Myers, DE., Irvin, JD., and Uckun, FM. (1999). X-ray crystallographic analysis of the structural basis for the interactions of pokeweed antiviral protein with its active site inhibitor and ribosomal Rna substrate analogs. *Protein Sci*, 8(9):1765-72.
- Laemmli, U.K. (1970). *Nature (London)* 227,680-685.
- Lau, CK., Wong, RN., Lo, SC., Kwok, F. (1998). Refolding of denatured trichosanthin in the presence of GroEL. *Biochem Biophys Res Commun*, 245(1):149-45.
- Lowry, O.H., Rosebrough, N.J., Farr, A.L., and Randall, R.J. (1951). *Biol. Chem.* 193, 223-234.
- Moon, YH., Song, SK., Choi, KW., and Lee, JS., (1997). Expression of a cDNA encoding *Phytolacca insularis* antiviral protein confers virus resistance on transgenic potato plants. *Mol Cells*, 7(6):807-15
- Nielsen, K. and Boston, R.S., (2001). Ribosome-inactivating proteins : a plant perspective. *Annu. Rev. Plant Physiol. Plant Mol. Biol.* 52, 785-816.
- Park, Vepachedu, R., Sharma, N., and Vivanco, J.M. (2004). Ribosome-inactivating proteins in plant biology. *Planta* 219, 1903-1906.
- Peumans, W.J., Hao, Q. and Van Damme, E.J.M. (2001). Ribosome-inactivating protein from plants: more than RNA N-glycosidases? *FASEB J.* 15, 1493-1506.
- Sawasaki, T., Nishihara, M., and Endo, Y. (2008). RIP and RALyase cleave the sarcin/ricin domain, a critical domain for ribosome function, during senescence of wheat coleoptiles. *Biochem Biophys Res Commun*, 370(4):561-5.
- Sikriwal, D., Ghosh, P., and Batra, JK., (2008). Ribosome inactivating protein saporin induces apoptosis through mitochondrial cascade, independent of translation inhibition. *Int J Biochem Cell Biol*, 40(12):2880-8
- Sribash, R., Sadhana, P., and Begum, M., (2006). Purification, characterization and cloning of antiviral/ribosome inactivating protein from *Amaranthus tricolor* leaves
- Stirpe, F., Gasperi, Campani, A., Barbieri, L., Falasca, A. I., Abbondanza, A., and Stevens, W.A. (1983). Ribosome-inactivating proteins from the seeds of *Saponaria officinalis* L. (soapwort), *Agrostemma githago* L. (corn cockle), *Asparagus officinalis* L. (asparagus) and from the latex of *Hura crepitans* L. (sandbox tree). *Biochem. J.*, 216, 617.
- Stirpe, F., Barbieri, L., Batelli, M.G., Soria, M., and Lappi, D.A. (1992). Ribosome inactivating proteins from plants: present status and future prospects, *BioTechnology*. 10:405-412.
- Taylor, B.E., and Irvin, J.D. (1990). Depurination of plant ribosomes by pokeweed antiviral proteins. *FEBS lett*, 273:144-146.
- Taylor, S., Massiah, A., Lomonosoff, G., Roberts, L.M., Lord, J.M., and Hartley, M. (1994). Correlation between the activities of five ribosome-inactivating proteins in depurination of tobacco mosaic virus infection. *Plant J* 5(6):827-835.
- Tumer, N.E., Hwang, D.J., and Bonness, M., (1997). C-terminal deletion mutant of Pokeweed antiviral protein inhibits viral infection but does not depurinate host ribosomes. *Proc. Natl. Acad. Sci. USA*, 94, 3866-3871.
- Van Damme, E.J.M., Hao, Q., Chen, Y., Barre, A., Vandenbussche, F., Desmyter, S., Rouge, P. and Peumans, W.J. (2001). Ribosome-inactivating proteins: a family of plant proteins do more than inactivate ribosomes. *Crit. Rev. plant Sci.* 20, 395-465.
- Vandenbussche, F., Desmyter, s., Ciani, M., Proost, P., Peumans, W.J., and Van Damme, E.J.M., (2004). Analysis of the in planta antiviral activity of elderberry ribosome-inactivating proteins. *Eur.J.Biochem.* 271, 1508-1515.
- Vepachedu, R., Park, SW., Sharma, N., and Vivanco, JM., (2005). Bacterial expression and enzymatic activity analysis of ME1, a ribosome-inactivating protein from *Mirabilis expansa*. *Protein Expr Purif*, Mar; 40(1):142-51
- Verma, H.N., Srivastava, S., Kumar, V., Kumar, D., (1996). Induction of systemic resistance in plants against viruses by a basic protein from *Clerodendrum aculeatum* leaves. *Biochem. Cell Biol.* 86, 485-491.
- Watanabe, K., Kawasaki, T., Sako, N., and Funatsu, G. (1997). Actions of pokeweed antiviral protein on virus-infected protoplasts. *Bioscience, Biotechnology and Biochemistry*, 61: 6, 994-997.
- Zoubenko, O., Hudak, K. and Tumer, N.E., (2000). A non-toxic pokeweed antiviral protein mutant inhibits pathogen infection via a novel salicylic acid-independent pathway. *Plant Mol.Biol.* 44, 219-229.



# Novel Chiral Compound: (*R*) and (*S*) 1-(2-Benzyloxy-3-Methoxyphenyl)-2,2,2-Trichloroethyl Benzenesulfonate, Synthesis and characterization

Mohammed Hadi Al-Douh

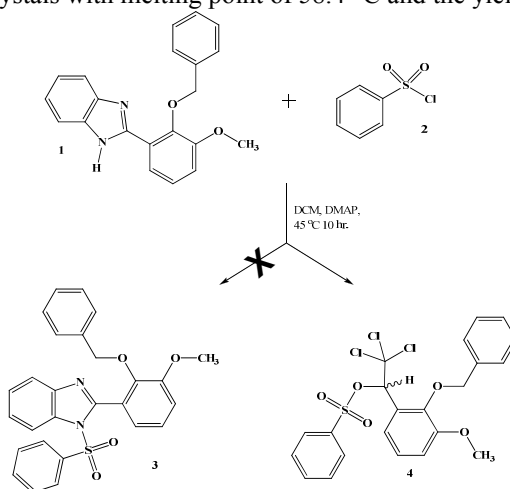
Chemistry Department, Faculty of Science, Hadhramout University of Science and Technology (HUST),  
50512, Mukalla, Hadhramout, Republic of Yemen  
mhd\_douh@yahoo.com

**Abstract:** The reaction between benzimidazole **1** and benzenesulfonyl chloride **2** in dichloromethane (DCM) at 45 °C for 10 hr in the presence of dimethyl aminopyridine (DMAP) as a catalyst was expected to obtain 2-(2-benzyloxy-3-methoxyphenyl)-1-(phenylsulfonyl)-1*H*-benzimidazole, **3**. Unfortunately, a novel chiral compound (*R*) and (*S*) 1-(2-benzyloxy-3-methoxyphenyl)-2,2,2-trichloroethyl benzenesulfonate **4** was obtained as a single crystal (59% yield) with melting point of 58.4 °C. However, the mechanism of this reaction still is under investigation. The molecular structure of this compound was confirmed by FTIR, HRMS, X-Ray crystallography, 1D and 2D NMR spectroscopy. The crystal of **4** is in the monoclinic space group *P*2<sub>1</sub>/*c* with *a* = 8.1638 (1) Å, *b* = 8.8536 (1) Å, *c* = 30.7221 (5) Å,  $\beta$  = 90.670 (1)°, *D*<sub>calc</sub> = 1.501 μg m<sup>-3</sup>, *V* = 2220.41 (5) Å<sup>3</sup> and *R*<sub>int</sub> = 0.059. The complete assignments of **4** were made using 1D and 2D NMR including APT, DEPT-135, COSY, HMQC and HMBC in CDCl<sub>3</sub>.

**Key words:** <sup>1</sup>H NMR; <sup>13</sup>C NMR; 2D NMR; X-Ray Crystallography; 2,2,2-Trichloroethyl Benzenesulfonate.

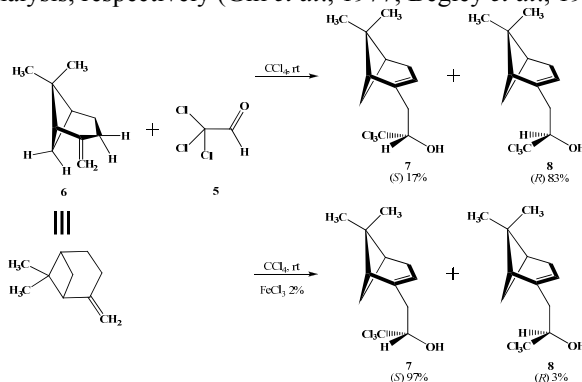
## Introduction

The reaction between benzimidazole **1** and benzene sulfonyl chloride **2** in DCM at 45 °C for 10 hr in the presence of DMAP as a catalyst was hoped to obtain 2-(2-benzyloxy-3-methoxyphenyl)-1-(phenylsulfonyl)-1*H*-benzimidazole **3** (Li *et al.*, 2006), but it was given (*R*) and (*S*) 1-(2-benzyloxy-3-methoxyphenyl)-2,2,2-trichloroethyl benzenesulfonate **4** (Al-Douh *et al.*, 2007, Scheme 1). It was obtained as single crystals with melting point of 58.4 °C and the yield was 59%.

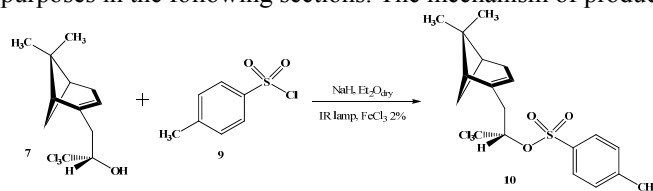


Scheme 1: Synthetic route towards the compound **4**.

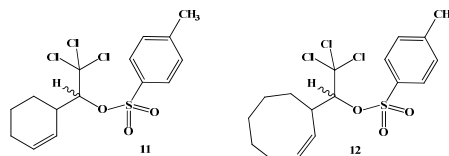
The addition of chloral **5** to (–)-(1*S*,5*S*)-pin-2(10)-ene **6** was formed diastereoisomers (*S*) **7** and (*R*) **8** with ratio 17:83, while the ratio was enhanced in the presence of FeCl<sub>3</sub> 2% as a bulky Lewis acid catalyst to 97:3, which were confirmed by <sup>1</sup>H and <sup>13</sup>C NMR experiments and X-ray analysis, respectively (Gill *et al.*, 1977; Begley *et al.*, 1978, Scheme 2).



Scheme 2: Gill *et al.* method to prepare derivative of **4**. Begley *et al.* (1978) were synthesized derivatives of **4** from the reaction of **7** with toluene-*p*-sulphonyl chloride or tosyl chloride **9** to produce **10** as (*S*) diastereoisomer (Scheme 3), while Gill *et al.* (1979) were synthesized other derivatives from the reaction of cyclohex-1-ene and cycloocta-1-ene with **9** to produce **11** and **12** as diastereoisomers (*R*) and (*S*), respectively (Scheme 4). Figure 1 shows the chemical structure and the numbering scheme of **4** for discussion purposes in the following sections. The mechanism of produce **4** still is unknown.



Scheme 3: Derivative **10** was prepared by Begley *et al.*



Scheme 4: Other derivatives of **4** were prepared by Gill *et al.*

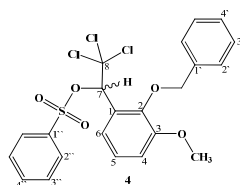


Figure 1: The chemical structure and the numbering scheme of **4**.

## Experimental Part

### General

All NMR experiments were performed on *Bruker Avance 400 Ultrashield*<sup>TM</sup> NMR for <sup>1</sup>H, operating at 400.132 MHz, and *Bruker Avance 300* NMR spectrometers for <sup>13</sup>C, operating at 71.478 MHz at 298 K using *Bruker XWINNMR* software equipped with a 5 mm BBI inverse gradient and QNP probes, respectively (Bruker, 1999; Berger and Braun, 2004). Chemical shifts were reported downfield in parts per million (ppm) from a tetramethylsilane (TMS) reference, and coupling constants (*J*) were measured in Hz. The concentration of solute molecule was 25 mg in 1.0 mL CDCl<sub>3</sub>.

High-resolution mass spectrum (HRMS) was recorded by a *Bruker Daltonics' micrOTOF-Q*<sup>TM</sup> mass spectrometer, operated in electrospray ionization source ESI mode. In DCM, the sample was prepared in 1.0 μL–1.0 mL/min. The crystal structure was determined by an *APEX2 Bruker* (APEX2, 2005) and *SHELXTL* (Sheldrick, 1998, 2008) crystallographic software packages for determining molecular structure, and Infrared spectrum was recorded on a *Perkin-Elmer 2000 FT* spectrometer and was expressed in cm<sup>-1</sup>. The compound was prepared using KBr cells. Melting point (uncorrected) was determined on Stuart melting point apparatus.

### Synthesis

The synthetic method of **4** was described previously (Li *et al.*, 2006; Al-Douh *et al.*, 2007).

## Results and Discussion

### FTIR Spectroscopy

The FTIR spectrum of **4** is depicted in Figure 2 and selected FTIR data are listed in Table 1. The bands with weak intensity observed of benzene rings at 3096, 3067 and 3028 cm<sup>-1</sup> are ascribed to the stretching of aromatic ν C=C–H. The bands observed at 2948 and 2873 cm<sup>-1</sup> are assigned to ν<sub>as</sub> and ν<sub>s</sub> CH<sub>3</sub> of methoxy group, respectively, while the bands observed at 2927 and 2855 cm<sup>-1</sup> assigned to ν<sub>as</sub> and ν<sub>s</sub> CH<sub>2</sub> of methylene group, respectively.

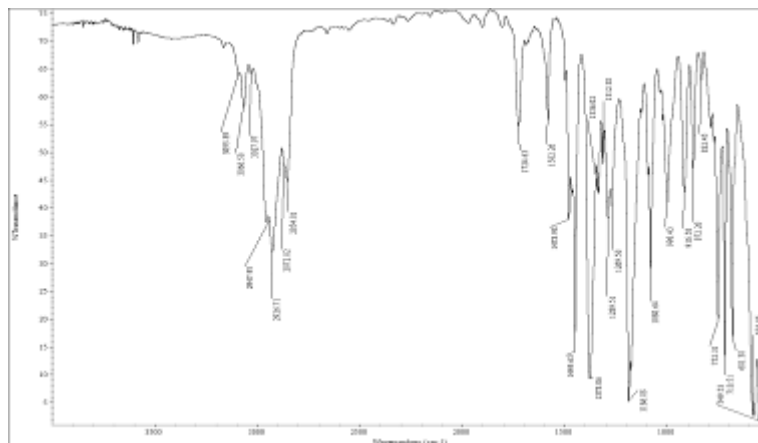


Figure 2: FTIR spectrum of **4**.

The asymmetrical bending vibration of  $\delta_{as}$  CH<sub>3</sub> occurred at 1479 cm<sup>-1</sup>, while the symmetrical bending vibration of  $\delta_s$  CH<sub>3</sub> appeared at 1336 cm<sup>-1</sup>, and the CH<sub>2</sub> scissoring vibration  $\delta_s$  CH<sub>2</sub> appeared at 1450 cm<sup>-1</sup>. The strong intensity bands appeared at 1378 and 1187 cm<sup>-1</sup> are assigned to  $\nu_{as}$  and  $\nu_s$  SO<sub>2</sub> sulfonic esters (Silverstein *et al.*, 2005). The free  $\nu$ N–H stretching band of benzimidazole **1** at 3354 cm<sup>-1</sup> was disappeared (Al-Douh, 2010).

Table 1: FTIR spectral data of compound **4** (cm<sup>-1</sup>):

$\nu$ C–H arom.	$\nu$ CH <sub>3</sub> aliph.	$\nu$ CH <sub>2</sub> aliph.	$\delta$ CH <sub>3</sub>	$\delta$ CH <sub>2</sub>	$\nu$ S=O ester	$\nu$ C–O–C aliph.	$\nu$ C–Cl aliph.	$\nu$ aromatic
3096	as 2948	as 2927	as 1479	as	as 1378	as 1270	998	833, 752,
3067	sy 2873	sy 2855	sy 1336	1450	sy 1187	sy 1081	917	719,
3028							872	681, 577 & 550

### HRMS Spectra

Figure 3 shows the HRMS spectrum of **4**. The HRMS of **4** shows a molecular formula of C<sub>22</sub>H<sub>19</sub>Cl<sub>3</sub>NaO<sub>5</sub>S<sup>-</sup> at  $m/z$  522.9933 (M+Na<sup>+</sup>). The peaks at  $m/z$  523.9940, 524.9903, 525.9912, 526.9862, 527.9885 and 528.9830 for the isotopes of the benzenesulfonate **4**, M+2, M+4, M+6, M+8, M+10 and M+12, respectively, which it has three chlorine atoms (Silverstein *et al.*, 2005).

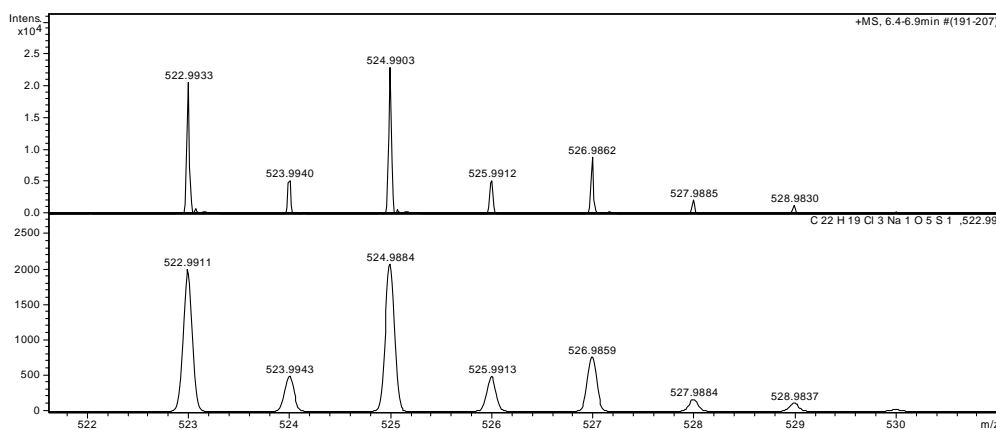


Figure 3: HRMS spectrum of **4**.

### <sup>1</sup>H NMR

The <sup>1</sup>H NMR spectrum in CDCl<sub>3</sub> of **4** was shown in Figure 4. The spectrum shows the chemical shift of the aromatic protons of the benzyloxy ring H<sub>2</sub> were observed signal as double doublet at  $\delta$  = 7.69–7.66 ppm ( $J$  = 8.46 and 1.19 Hz), and H<sub>3</sub> were exhibited signal as a triplet at  $\delta$  = 7.36–7.32 ppm ( $J$  = 7.92 Hz), while proton H<sub>4</sub> was displayed triplet at  $\delta$  = 7.52 ppm ( $J$  = 1.05 Hz), due to its coupled with H<sub>3</sub>. The signals as multiplet at  $\delta$  = 7.58–7.54, 7.48–7.43 and 7.41–7.38 ppm are proposed to be assigned to H<sub>2</sub>, H<sub>3</sub> and H<sub>4</sub> in the benzenesulfonyl ring, respectively. The double doublet were overlapped with CDCl<sub>3</sub> peak and were observed at  $\delta$  = 7.28–7.25 ppm ( $J$  = 7.56 and 1.82 Hz) was assigned to H<sub>6</sub> in the trisubstituted ring, while both protons H<sub>5</sub> and H<sub>4</sub> were observed two signals as triplet and double doublet at  $\delta$  = 7.06–7.01 and 7.00–6.96 ppm ( $J$  = 7.92, 8.21 and 1.83 Hz), respectively. The methoxy group OCH<sub>3</sub> of **4** was shown as singlet at  $\delta$  = 3.89 ppm, and the methine H<sub>7</sub> was also observed signal at  $\delta$  = 6.46 ppm as singlet.

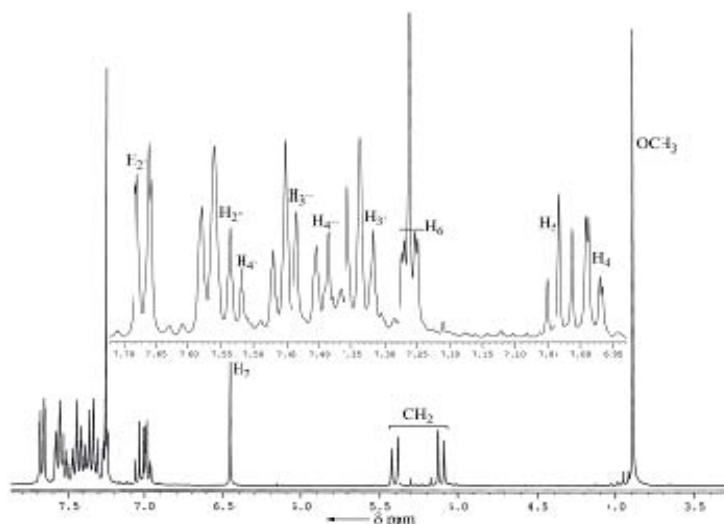


Figure 4:  $^1\text{H}$  NMR spectrum of **4** in  $\text{CDCl}_3$ .

On the other hand, the methylene group  $\text{CH}_2$  was exhibited signal as double doublet at  $\delta = 5.41\text{--}5.12$  ppm, ( $J = 88.34$  and  $11.48$  Hz). These values of coupling constant are unexpected specially  $88.34$  Hz. We suggest the reasons of these values to be due to the configuration of those hydrogen atoms between benzyloxy ring and the 2,2,2-trichloroethyl benzenesulfonate group, which  $^1\text{H}\text{--}^1\text{H}$  COSY experiment was performed to further confirmed the assigned peak between the methine proton  $\text{H}_7$  with one proton of methylene group  $\text{CH}_2$  and one proton of benzene ring  $\text{H}_2$  (see  $^1\text{H}\text{--}^1\text{H}$  COSY analysis, Figure 7), while  $^1\text{H}\text{--}^{13}\text{C}$  HMBC experiment was performed to further confirmed the assigned peak between the protons of benzene ring  $\text{H}_2$  and the protons of methylene group  $\text{CH}_2$  (see  $^1\text{H}\text{--}^{13}\text{C}$  HMBC, Figure 11). Additionally, the crystal structure of **4** confirmed the posture of that groups (see X-ray analysis, Figures 5, 13 and 14).

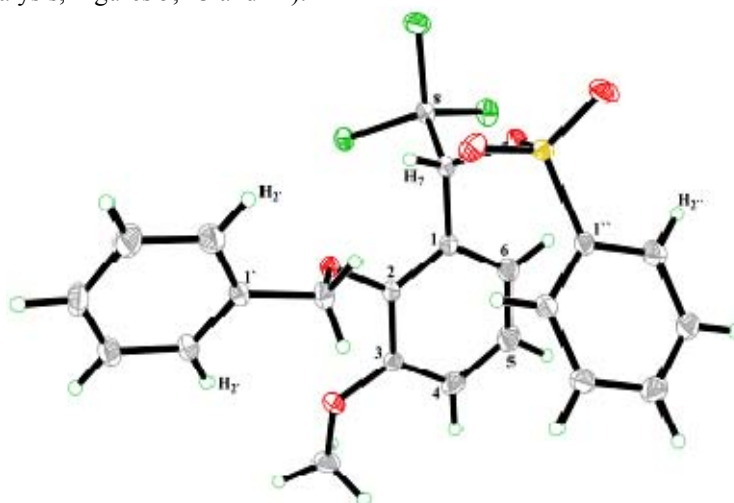
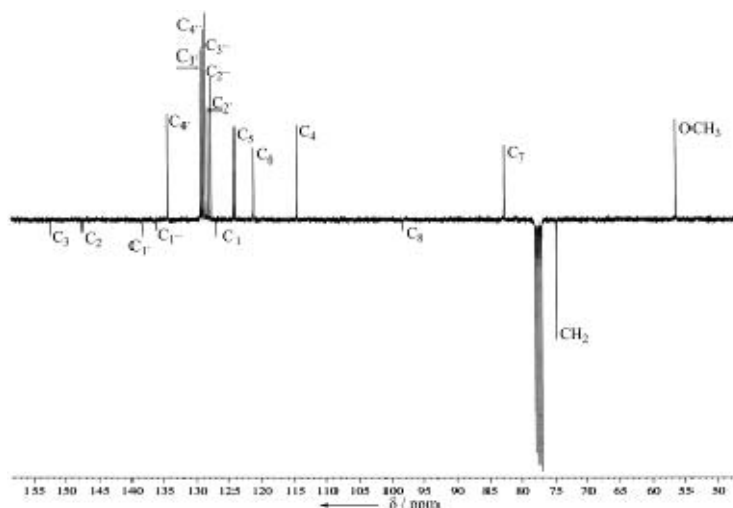


Figure 5: The crystal structure of **4**.

### $^{13}\text{C}$ APT NMR

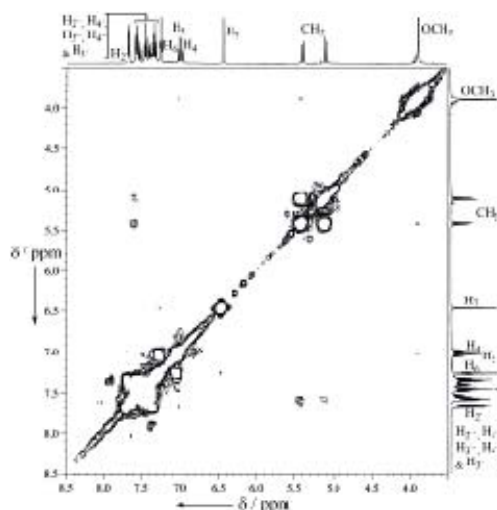
The  $^{13}\text{C}$  NMR spectrum of **4** was obtained with using APT NMR experiment and shown in Table 2 and Figure 6. The peak in  $\text{CDCl}_3$  appears at  $\delta = 56.26$  ppm of **4** was assigned to the methoxy group  $\text{OCH}_3$ , while methylene group  $\text{CH}_2$  and methine carbon  $\text{C}_7$  were showed at  $\delta = 74.79$  and  $82.70$  ppm, respectively. The quaternary carbon signals were observed at  $\delta = 152.42$ ,  $147.40$ ,  $138.35$ ,  $136.18$ ,  $126.84$  and  $98.35$  ppm for  $\text{C}_3$ ,  $\text{C}_2$ ,  $\text{C}_{1'}$ ,  $\text{C}_{1''}$ ,  $\text{C}_1$  and  $\text{C}_8$ , respectively. Other aromatic carbon signals of benzenesulfonyl ring were observed at  $\delta = 128.97$ ,  $128.56$  and  $127.62$  ppm for  $\text{C}_{4'}$ ,  $\text{C}_{3'}$  and  $\text{C}_{2'}$ , respectively, while  $\text{C}_4$ ,  $\text{C}_6$  and  $\text{C}_5$  at the trisubstituted aromatic carbon showed signals at  $\delta = 114.47$ ,  $121.13$  and  $124.08$  ppm, respectively. Aromatic carbons of benzyloxy ring observed signals of  $\text{C}_{2'}$ ,  $\text{C}_{3'}$  and  $\text{C}_{4'}$  at the respective  $\delta = 128.16$ ,  $129.31$  and  $134.30$  ppm. Table 2 summarizes the  $^1\text{H}$  and APT NMR of **4** in  $\text{CDCl}_3$ .

Figure 6: APT NMR spectrum of **4** in  $\text{CDCl}_3$ .**Table 3.**  $^1\text{H}$  and  $^{13}\text{C}$  APT NMR chemical shifts (ppm) and coupling constants (Hz) of **4** in  $\text{CDCl}_3$ :

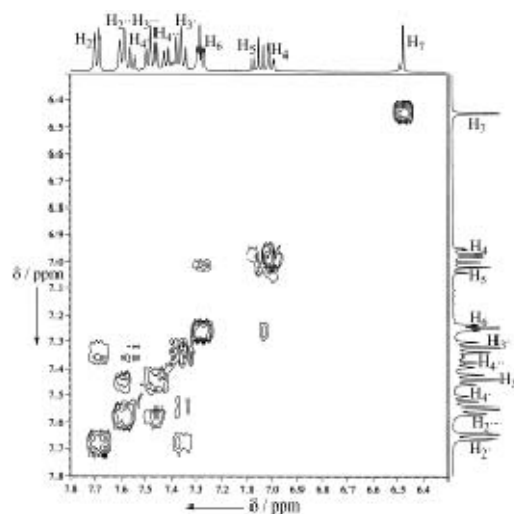
Atom No.	$^1\text{H}$ NMR		$^{13}\text{C}$ NMR
	$\delta$	$J$	$\delta$
$\text{OCH}_3$	3.89, <i>s</i>	—	56.26
$\text{CH}_2$	5.41–5.12, <i>dd</i>	88.34, 11.48	74.79
1	—	—	126.84
2	—	—	147.40
3	—	—	152.42
4	7.00–6.96, <i>dd</i>	8.21, 1.83	114.47
5	7.06–7.01, <i>t</i>	7.92	124.08
6	7.28–7.25, <i>dd</i>	7.56, 1.82	121.13
7	6.46, <i>s</i>	—	82.70
8	—	—	98.35
1'	—	—	138.35
2'	7.69–7.66, <i>dd</i>	8.46, 1.19	128.16
3'	7.36–7.32, <i>t</i>	7.92	129.31
4'	7.52, <i>t</i>	1.05	134.30
1''	—	—	136.18
2''	7.58–7.54, <i>m</i>	—	127.62
3''	7.48–7.43, <i>m</i>	—	128.56
4''	7.41–7.38, <i>m</i>	—	128.97

 **$^1\text{H}$ – $^1\text{H}$  COSY**

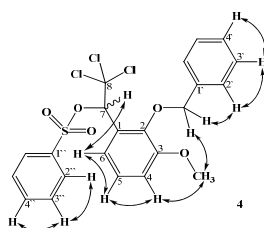
Figures 7 and 8 were shown the  $^1\text{H}$ – $^1\text{H}$  COSY NMR spectra of **4** in  $\text{CDCl}_3$  and the most important correlations observed were shown in Figure 9. In COSY spectrum confirmed the correlation assignments of  $\text{H}_4$  with methoxy group  $\text{OCH}_3$  and one proton of methylene group  $\text{CH}_2$  in benzyloxy ring at  $\delta = 3.89$  and 5.41 ppm, respectively, but low correlation were observed with the second proton of  $\text{CH}_2$  at  $\delta = 5.12$  ppm.

Figure 7:  $^1\text{H}$ – $^1\text{H}$  COSY NMR spectrum of **4** in  $\text{CDCl}_3$ .

On the other side, both CH<sub>2</sub> protons were correlated with H<sub>3'</sub> in the benzyloxy ring, but the second proton showed more correlated with H<sub>3'</sub> than the other one. The methine proton H<sub>7</sub> was observed assignment with H<sub>6</sub> in the trisubstituted ring at  $\delta = 7.28\text{--}7.25$  ppm. In the trisubstituted ring, proton H<sub>4</sub> in **4** showed  $^3J$  with H<sub>5</sub> at  $\delta = 7.06\text{--}7.01$  ppm, while proton H<sub>5</sub> was showed  $^3J$ -correlation with both H<sub>4</sub> and H<sub>6</sub> protons at  $\delta = 7.00\text{--}6.96$  and  $7.28\text{--}7.25$  ppm, respectively. However, the correlations between H<sub>3'</sub> with both protons H<sub>2'</sub> and H<sub>4'</sub> in benzyloxy ring were shown clearly at  $\delta = 7.69\text{--}7.66$  and  $7.52$  ppm, respectively, while in the benzenesulfonyl ring, H<sub>3''</sub> was observed  $^3J$ -correlation with H<sub>2''</sub> at  $\delta = 7.58\text{--}7.54$  ppm (Figure 8).



**Figure 8:**  $^1\text{H}$ - $^1\text{H}$  COSY NMR spectrum of the aromatic protons range of **4**.



**Figure 9:** The most important correlations observed in COSY spectrum of **4**.

 $^1\text{H}-^{13}\text{C}$  HMQC

The HMQC NMR spectrum for **4** was shown in Figure 10 in CDCl<sub>3</sub>. The signals owing to C<sub>4'</sub>, C<sub>3'</sub>, C<sub>4''</sub>, C<sub>3''</sub>, C<sub>2'</sub>, C<sub>2''</sub>, C<sub>5</sub>, C<sub>6</sub> and C<sub>4</sub> atoms were observed at  $\delta$  = 134.30, 129.31, 128.97, 128.56, 128.16, 127.62, 124.08, 121.13 and 114.47 ppm. The one bond <sup>1</sup>H–<sup>13</sup>C connectivities were also well observed for OCH<sub>3</sub>, CH<sub>2</sub> and C<sub>7</sub> atoms whereby the cross peaks appeared at the respective  $\delta$  = 56.26, 74.79 and 82.70 ppm.

 $^1\text{H}-^{13}\text{C}$  HMBC

The HMBC NMR spectrum for **4** was shown in Figure 11 and the most important correlations observed shown in Figure 12. The long-range HMBC cross peaks of the methylene group CH<sub>2</sub> protons with C<sub>2</sub> and C<sub>1</sub> in the benzyloxy ring were appeared at  $\delta$  = 128.16 and 138.35 ppm, respectively. The HMBC cross peaks of the methoxy protons OCH<sub>3</sub> with C<sub>3</sub> was observed at  $\delta$  = 152.42 ppm. On the other hand, the methine proton H<sub>7</sub> was correlated with C<sub>8</sub>, C<sub>6</sub>, C<sub>1</sub> and C<sub>2</sub>, at  $\delta$  = 98.35, 121.13, 126.84 and 147.40 ppm, respectively.

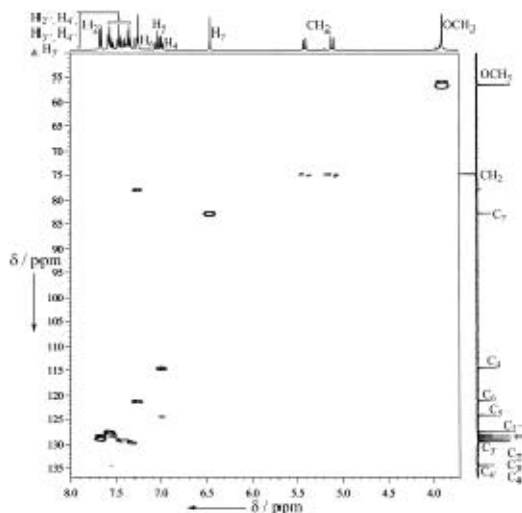


**Figure 10:**  $^1\text{H}$ - $^{13}\text{C}$  HMQC NMR spectrum of **4** in  $\text{CDCl}_3$ .



Additionally, the correlation between  $H_5$  with both  $C_1$  and  $C_3$ , both protons  $H_4$  and  $H_6$  with  $C_2$ , and  $CH_2$  with  $H_2'$  in the benzyloxy ring were observed clearly as  $^3J$ -correlation. The homonuclear connectivities were observed between protons in  $C_4$  with  $H_6$  and  $C_6$  with  $H_5$  as  $^3J$ -correlation, and  $C_5$  with both  $H_4$  and  $H_6$  as  $^2J$ -correlation. In addition,  $C_4'$  was correlated with  $H_2'$  in the same ring at  $\delta = 7.58$ – $7.54$  ppm, while  $C_1'$  was correlated as  $^3J$ -correlation with  $H_3'$  at  $\delta = 7.36$ – $7.32$  ppm. However, in the benzenesulfonyl ring, the homonuclear connectivities were shown between  $C_{1''}$  with  $H_{3''}$  as  $^3J$ -correlation. Other observed correlations between the aromatic protons and the carbons were showed in Table 3. All these correlation assignments were demonstrated and consistent with the crystal structure of **4**. Table 3 summarizes the values of COSY, HMQC and HMBC experiments in  $CDCl_3$ .

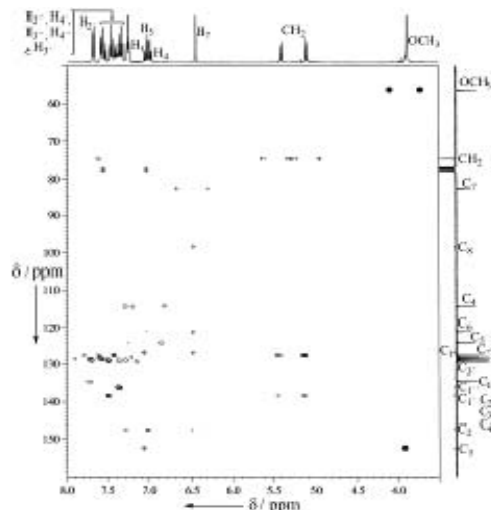


**Figure 11:**  $^1H$ – $^{13}C$  HMBC NMR spectrum of **4** in  $CDCl_3$ .

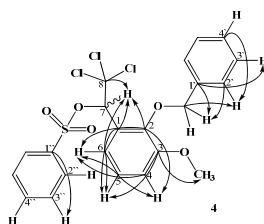


**Figure 12:** The most important correlations observed in HMBC spectrum of **4**.

**Table 3:** 2D  $^1H$ – $^1H$  COSY,  $^1H$ – $^{13}C$  HMQC and HMBC correlations for **4** in  $CDCl_3$ :

Atom No.	COSY $^1H$ – $^1H$	HMQC $^1J$	$^2J$	HMBC $^3J$	$^4J$
OCH <sub>3</sub>	CH <sub>2</sub> , H <sub>4</sub>	56.26	—	152.42, C <sub>3</sub>	—
CH <sub>2</sub>	OCH <sub>3</sub> , H <sub>2'</sub>	74.79	138.35, C <sub>1'</sub>	128.16, C <sub>2'</sub>	—
H <sub>4</sub>	OCH <sub>3</sub> , H <sub>5</sub>	114.47	124.08, C <sub>5</sub>	147.40, C <sub>2</sub>	—
H <sub>5</sub>	H <sub>4</sub> , H <sub>6</sub>	124.08	121.13, C <sub>6</sub>	152.42, C <sub>3</sub>	—
H <sub>6</sub>	H <sub>5</sub> , H <sub>7</sub>	121.13	124.08, C <sub>5</sub>	114.47, C <sub>4</sub>	—
				147.40, C <sub>2</sub>	
H <sub>7</sub>	H <sub>6</sub>	82.70	98.35, C <sub>8</sub>	121.13, C <sub>6</sub>	—
			126.84, C <sub>1</sub>	147.40, C <sub>2</sub>	
H <sub>2'</sub>	H <sub>3'</sub>	128.16	— <sup>x</sup>	74.79, CH <sub>2</sub>	—
				134.30, C <sub>4'</sub>	
H <sub>3'</sub>	H <sub>2'</sub> , H <sub>4'</sub>	129.31	— <sup>x</sup>	138.35, C <sub>1'</sub>	—
H <sub>4'</sub>	H <sub>3'</sub>	134.30	— <sup>x</sup>	— <sup>x</sup>	—
H <sub>2''</sub>	H <sub>3''</sub>	127.62	— <sup>x</sup>	— <sup>x</sup>	—
H <sub>3''</sub>	H <sub>2''</sub> , H <sub>4''</sub>	128.56	— <sup>x</sup>	136.18, C <sub>1''</sub>	—
H <sub>4''</sub>	H <sub>3''</sub>	128.97	— <sup>x</sup>	— <sup>x</sup>	—

<sup>x</sup>: is not observed

### X-Ray Crystallography

The previous results of **4** by FTIR, HRMS,  $^1H$  NMR and  $^{13}C$  NMR were consistent with the result of X-ray crystallography, which the golden single crystal of **4** was obtained and determined by X-ray crystallography, Figures 13 and 14. Bond lengths and angles in **4** have normal values, and are comparable with those in the related structures (Begley *et al.*, 1978; Gill *et al.*, 1979). The methoxy group at C9 is slightly twisted from the plane of the attached benzene ring C22–O2–C9–C10 with a torsion angle of  $-18.96$  ( $14$ )°. The dihedral angle between the benzene rings [(C1–C6) and (C8–C13)] is  $22.64$  ( $5$ )° whereas the torsion angle of C8–O1–C7–C6 is  $-157.96$  ( $7$ )°. In the crystal structure, the intramolecular C7–H7B...O2 interaction generated

an  $S(6)$  ring motifs, while other intramolecular  $C14-H14A \cdots O1$ ,  $C14-H14A \cdots O3$  and  $C21-H21A \cdots O3$  interactions generate  $S(5)$  ring motifs (Bernstein *et al.*, 1995), Table 4, Figure 13. The molecules of benzenesulfonate **4** are linked by short inter  $Cl2 \cdots O4^{ii}$  contact of 3.0170 (8) Å (symmetry code: (ii)  $-x, -y, -z$ ) into cyclic centrosymmetric  $R^2_2$  (12) dimers. These dimers are interlinked by the  $C3-H3A \cdots O2^i$  (symmetry code: (i)  $-x, y + 1/2, -z + 1/2$ ) intermolecular interactions, Figure 14. H atoms were placed in calculated positions and constrained to ride on their carrier atoms, with C–H distances in the range 0.93–0.98 Å. Table 4 shows the summarized value for inter and intra hydrogen bonds of **4**. The crystal data of **4** was showed in Table 5 (Al-Douh *et al.*, 2007).

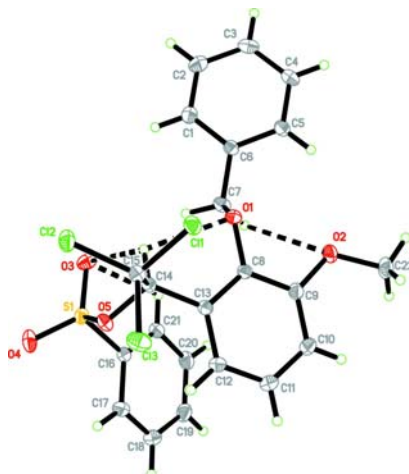


**Figure 13:** The crystal structure of **4** showing 50% probability displacement ellipsoids and the atomic numbering. The dashed lines indicate intramolecular hydrogen bonds.

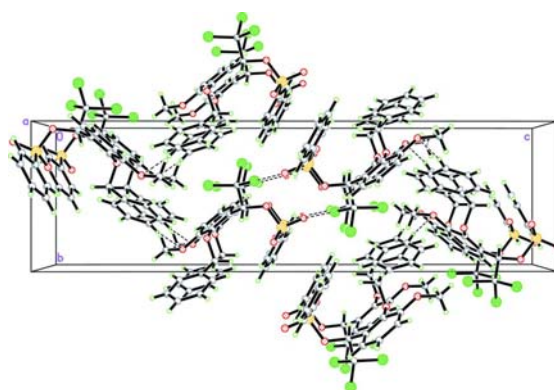


**Figure 14:** The crystal packing of **4**, viewed down the  $a$  axis. The intermolecular  $C-H \cdots O$  hydrogen bonds and the short inter  $Cl \cdots O$  contacts are shown as dashed lines.

**Table 4:** Hydrogen bond geometry of **4** (Å, °):

$D-H \cdots A$	$D-H$	$H \cdots A$	$D \cdots A$	$D-H \cdots A$
$C7-H7B \cdots O2$	0.97	2.56	3.040 (1)	110
$C14-H14A \cdots O1$	0.98	2.38	2.820 (1)	107
$C14-H14A \cdots O3$	0.98	2.34	2.838 (1)	111
$C21-H21A \cdots O3$	0.93	2.55	2.919 (1)	104
$C3-H3A \cdots O2^i$	0.93	2.49	3.414 (1)	172

Symmetry code: (i)  $-x, y + \frac{1}{2}, -z + \frac{1}{2}$

**Table 5:** Crystal data of **4**

Empirical formula, Formula weight	$C_{22}H_{19}Cl_3O_5S$ , 501.78
$T$ , $\lambda$	293(2) K, 0.71073 Å
Crystal system, space group	$P2_1/c$ , monoclinic
Unit cell dimensions	$a = 8.1638(1)$ Å, $b = 8.8536(1)$ Å, $c = 30.7221(5)$ Å, $\alpha = 90^\circ$ , $\gamma = 90^\circ$ , $\beta = 90.670(1)^\circ$
$V$ , Crystal size	$2220.41(5)$ Å <sup>3</sup> , $0.48 \times 0.30 \times 0.29$ mm
$Z$ , Calculated density	4, 1.501 µg/m <sup>3</sup>
$\mu$ , $F(000)$ , $\theta$	$0.54 \text{ mm}^{-1}$ , 1032, 1.33 to $40.00^\circ$
Limiting indices	$-14 \leq h \leq 14$ , $-16 \leq k \leq 16$ , $-54 \leq l \leq 54$
Reflections collected / unique	122837 / 13669 [ $R_{(int)} = 0.059$ ]
Data / restraints / parameters, $S$	11428 / 0 / 280, 1.08
Final $R$ indices [ $I > 2\sigma(I)$ ]	$R_1 = 0.040$ , $wR_2 = 0.108$
Largest diff. peak and hole	0.56 and $-0.55 \text{ e.Å}^{-3}$

## Conclusions

We have reported the complete assignments of the novel chiral compound (*R*) and (*S*) 1-(2-benzyloxy-3-methoxyphenyl)-2,2,2-trichloroethyl benzenesulfonate **4** using  $^1\text{H}$ ,  $^{13}\text{C}$  APT, COSY, HMQC and HMBC NMR in  $\text{CDCl}_3$ . Compound **4** was obtained as single crystal and it was studied by X-ray crystallography. Further, it using the compound in biologically important is in progress. The formation mechanism of **4** is in progress to identify.

## Acknowledgement

Thanks go to Hadhramout University of Science and Technology (HUST), Ministry of Higher Education and Scientific Research for HESR-HUST grant [1594/1/16/92] and for the financial support and to the Malaysian Government and Universiti Sains Malaysia (USM) for USM-RU-PGRS grant [1001/PKIMIA/842024] to conduct this work. Thanks to Assoc. Prof. Dr. Shafida A. Hamid, Kulliyah of Science, International Islamic University Malaysia (IIUM), Kuantan, Pahang, Assoc. Prof. Dr. Hasnah Osman School of Chemical Sciences, USM, Penang, Malaysia, for their help in chemical analyses, Prof. Dr. Hoong K. Fun and his team for X-ray crystallography analyses, X-ray Crystallography Unit, School of Physics, USM, Pulau Pinang, Malaysia and Prof. Dr. David S. Larsen and his team for HRMS analyses, Dept. of Chem., Univ. Otago, Dunedin, New Zealand.

## References

- Al-Douh, M. H. (2010). *Synthesis, Characterization and Anti-Proliferation Study of Some Benzimidazole Derivatives*. PhD thesis. Universiti Sains Malaysia (USM), Malaysia, ISBN: 978-3-8443-3294-0, LAP LAMBERT Academic Publishing GmbH & Co. KG, Dudweiler Landstr, 99, 66123 Saarbrücken, Germany.
- Al-Douh, M. H., Hamid, S. A., Osman, H., Ng, S. L. and Fun, H. K. (2007). (*R*) and (*S*)-1-(2-Benzyloxy-3-methoxyphenyl)-2,2,2-trichloroethyl benzenesulfonate. *Acta Crystallogr. E*, 63: o3233.
- APEX2 (Version 1.27), SAINT (Version 7.12A), and SADABS (Version 2004/1), (2005), Bruker AXS Inc., Madison, Wisconsin, USA.
- Begley, M. J., Gill, G. B. and Wallace, B. (1978). X-ray structure analysis of the tosylate ester of (1*S*,5*S*)-6,6-dimethyl-2-[(2*S*)-3,3,3-trichloro-2-hydroxypropyl] bicycle[3.3.1]hept-2-ene, the major product of the iron(III) chloride-catalysed *ene* addition of chloral to (–)-(1*S*,5*S*)-pin-2-(10)-ene. *J. Chem. Soc., Perkin Trans. 1*, 93.
- Berger, S. and Braun, S. (2004). *200 and more NMR experiments, A practical course*. Wiley-VCH, Weinheim, Germany, 44.
- Bernstein, J., Davis, R. E., Shimon, L. and Chang, N. L. (1995). Patterns in hydrogen bonding: Functionality and graph set analysis in crystals. *Angew. Chem. Int. Ed. Engl.*, 34: 1555.
- Bruker, Analytik GmbH program, (1999). NMR Suite Ver. 2.6.
- Gill, G. B., Marrison, K., Parrot, S. J. and Wallace, B. (1979). Stereoselection in the  $\text{AlCl}_3$ -catalysed *ene* additions of chloral to 1,2-dialkyl ethylenes. *Tetrahedron Lett.*, 50: 4867.
- Li, Y. F., Wang, G. F., He, P. L., Huang, W. G., Zhu, F. H., Gao, H. Y., Tang, W., Luo, Y., Feng, C. L., Shi, L. P., Ren, Y. D., Lu, W. and Zuo, J. P. (2006). Synthesis and anti-Hepatitis B virus activity of novel benzimidazole derivatives. *J. Med. Chem.*, 49: 4790.
- Sheldrick, G. M., *SHELXTL*. (Version 5.1), (1998). Program for the solution of crystal structures. Bruker AXS Inc., Madison, Wisconsin, USA.
- Sheldrick, G. M. (2008). A short history of *SHELX*. *Acta Crystallogr. A*, 64: 112.
- Silverstein, R. M., Webster, F. X. and Kiemle, D. J. (2005). *Spectrometric Identification of Organic Compounds*, WileyVCH, New York, USA, 72.

# Prediction of Slope Stability Using Statistical Method and Fuzzy Logic

Tarig Mohamed, Anuar Kasa, Muhammad Mukhlisin

Civil and Structural Engineering, The National University of Malaysia, Bangi, Selangor, 43600, Malaysia

tarigmohal@yahoo.com

**Abstract:** The main goal of this research is to predict the stability of slope using fuzzy logic, Adaptive Neuro Fuzzy Inference System (ANFIS), and statistical method, Multiple Linear Regression (MLR). Four limit equilibrium methods (LEM) i.e. Morgenstern-Price, Janbu, Bishop and Ordinary were used to calculate the safety factors for various designs of slope. For prediction, five parameters were used as the inputs i.e. height of slope, unit weight of slope material, angle of slope, coefficient of cohesion, and internal angle of friction, while the output parameters are factors of safety. MLR obtained regression square ( $R^2$ ) of 0.470 for Bishop, 0.459 for Janbu, 0.470 for Morgenstern-Price, and 0.468 for Ordinary Method, while ANFIS obtained regression square ( $R^2$ ) of 0.9996 for Bishop, 0.9994 for Janbu, 0.9995 for Morgenstern-Price, and 0.9997 for Ordinary Method. The result showed that ANFIS could predict the safety factors with high accuracy compare with MLR.

**Key words:** Fuzzy logic, Slope stability

## Introduction

Slopes either occur naturally or engineered by humans. Slope stability problems have been faced throughout history when men and women or nature has disrupted the delicate balance of natural soil slopes, so the slope failure become a common natural disaster which takes place around the world. In addition, the increasing demand for engineering cut and fill slopes on construction has only increase the need to understand analytical methods, investigative tools, and stabilization methods to solve slope stability problems. Slope stabilization methods involve specialty construction techniques that must be understood and modeled in realistic ways. An understanding of geology, hydrology, and soil properties is central to applying slope stability principles properly. Investigations of failures of soil masses are subjects touching both geology and engineering. These investigations call the joint efforts of engineering geologists and geotechnical engineers. Slope stability problem has been an important issue in geotechnical engineering. The evolution of slope stability analyses in geotechnical engineering has followed closely the developments in soil. Geotechnical engineers have to pay particular attention to geology, ground water, and shear strength of soils in assessing slope stability. Analyses must be based upon a model that accurately represents site subsurface conditions, ground behavior, and applied loads. Judgments regarding acceptable risk or safety factor must be made to assess the results of analyses. Therefore, slope investigation and classification are important for the community (Lee et al. 2002; Choobbasti et al. 2009; Ping et al. 2009; Vector 2008).

The limit equilibrium methods (LEMs) (i.e. linear methods: infinite slope analysis, wedge analysis, circular arc methods; non-linear methods: Bishop's routine method, Janbu's simplified method, Spencer's method, Morgenstern and Price's method, Janbu's rigorous analysis) are widely used for the analysis of slopes (Nash 1987). Historically, these methods were developed before the advent of computers; computationally more complex methods followed later. These computational methods have varying degrees of accuracy, depending on the suitability of the simplifying assumptions for the situation being analyzed. A useful concept in the application of limit equilibrium methods for slope stability analysis and design is the idea of mobilized shear strengths and mobilized shear strength parameters (Bromhead 1999; Sakellariou & Ferentinou 2005).

The power of Artificial Intelligent (AI) becomes more authoritative when the system is programmed to cater the need of complex applications. Adaptive Neuro-fuzzy Inference System (ANFIS) Model using neuro adaptive learning techniques which are similar to those of neural networks was originally presented by Jang. Given an input/output data sets, ANFIS constructs fuzzy Inference System (FIS) whose membership function (MF) parameters are adjusted using back propagation algorithm or other similar optimization techniques. Hence, the advantages of a fuzzy system can be combined with a learning algorithm (Sivarao et al. 2009; Merikoski et al. 2001; Jang 1996; MathWorks 2009 and Sakellariou & Ferentinou 2005).

Regression is most often used by scientists and engineers to visualize and plot the curve that best describes the shape and behavior of their data. As with most statistical analyses, the goal of regression is to summarize observed data as simply, usefully, and elegantly as possible. Researchers are often interested in the relationships between one variable and several other variables. Regression procedures find an association between independent and dependent variables that, when graphed on a Cartesian coordinate system, produces a straight line, plane or curve. The general purpose of Multiple Linear Regression (MLR) is to seek for the linear relationship between a dependent variable and several independent variables. (SigmaPlot 9 2004; SigmaPlot 11 2008; Sanford 2005; Xin & Xiaogang 2009).

The main objectives of this research are; calculate safety factors of various slopes using limit equilibrium methods (LEM), predict the result using Adaptive Neuro-fuzzy Inference System model and Multiple Linear Regression and develop a computer program to present the stability of slopes using Graphical User Interface (GUI).

## Method

In this research 210 different designs of slope which created by software that applied limit equilibrium methods were used. The range for the input parameters for those designs are: height of slope,  $H$  (1–6 m), unit weight of slope material,  $\gamma$  (15–22 kN/m<sup>3</sup>), angle of slope,  $\theta$  (11.31°–78.69°), coefficient of cohesion,  $c$  (0–50 kN/m<sup>2</sup>) and internal angle of friction,  $\phi$  (20°–40°) and the output is factors of safety. The comprehensive formulation of the software made it possible to easily analyze both simple and complex slope stability problems using a variety of methods to calculate the safety factors (Geo-Slope 2004). After carrying out the stability analyses, ANFIS model were used to predict the result for over all safety factors for all LEMs. The prediction constructed the rule statements based on the descriptions of the input and output variables defined with the fuzzy inference system. Another prediction method using Multiple Linear Regression applied for the same over all safety factors for all LEMs. From predicted data, Graphical User Interface program was generated to present the stability of slopes for all LEMs.

## Results and discussion

Five inputs, height of slope, unit weight of slope material, angle of slope, coefficient of cohesion, and internal angle of friction, and one output, factor of safety, were used as membership functions to build the fuzzy inference system with 243 rules and three epochs. On the other hand, the five input parameters and the over all output safety factors were used also for Multiple Linear Regression prediction.

The regression square ( $R^2$ ) which obtained by Adaptive Neuro-fuzzy Inference System prediction are 0.9996 for Bishop, 0.9994 for Janbu, 0.9995 for Morgenstern-Price, and 0.9997 for Ordinary Method, while the regression square ( $R^2$ ) which obtained by Multiple Linear Regression prediction are 0.470 for Bishop, 0.459 for Janbu, 0.470 for Morgenstern-Price, and 0.468 for Ordinary Method. Figure 1 until 4 for Bishop, Janbu, Morgenstern-Price, and Ordinary, respectively, showed the calculated values using SLOPE/W and the predicted values using Adaptive Neuro Fuzzy Inference System. The result showed that Adaptive Neuro Fuzzy Inference System could predict the safety factor with high accuracy and close to the target data. In addition, figure 5 until 8 for all LEMs, showed the calculated values using SLOPE/W and the predicted values using Multiple Linear Regression. The result showed that Multiple Linear Regression could predict the safety factor with low accuracy compared with Adaptive Neuro Fuzzy Inference System. Figure 9 until 12 showed the comparison between ANFIS and MLR prediction and the calculated data for all LEMs.

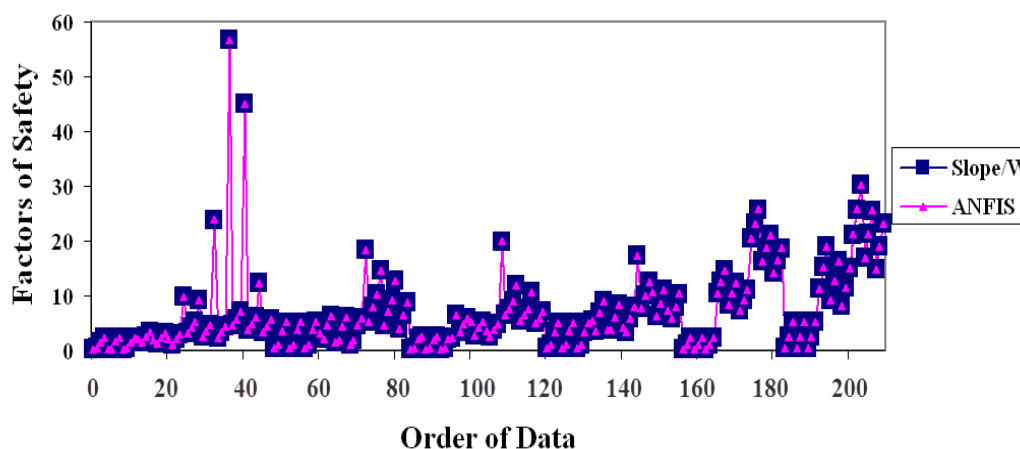


**Figure 1** Comparison of calculated factor of safety using Bishop and predicted using ANFIS

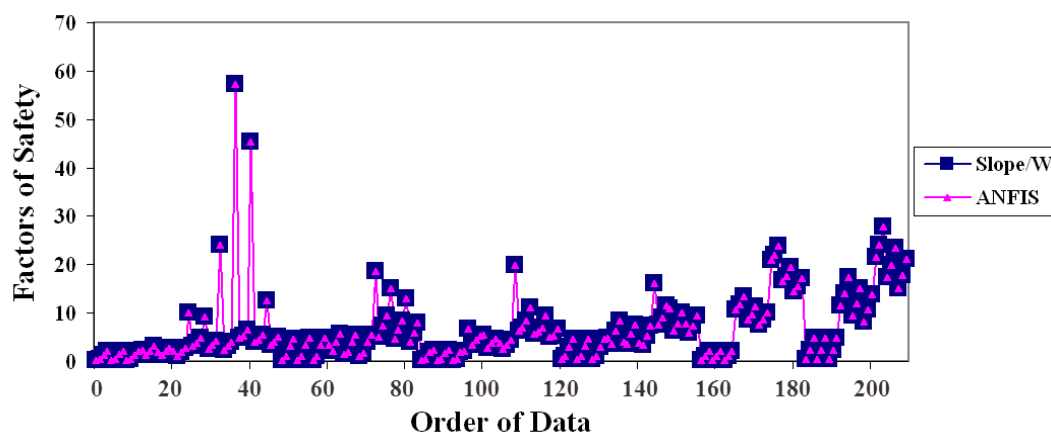


**Figure 2** Comparison of calculated factor of safety using Janbu and predicted using ANFIS

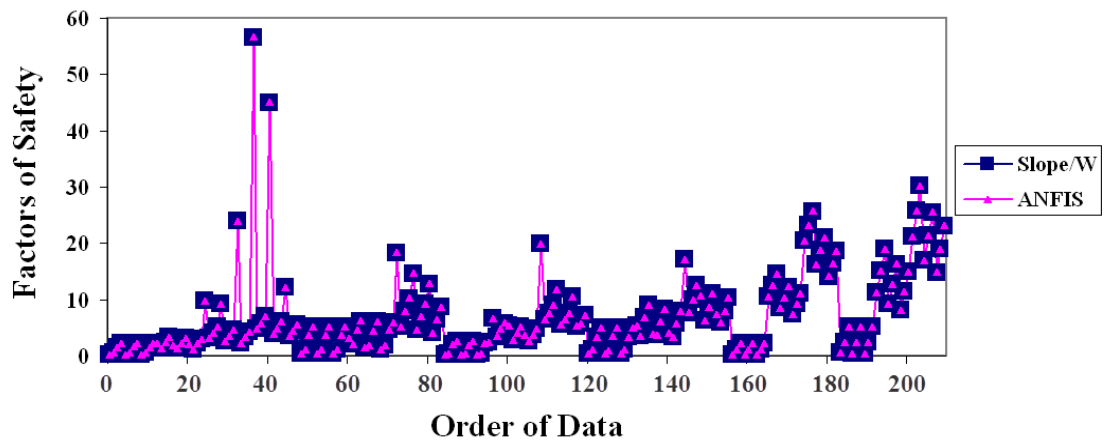


**Figure 3** Comparison of calculated factor of safety using Morgenstern-Price and predicted using ANFIS

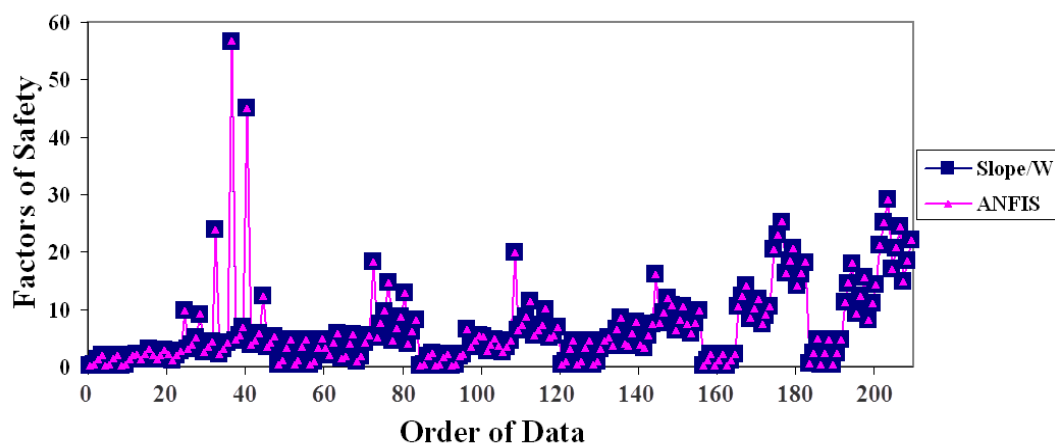


**Figure 4** Comparison of calculated factor of safety using Ordinary and predicted using ANFIS

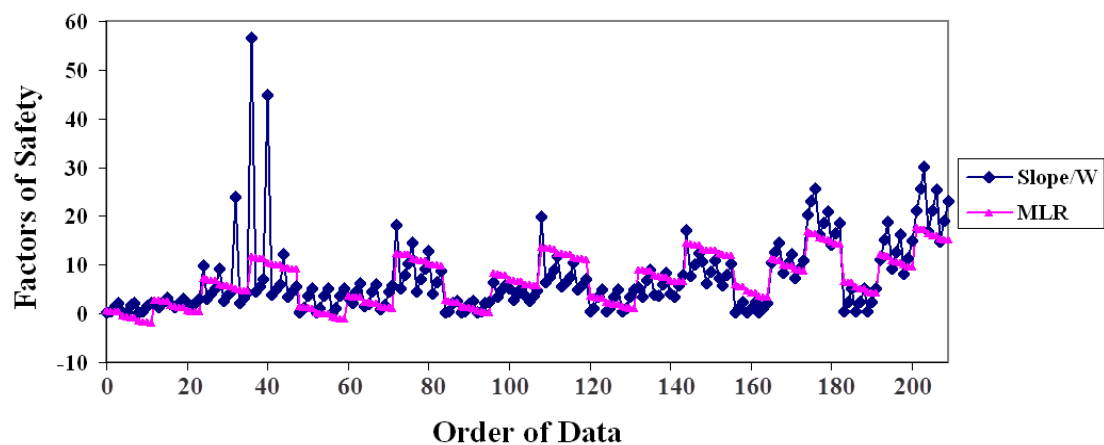


**Figure 5** Comparison of calculated factor of safety using Bishop and predicted using MLR



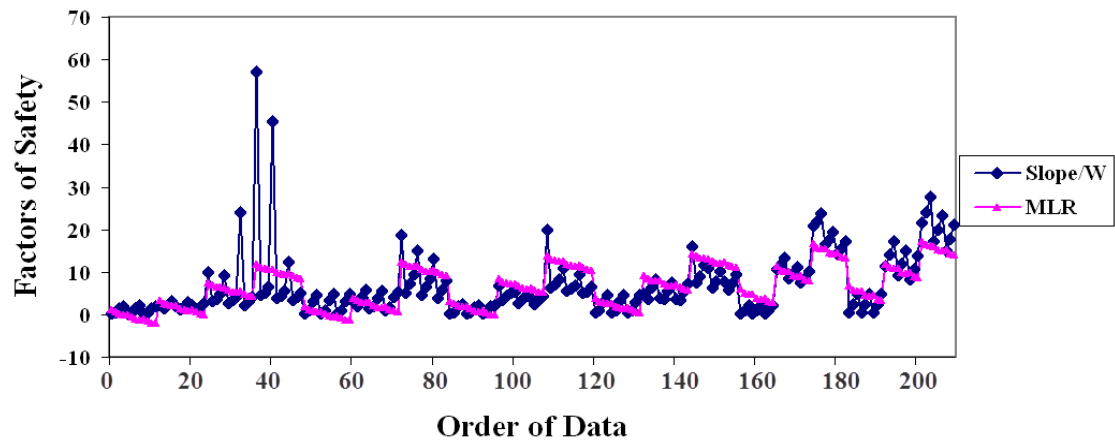


**Figure 6** Comparison of calculated factor of safety using Janbu and predicted using MLR

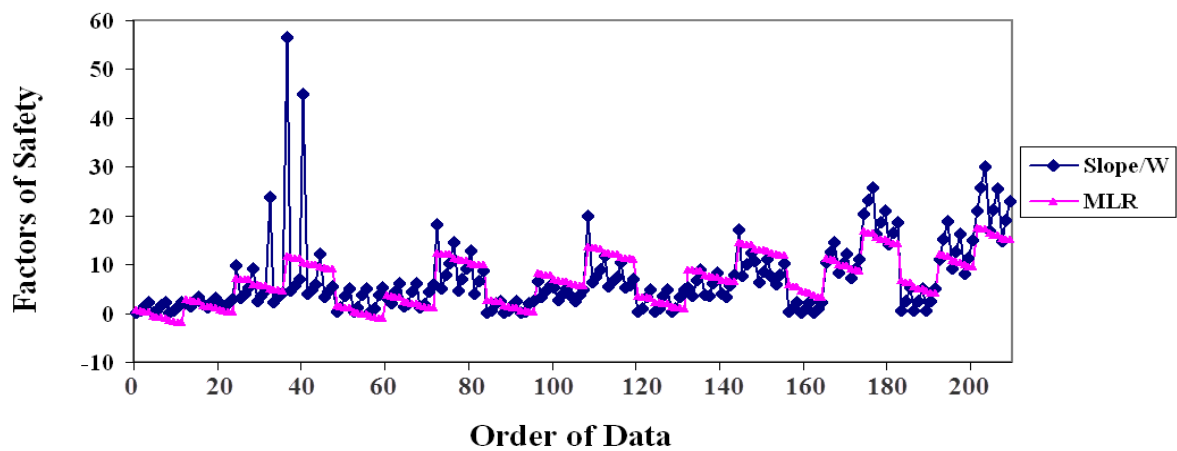


**Figure 7** Comparison of calculated factor of safety using Morgenstern-Price and predicted using MLR

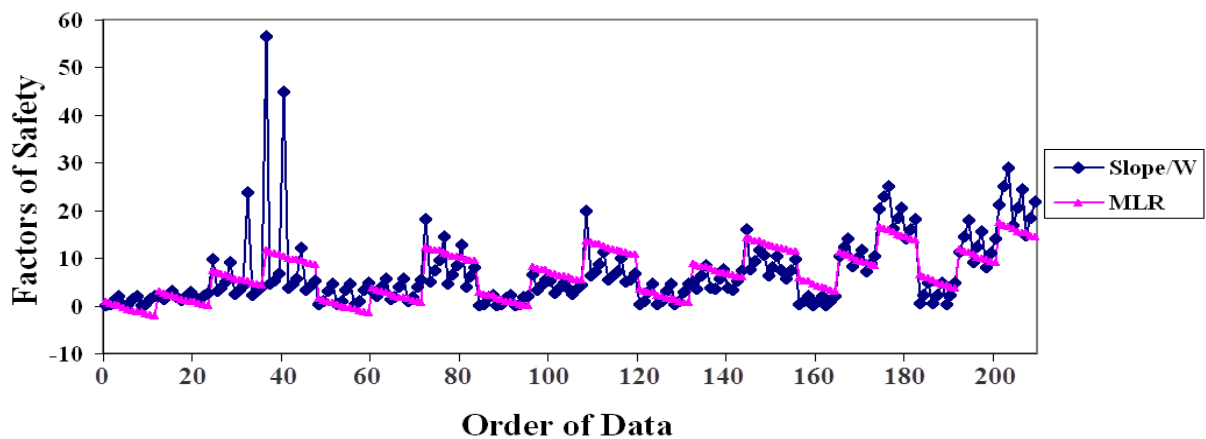


**Figure 8** Comparison of calculated factor of safety using Ordinary and predicted using MLR

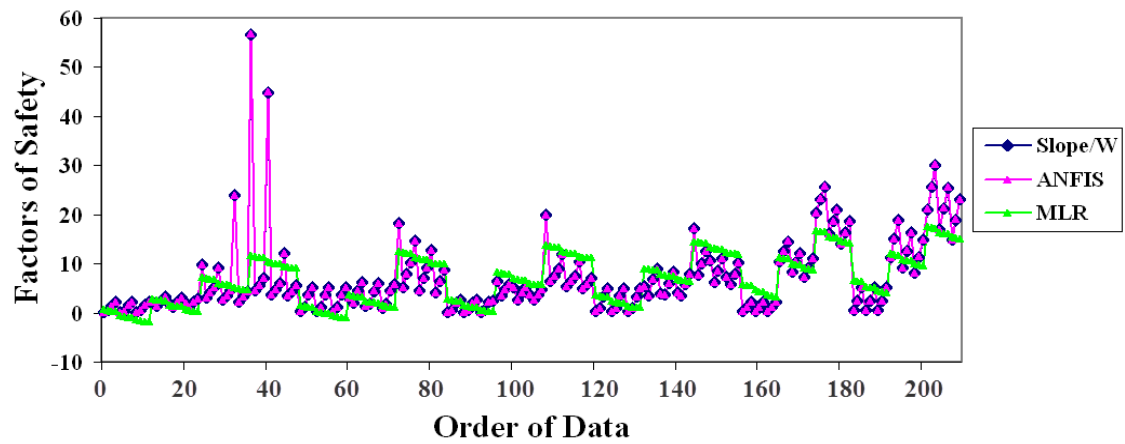


**Figure 9** Comparison of ANFIS and MLR for Bishop

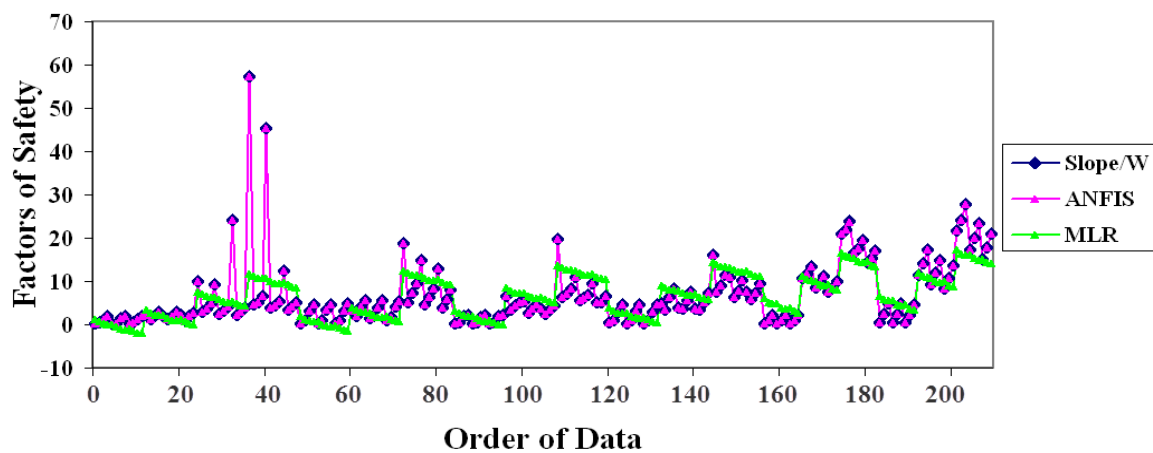


**Figure 10** Comparison of ANFIS and MLR for Janbu

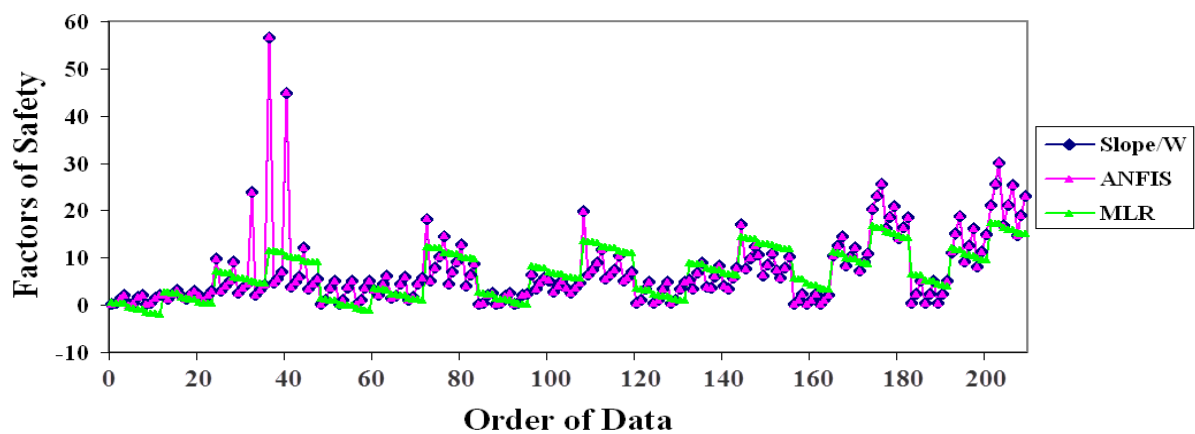


**Figure 11** Comparison of ANFIS and MLR for Morgenstern-Price

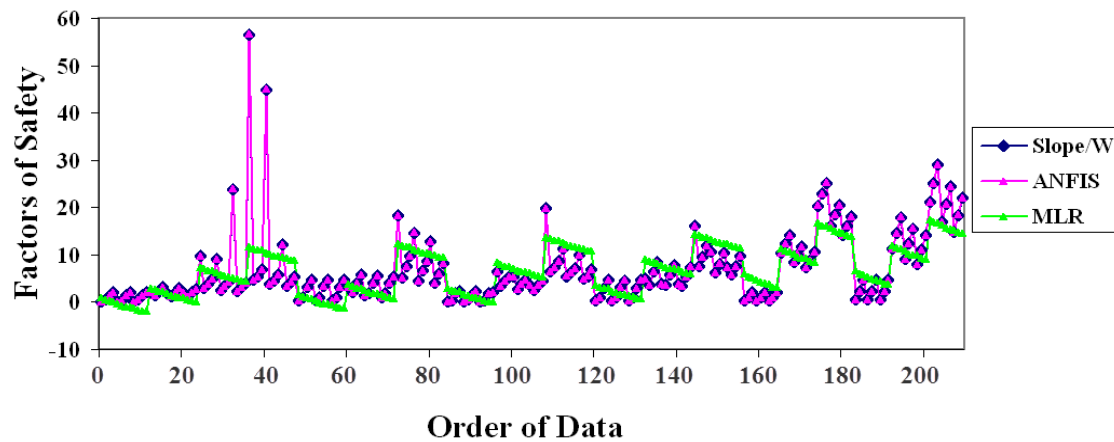


**Figure 12** Comparison of ANFIS and MLR for Ordinary

## Conclusion

Limit equilibrium methods were used to calculate safety factors for 210 different designs with five input parameters: height of slope, unit weight of slope material, angle of slope, coefficient of cohesion, and internal angle of friction. Adaptive Neuro Fuzzy Inference System model and Multiple Linear Regression were used to predict the five input parameters and the overall output safety factors. From predicted data, Graphical User Interface program was generated to present the stability of slopes. The result seemed that Adaptive Neuro Fuzzy Inference System model could predict the safety factors with high accuracy compared with Multiple Linear Regression model.

## References

- Bromhead, E.N. (1999). *The stability of slopes*, Second Eds., Spon press.
- Choobbasti, A.J., Farrokhzad, F. & Barari, A. (2009). Prediction of slope stability using artificial neural network, *Arabian Journal of Geosciences*, 2(4): 311-319.
- Jang, R. (1996). *Neuro-Fuzzy and Soft Computing: A Computational Approach to Learning and Machine Intelligence*. New Jersey: Prentice Hall.
- Lee, W.A., Thomas, S.L., Sunil, S. & Glenn, M. (2002). *Slope stability and stabilization methods*, Second Eds., John Wiley & Sons.
- MathWorks (2009). *Fuzzy Logic Toolbox, User's Guide*, MathWorks.
- Merikoski, S., Laurikkala, M. & Koivisto, H. (2001). An adaptive neuro-fuzzy inference system as a soft sensor for viscosity in rubber mixing process. *Automation and Control Institute: Tampere*.
- Nash, D. (1987). Comparative review of limit equilibrium methods of stability analysis, *Geotechnical Engineering and Geomorphology*, 11-75.
- Ping, K.Z. & Zhi, Q.C. (2009). Stability prediction of tailing dam slope based on neural network pattern recognition, *Proceeding of the International Conference on Environmental and Computer Science*, 380-383.
- Sakellariou, M.G. & Ferentinou, M.D (2005). A study of slope stability prediction using neural networks, *Geotechnical and Geological Engineering*, 23: 419-445.
- Sanford, W. (2005). *Applied linear regression*. New Jersey: John Wiley & Sons.
- SigmaPlot (2004). *SigmaPlot 9: user's guide*. Chicago: Systat Software.
- SigmaPlot (2008). *SigmaPlot 11 part 1: user's guide*. Chicago: Systat Software.
- Sivarao, Peter, B. & El-Tayeb, N.S.M. (2009). A new approach of adaptive network- based fuzzy inference system modeling in laser processing-a graphical user interface (GUI) based. *Journal of Computer Science* 5(10): 704-710.
- Vector, Y. (2008). *Application of soil nailing for slope stability purpose*, Thesis B.Sc. University of Technology.
- Xin, Y. & Xiaogang, S. (2009). *Linear regression analysis: theory and computing*. Singapore: World Scientific.

# Removal of Cr(III) Ions from Tannery Waste Water Through Fungi

Amna Shoaib

Institute of Agricultural Sciences, University of the Punjab, Quaid-e-Azam Campus 54590-Lahore, Pakistan  
aamnaa29@yahoo.mail.com

**Abstract:** Cr(III) removal potential of a wood-rotting fungus viz., *Ganoderma lucidum* (Curt. Fr.) P. Karst was studied from tannery wastewater. Preliminary laboratory assays indicate an optimum pH, 4.5, stirring intensity 150 rpm with increase in removal rate on increasing initial metal ion concentration ( $4\text{--}20\text{ mg L}^{-1}$ ) in the medium. The maximum biosorption capacity of fungus biomass was  $2.16\text{ mg g}^{-1}$  with suitability of Langmuir and Freundlich models on acquired experimental data. In tannery wastewater, fungus showed a maximum of  $1.6\text{ mg g}^{-1}$  biosorption capacity and 43% efficiency. To make this technique practically applicable and economically feasible, the study was further extended by mass cultivated this fungus on agro-wastes followed by assessment of its biosorption potency for Cr(III) ions. Rice straw colonized with *G. lucidum* mycelia could be utilized as an excellent biosorbent thus exhibited 73-76% efficiency for Cr(III) adsorption from tannery wastewater at low concentration of the metal ( $4\text{--}20\text{ mg L}^{-1}$ ).

**Keywords:** Removal of Cr(III), Waste water, Fungi.

## Introduction

Biosorption, metal removal ability of the certain biomass e.g. algae, fungi and bacteria is well-recognized, attractive and cost effective biotechnology for treatment of metal-loaded water. Fungi have been well known for metal removal ability from aqueous phase. Gadd (2001) stated filamentous network of hyphae help them to grow and survive in variety of ecosystems thus provides additional metal binding potential from the contaminated environment. The multilaminar and microfibrillar structure of fungal cell wall along with distinctive aspects of high percentage of cell wall material attributes excellent metal-binding properties. Generally on the basis of sizes, fungi are recognized as micromycetes and macromycetes. So far, numbers of micromycetes like species of *Aspergillus*, *Rhizopus*, *Penicillium*, *Mucor* and *Absidia* have been studied for their metal sorption capability (Dursun *et al.*, 2006; Congeevaram *et al.*, 2007; Subudhi and Kar, 2008). The role of wood rotting fungi or macromycetes in removing heavy metals from the metal-loaded medium could not be negated. Number of macromycetes like *Pleurotus ostreatus*, *Ganoderma lucidum*, *Schizophyllum commune*, *Phanerocheate chrysogenum*, *Coriolus versicolor*, *Agaricus bisporus* and *Pycnoporus cinnabarinus* has been investigated for their metal uptake capability with very promising results (Arica *et al.*, 2003, 2004; Javaid *et al.*, 2008, 2010, 2011).

Macromycetes are commonly famous as mushrooms are found in world humid environment. Mushrooms are a appetizing and nutritious food group of fungi. Reshi mushroom or *Ganoderma lucidum* is well-known oldest medicinal mushroom and is very important economically. Its fruit bodies typically grow in a fanlike or hoof like form on the trunks of living or dead trees. Spores have double-walled, truncate with yellow to brown ornamented inner layers. *G. lucidum* produces a group of triterpenes, called ganoderic acids, having similarity in molecular structure to steroid hormones. Other common compounds of this mushroom are variety of polysaccharides (beta-glucan, coumarin, mannitol) and alkaloids (Paterson, 2006). The potential of both fruiting body and mycelium of *G. lucidum* in bioremediation of heavy metal is well known.

The most compelling reasons for using biosorption technology are utilization of renewable or waste raw materials in economic way. The application of biosorption technology could become more effective keeping economic feasibility through utilization some cheap source for mycelial production of fungi. By doing this practice we not only get economic substrate for mycelial mass cultivation but there would be addition adsorbent having plant cell wall properties. The plant by products e.g. wheat straw and husk, rice straw and husk and cotton waste etc are easily available substrates for raising fungal mycelium in bulk. However, the biosorption potential of macromycetes preparation on agro-waste especially for industrial heavy metal ions removal has not been extensively attempted.

The aim of current research work was to explore the role of *G. lucidum* in removing Cr(III) from tannery wastewater. For large scale industrial application mycelium of *G. lucidum* was mass cultivated on rice straw and colonized straw was used for removal of Cr(III) from tannery water.

## Methodology

Fungal biomass was prepared in liquid phase in 250 ml Erlenmeyer flasks filled with 100 mL of a culture medium i.e. 2% Malt Extract (ME) composed of  $20\text{ g L}^{-1}$  ME powder (DIFCO). The prepared fungal mat after 10 days of incubation was collected, washed with generous amounts of distilled water as long as the pH of the washing solution was in the near-neutral range (7.0-7.2). Dried at  $60 \pm 1\text{ }^{\circ}\text{C}$  was utilized in metal sorption assays.

Batch experiments were performed by taking 0.2 g of oven dried biomass of test fungus in 250 mL flask containing 100 mL of  $14.35\text{ mg L}^{-1}$  (particular concentration chosen on the basis of quantitative measurement of Cr(III) present in tannery water) of Cr(III) solution at 150 rpm and  $25^{\circ}\text{C}$  for 3 hours. To select the optimum pH, this parameter was varied over the range of 2-6.

The rotation speed was monitored at low (50 rpm), medium (100 rpm) and high (150 and 200 rpm) taking non-agitated system as the control. Effect of initial metal ion concentration was investigated by changing the initial concentration of Cr(III) ions within the range of 4-20 mg L<sup>-1</sup> at constant pH and temperature. At the end of experiment, remaining Cr(III) in the supernatant was measured on Atomic absorption spectrophotometer (Model, Varian AA 1275 series).

Cr(III) removal ability of fungus was checked with water of tannery by repeating batch biosorption experiment in same way mentioned above. Acid digestion of the samples was carried out with aquaregia for measurement of residual metal ion concentrations.

Rice straw was used for mycelial cultivation *G. lucidum*. The pre autoclaved inoculated plastic bags (20 x 30 cm) were kept in an incubator at 25°C for 12-15 days. The prepared straw colonized with fungus mycelia was dried in oven and sun. Oven drying was carried out at 60°C for 24 hours and for sun drying prepared material was exposed directly to sun light (40-42°C) for 12-14 hours at 40-50 °C. The biosorption experiments were performed with tannery water under pre optimized biosorption conditions as mentioned in section batch biosorption experiments.

## Results and Discussion

### Effect of pH

The biosorption capacity/efficiency of the candidate fungus for Cr(III) was recorded to increase significantly at appreciable amount on increasing pH from 4.5 (2.0 mg g<sup>-1</sup>/28%) to 5.5 (2.0 mg g<sup>-1</sup>/27%) with slight reduction at pH 6.0 (1.63 mg g<sup>-1</sup>/23%). However, at high acidic pH range i.e., 2.0-4.0 the test fungus exhibited only up to 7-18% efficiency. Consequently, predilection of pH by the test fungus for the highest adsorption of metal ion exhibited following sequence 4.5 > 5.0 ≥ 5.5 > 6.0 > 4.0 > 3.5 (Fig.1). Similar to present records, pH range 4.5-6.0 has been reported as optimal for biosorption of Cr(III), Cu(II), Ni(II) and Zn(II) ions both by micro and macro fungi in several previous studies (El-Syed and El-Morsey, 2004; Javaid et al., 2010; Javaid et al, 2011). These authors attribute that low pH (4.0 and below) limits the biosorption metal ions on to fungal biomass surfaces, probably due to the ion exchange between metallic species and competition effects with oxonium (hydronium) ion to some extent in the biosorption mechanism.

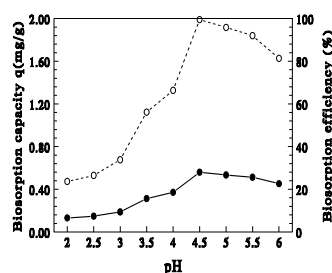


**Figure 1:** Effect of pH on biosorption potential of the *G. lucidum* for Cr(III) ions. Initial concentration of Cr(III) ion in the reaction mixture: 14.35 mg L<sup>-1</sup>. Biosorption conditions: biosorbent concentration, 0.2 g 100 mL<sup>-1</sup>; pH range (2.0-6.0); 150 rpm and 25°C for 5 hours.

### Effect of Stirring Intensity

The effect of the agitation of the sorbent/sorbate system indicated that all agitation speeds exerted a remarkable increase in biosorption efficiency of 21-27% over the non-agitated system that holds only 3.48% efficiency. Therefore, metal removal capacity reached its maximum level at 150 rpm (1.92 mg g<sup>-1</sup>) and then decreased slightly at 200 rpm (1.68 mg g<sup>-1</sup>) followed by 50 and 100 rpm (1.50 mg g<sup>-1</sup>) in comparison to control (0.25 mg g<sup>-1</sup>) (Fig. 2). Agitation facilitates proper contact between the metal ion in solution and the biomass binding sites and thereby, promotes effective transfer of sorbate ion to the sorbent sites (Chergui *et al.*, 2007).

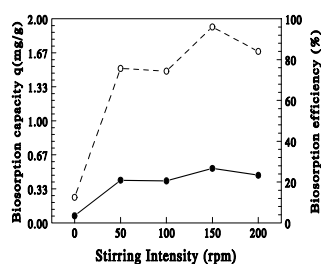


**Figure 2:** Effect of stirring intensity on sorption potential of *G. lucidum* for Cr(III) ions. Initial concentration of Cr(III) ion in the reaction mixture: 14.35 mg L<sup>-1</sup>. Biosorption conditions: biosorbent concentration, 0.2 g 100 mL<sup>-1</sup>; pH, 5.0 at 25°C for 5 hours.

### Effect of Initial Concentration of Metal ions

The fungus subjected to varied concentrations of Cr(III) from 4-20 mg L<sup>-1</sup>, exhibited an increase in sorption capacity of 1.02-2.40 mg g<sup>-1</sup> on increasing metal ion concentrations and maximum uptake was evident at the highest applied concentration (Fig. 3). There is evidence that at high metal ion concentration the number of ions sorbed is more than at low metal concentration, where more binding sites were free for interaction (Cossich *et al.*, 2002; Loukidou *et al.*, 2004).

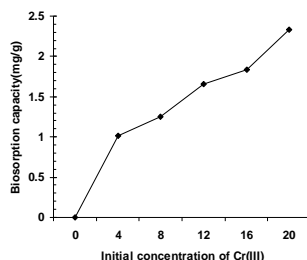


**Figure 3:** Biosorption capacity of *G. lucidum* for Cr(III) ions at various initial concentrations.

### Isotherm Assessment

Through the scatter diagram the analysis of Langmuir (1906) and Freundlich (1916) isotherm models were obtained for the test fungal biomass (Table 2, Fig. 4 A, B). The distribution of  $q_{eq}$  point calculated by the model in function of the experimental values of  $q_{eq}$  shows a linear tendency among the observed and predicted values. This indicated that the experimental data were very well adjusted to the two models.

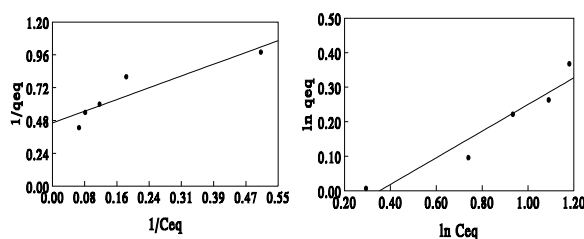


**Figure 4 A & B:** The linearized Langmuir (A) and Freundlich (B) adsorption isotherm for Cr(III) ion biosorption by *G. lucidum*.

### Physicochemical Analyses of Tannery Wastewater

The results obtained on physicochemical analyses of the tannery wastewater are shown in Table 1. All analytical techniques employed were item standard methods (APHA, 1995) and chemicals used in the experiment were of analytical grade (MERCK).

**Table 1:** Physico-Chemical Characterization of Tannery Treatment Plant.

Parameters	Tannery Treatment Plant, Current status	NEQS Acceptable limits	WHO Acceptable limits
Copper (II), mg L <sup>-1</sup>	1.21	1.00	0.20
Chromium (III), mg L <sup>-1</sup>	14.35	1.00	0.10
Nickel (II), mg L <sup>-1</sup>	0.05	1.00	0.20
Zinc (II), mg L <sup>-1</sup>	0.54	5.00	2.00
pH Value (acidity/basicity)	8.5-9.5	6.0-10	No guideline
Temperature (°C)	27-29	40	No guideline
Biochemical Oxygen Demand (BOD) at 20 °C, mg L <sup>-1</sup>	500	80	No guideline
Chemical Oxygen Demand (COD), mg L <sup>-1</sup>	4000	150	No guideline
Total Dissolved Solids (TDS), mg L <sup>-1</sup>	1510	3500	No guideline

National Environmental Quality Standards (NEQS) for liquid Industrial Effluents (2001); World Health organization Standards (WHO) for drinking water (2006).



**Table 2:** Isotherm parameters for the biosorption of Cr(III) ion onto fungal biomass.

Test fungus	$q_{\text{exp}}$ (mg g <sup>-1</sup> )	Langmuir			Freundlich		
		$q_m$ (mg g <sup>-1</sup> )	$b$ (mg L <sup>-1</sup> )	$R^2$	$K_F$	$n$	$R^2$
<i>G. lucidum</i>	1.92	2.16	0.42	0.91	1.37	2.59	0.96

### Biosorption Assays with Tannery Water

The optimized conditions determined from preliminary biosorption assays were used to conduct biosorption experiment with tannery water. For comparison parallel batch experiment was conducted with synthetic solution. Results acquired indicate only 1% reduction in biosorption efficiency of the biosorbent in tannery wastewater in comparison to control (synthetic solution) (Table 3). Similar findings were recorded by Matheickal and Yu (1999) while investigating the effect of light metal ions Na<sup>+</sup>, K<sup>+</sup>, Mg<sup>2+</sup> and Ca<sup>2+</sup> on the biosorption of Pb(II) by *Durvillaea potatorum* and *Ecklonia radiata*. They found that biosorbents had much higher relative affinity for heavy metals than for light metals.

**Table 3:** Comparison of biosorption capacity and efficiency of the test fungus for Cr(III) ions in synthetic solution and Tannery Treatment Plant Water.

Treatments	Rice straw (OD)	Rice straw (SD)
Control (uncolonized agro-waste)	67.73c	69.82b
Colonized agro-waste with mycelia of <i>G. lucidum</i>	73.98ab	75.84a

Initial concentrations of Cr(III) ion in both systems: 14.35 mg L<sup>-1</sup>. Biosorption conditions: pH 4.5, 150 rpm for 3 hours.

**Table 4:** Comparison of biosorbents biosorption efficiency (%) for uptake of Cr(III) ions from Tannery wastewater

Parameters	Synthetic solution of Cr(III)	Actual wastewater of Tannery treatment plant
Biosorption capacity (mg/g)	1.57	1.51
Biosorption efficiency (%)	43.87	42.51

Values with the different letters showed significant difference among treatments at  $p < 0.01$  according to Duncan's multiple comparison tests.

### Biosorption Assays with Colonized and Uncolonized Agro-waste

Both uncolonized and colonized straw with *G. lucidum* mycelia exhibited significantly greater metal removal potential from tannery water (Table 4). However, colonized agro-wastes exhibited greater biosorption potential (70-76%) as compared to uncolonized (60-70%). Enhancement in adsorption ability of colonized rice straw could be owing to fungal lignin and cellulose degradation of agro-wastes. As results of this degradation, the polymer core of straw turn into soluble form and more binding sites on straw are available for metal binding in addition to fungal cell wall molecular binding sites on mucelium (Lee and Rowel, 2004). Results showed that sun dried rice straw exhibited significantly greater adsorption capacity/efficiency (1.36 mg g<sup>-1</sup>/75.84%) in comparison to oven dried straw (1.33 mg g<sup>-1</sup>/73.98%). There might be possibility that oven drying cause denaturtaion of some important chemical groups on the cell wall of biosorbents which remain intact in case of natural drying under sun (Huang and Hunag, 1996).

### Conclusion

Due to low cost involved and simplicity of the technique, rice straw colonized with *G. lucidum* mycelia could be utilized as an excellent biosorbent exhibited efficiency of 73-76% for removal of Cr(III) ions from tannery water containing diluted concentration of the metal (4-20 mg L<sup>-1</sup>).

## References

- American Public Health Association (APHA) (1995). Standard Method for the Examination of Water and Wastewater, American Water Work Association and Water Environment Federation 19<sup>th</sup> Ed.
- Arica, M.Y., Arpa, C., & Kaya, B. (2003). Comparative biosorption of mercuric ions from aquatic systems by immobilized live and heat-inactivated *Trametes versicolor* and *Pleurotus sajor-caju*. *Bioresource Technology*, 89, 145-154.
- Arica, M. Y., Bayramoglu, G., Yilmaz, M., Bektas, S., & Genc, O. (2004). Biosorption of  $Hg^{2+}$ ,  $Cd^{2+}$  and  $Zn^{2+}$  by Ca-alginate and immobilized wood-rotting fungus *Funalia trogii*. *Journal of Hazardous Material*, 109, 191-199.
- Chergui, A., Bakhti, M. Z., Chahboub, A., Haddoum, S., Selatnia, A., & Junter, G. A. (2007). Simultaneous biosorption of  $Cu^{2+}$ ,  $Zn^{2+}$  and  $Cr^{6+}$  from aqueous solution by *Streptomyces rimosus* biomass. *Desalination*, 20, 179-184.
- Congeevaram, S., Dhanarani, S., Park, J., Dexilin, M., & Thamaraselvi, K. (2007). Biosorption of chromium and nickel by heavy metal resistant fungal and bacterial isolates. *Journal of Hazardous Materials*, 146, 270-277.
- Cossich, E. S., Tavares, C. R. G., & Ravagnani, T. M. K.. (2002). Biosorption of chromium(III) by *Sargassum* sp. biomass. *Electronic Journal of Biotechnology*, 5, 133-137.
- Dursun, A.Y. (2006). A comparative study on determination of the equilibrium, kinetic and thermodynamic parameters of biosorption of copper(II) and lead(II) ions onto pretreated *Aspergillus niger*. *Biochemical Engineering Journal*, 28, 187-195.
- El-Sayed. M., & El-Morsy, (2004) *Cunninghamella echinulata* a new biosorbent of metal ions from polluted water in Egypt. *Mycologia*, 96, 1183-1189.
- Freundlich, H. M. F. (1906) Over the adsorption in solution. *Journal of Physical Chemistry*, 57, 385-470.
- Gadd, G. M. (2001). *Fungi in Bioremediation*. Published by British Mycological Society. Cambridge University Press.
- Huang, C. P., & Huang, C. P. (1996). Application of *Aspergillus oryzae* and *Rhizopus oryzae*. *Water Research*, 30, 1985-1990.
- Javaid, A., & Bajwa, R. (2008). A new approach of utilizing plant by-products colonized by fungal mycelia for sorption of industrial heavy metal ions. *Pakistan Journal of Phytopathology*, 20, 101-107.
- Javaid, A., Bajwa, R., & Javaid, A. (2010). Biosorption of heavy metals using a Dead Macro Fungus: Evaluation of Equilibrium and Kinetic Models. *Pakistan Journal of Botany*, 42, 2105-2118.
- Javaid, A., Bajwa, R., Shafique, U., & Anwar, J. (2011). Removal of heavy metals by adsorption on *Pleurotus ostreatus*. *Biomass Bienergy*, 35, 1675-1682.
- Langmuir, I. (1916) The constitution and fundamental properties of solids and liquids. Part. I: Solids. *Journal of the American Chemical Society*, 38, 2221-2295.
- Lee, B. G., & Rowell, R. M. (2004). Removal of heavy metal ions from aqueous solutions using lignocellulosic fibers. *Journal of Natural Fibers*, 1, 97-108.
- Loukidou, M. X., Zouboulis, A.I., Karapantsios, T. D., & Matis, K. A. (2004). Equilibrium and kinetic modeling of chromium(VI) biosorption by *Aeromonas caviae*. *Colloids and Surfaces, A: Physicochemical and Engineering Aspects*, 242, 93-104.
- National Environmental Quality Standards for Municipal and Liquid Industrial Effluents NEQS. (1999) Pakistan.
- Paterson, R. R. (2006). "Ganoderma - a therapeutic fungal biofactory". *Phytochemistry*, 67, 1985-2001.
- Subudhi, E., & Kar, R. N. (2008). *Rhizopus arrhizus* – An efficient fungus for copper effluent treatment. *International journal of integrative Biology*, 2, 166-171.
- World Health Organization WHO. (2006) Guidelines for drinking-Water Quality. 3<sup>rd</sup> Eds. Vol 1.

# Steady-State Electron Drift Velocity at Different Temperatures in $\text{Al}_x\text{Ga}_{1-x}\text{N}$ and $\text{In}_x\text{Ga}_{1-x}\text{N}$ Alloys: Monte Carlo Simulation

Hamdoune, A., and Bachir, N.

Unity of Research Materials and Renewable Energies. Faculty of Science. University of Abou-bekr BELKAID. P.O. Box 230. 13000, Tlemcen, Algeria

ahamdoune@gmail.com

**Abstract:** The  $\text{Al}_x\text{Ga}_{1-x}\text{N}$  and  $\text{In}_x\text{Ga}_{1-x}\text{N}$  alloys are widely used in optoelectronic devices operating in the visible and ultraviolet. They are also attractive for high power, high temperature and high frequency electronic applications. The specific properties of these materials are the source of the charges induced by the effects of spontaneous and piezo-electric polarizations at the interfaces of quantum wells and super lattices. They are used in heterojunction field effect transistors HFET, modulated doping field effect transistors MODFET, and heterojunction bipolar transistors HBT.

We study  $\text{Al}_x\text{Ga}_{1-x}\text{N}$  and  $\text{In}_x\text{Ga}_{1-x}\text{N}$  in the cubic phases because they would have better electronic and optical performances than in their hexagonal phases. We first present GaN, AlN, InN and their alloys  $\text{Al}_x\text{Ga}_{1-x}\text{N}$  and  $\text{In}_x\text{Ga}_{1-x}\text{N}$ . In the second section, we describe the main steps of Monte Carlo simulation method that we use. In the third section, we calculate steady-state electron drift velocity versus electric field for different temperatures and various molar fractions  $x$ . We consider the acoustic, piezo-electric, ionized impurities and polar optical phonon scatterings. We compare our results with published work and are in satisfactory agreement.

**Key words:**  $\text{Al}_x\text{Ga}_{1-x}\text{N}$ ,  $\text{In}_x\text{Ga}_{1-x}\text{N}$ , Temperature (T), electric field (E), velocity (v)

## Introduction

The gallium nitride GaN is the most studied of III-N and even more all other semiconductors. Its large gap and its possibility of alloys with indium nitride (InN) and aluminium nitride (AlN) raised great hopes for these materials as devices in both optical and electronic applications (G. Roosen, 2003). The  $\text{In}_x\text{Ga}_{1-x}\text{N}$  and  $\text{Al}_x\text{Ga}_{1-x}\text{N}$  alloys are often used as barriers of confinement in the optoelectronic-based nitrides structures, and in transistors such MODFET, HEMT and HBT. Their lattice parameters can be deduced from those of GaN, InN and AlN by Vegard's law; they are given respectively by equations (1) and (2) whose are linear interpolations but not sufficient to obtain more accurate values (Fabrice Enjalbert, 2004). The usual lattice parameters of binary compounds in their cubic phase are given in Table 1. The difference between experimental and theoretical values is due to differences in the quality and structural constraints existing in the layers.

$$a_{\text{In}_x\text{Ga}_{1-x}\text{N}} = x \times a_{\text{InN}} + (1-x) \times a_{\text{GaN}} \quad (1)$$

$$a_{\text{Al}_x\text{Ga}_{1-x}\text{N}} = x \times a_{\text{AlN}} + (1-x) \times a_{\text{GaN}} \quad (2)$$

**Table.1** lattice parameters of GaN, InN and AlN compounds, in their cubic phase

Material	Calculated $a_0$ (Å) (S. K. Pugh et al. 1999)	Experimental $a_0$ (Å)
GaN	4.423 - 4.462 - 4.452	4.50 (Xu et al. 2000) - 4.53 (R. C. Powell et al. 1993)
InN	4.996 - 4.392 - 4.981	4.98 (M. Guerrero and Esteban, 2002) - 4.97 (F. Dessenne, 1998)
AlN	4.301 - 4.392 - 4.34	4.38 (I. Petrov et al. 1992) - 4.3996 (Okumaru et al. 1998)

The effective masses of  $\text{In}_x\text{Ga}_{1-x}\text{N}$  and  $\text{Al}_x\text{Ga}_{1-x}\text{N}$  ternary compounds are also often deduced by linear interpolation from those of GaN, InN and AlN. In the  $\Gamma$  valley, they are respectively  $m_e^* = 0.15m_0$ ,  $m_e^* = 0.10m_0$  and  $m_e^* = 0.25m_0$  in the cubic phase ( $m_0$  is the electron mass in vacuum).

At 300K; GaN, InN and AlN admit gaps about 3.2eV, 1.9eV and 6eV in their cubic phases. The variations of the alloys energy band gaps, depending on the composition, are given by equations (3) and (4) where the bowing parameter  $b$  is approximately equal to  $1.13 \pm 0.23\text{eV}$  (Fabrice Enjalbert, 2004).

$$E_{\text{In}_x\text{Ga}_{1-x}\text{N}}^g = x \times E_{\text{InN}}^g + (1-x) \times E_{\text{GaN}}^g - b \times x \times (1-x) \quad (3)$$

$$E_{\text{Al}_x\text{Ga}_{1-x}\text{N}}^g = x \times E_{\text{AlN}}^g + (1-x) \times E_{\text{GaN}}^g - b \times x \times (1-x) \quad (4)$$

## Monte Carlo Simulation

The Monte Carlo method is based on a drawing of lots process of interactions sustained by the carriers during their movement in the compound, from probability laws. The method consists to follow the behavior of each electron in real space and in wave-vectors space. Let us consider an electron which has energy  $\varepsilon(t)$ , wave-vector  $k(t)$ , and which is placed in  $r(t)$ . Under action of an electric field  $E(r, t)$ ; the exchange of energy and momentum with the lattice, and the deviation of its trajectory by impurities, will modify energy, wave-vector and position of the electron. Using mechanical and electrodynamic laws, we determine the behavior of each electron in time and space. To be more realistic:

1. We statistically study possible energy exchange between electrons, modes of lattice vibrations and impurities; this allows us to calculate the probability of these interactions and their effect on the electron energy and wave-vector.
2. We assume that these interactions are instantaneous. We can now do move electrons in free-flight under the only effect of electric field, between two shocks. The free-flight time is determined by drawing lots. When there is interaction, we determine its nature by drawing of lots, and we change the energy and wave-vector of the electron, in this case. The distribution of electrons changes, we then compute the resulting electric field at sufficiently small time intervals. Thus, we can assume the electric field constant between two calculations (Thobel, 1980) – (S. Galden, 1992) – (O. Mouton et al. 1993).

## Results and Discussion

We consider a simplified model of three isotropic and nonparabolic valleys, with a maximum alloy scattering rate. We consider the acoustic, piezoelectric, ionized impurities and polar optical phonon scatterings. We calculate the electron mass in the higher valleys, by the relationship (5) (A.F.M. Anwar et al. 2001) (where  $m^*$  is their effective mass in  $\Gamma$  valley, and  $\alpha$  is the nonparabolicity factor of the considered valley):

$$m = m^* \times (1 + \alpha\varepsilon) \quad (5)$$

In the steady-state, we calculate the electron drift velocity as a function of applied electric field for different temperatures namely 300, 500 and 700K; and for various molar fractions  $x$ , in the  $Al_xGa_{1-x}N$  and  $In_xGa_{1-x}N$  ternary compounds with an electron concentration equal to  $10^{17}cm^{-3}$ . The results are illustrated respectively by Fig.1 to 6. To validate our results, we compare them with those of reference 14 where the authors study the same ternary compounds, at room temperature.

By increasing the temperature, the gap decreases. That of InN is small; the  $In_xGa_{1-x}N$  ternary compound will have its gap towards zero quickly enough. For this reason, we limit ourselves to a temperature equal to 700K.

- Increasing the molar fraction  $x$  of aluminium in the  $Al_xGa_{1-x}N$  ternary compound, or decreasing the molar fraction  $x$  of indium in the  $In_xGa_{1-x}N$  ternary compound:

- The band gap energy increases.
- The energy separating the upper valleys and the  $\Gamma$  valley increases; then there is an increasing critical electric field for which the velocity reaches its maximum while the peak velocity decreases.
- The electron effective mass increases also, resulting in a decrease of electron drift velocity.

- At room temperature, we obtain respectively for GaN, InN and AlN peaks about:  $3 \times 10^7 cm/s$  for  $E=110kV/cm$ ,  $3.24 \times 10^7 cm/s$  for  $E=50kV/cm$  and  $2.13 \times 10^7 cm/s$  for  $E=400kV/cm$ . Their saturation velocities are respectively about  $2 \times 10^7 cm/s$ ,  $2.35 \times 10^7 cm/s$  and  $1.75 \times 10^7 cm/s$ .

- The increase in temperature allows a higher kinetic energy gain for electrons; they move more and then come into collisions with other atoms by transferring their energy. Then for the same molar fraction  $x$ ; the peak velocity decreases and moves slightly toward the highest fields, and the saturation velocity decreases also.

The alloy scattering mechanism dominates in the ternary compounds under the present simulation conditions; the total scattering rate is higher. Thus a higher field is required to the free carriers for reaching the higher valleys, and the peak velocity occurs at a higher field.

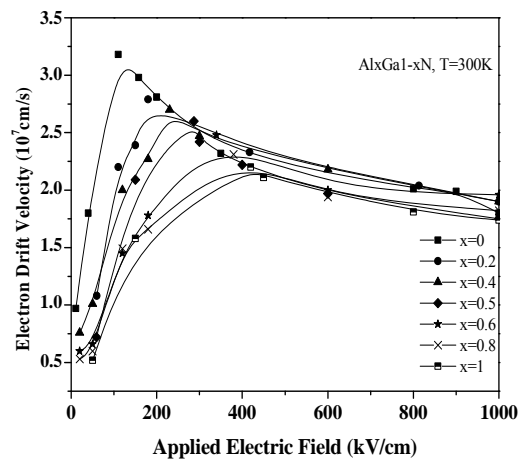


**Fig. 1** The electron drift velocity versus applied electric field for different molar fractions  $x$  at 300K, within  $\text{Al}_x\text{Ga}_{1-x}\text{N}$

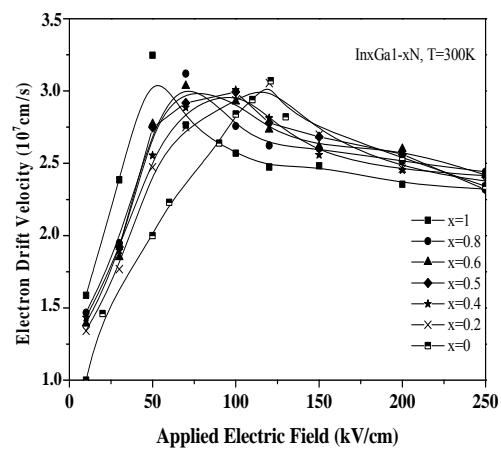


**Fig. 2** The electron drift velocity versus applied electric field for different molar fractions  $x$  at 300K, within  $\text{In}_x\text{Ga}_{1-x}\text{N}$

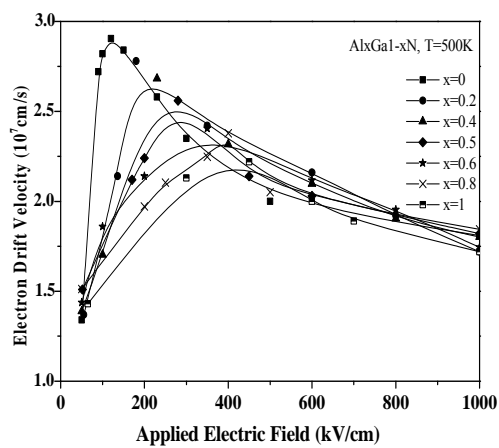


**Fig. 3** The electron drift velocity versus applied electric field for different molar fractions  $x$  at 500K, within  $\text{Al}_x\text{Ga}_{1-x}\text{N}$

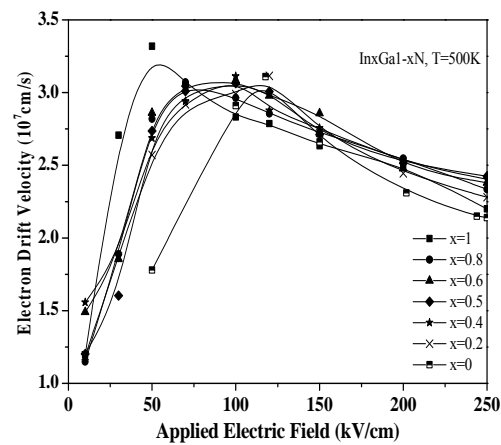


**Fig. 4** The electron drift velocity versus applied electric field for different molar fractions  $x$  at 500K, within  $\text{In}_x\text{Ga}_{1-x}\text{N}$

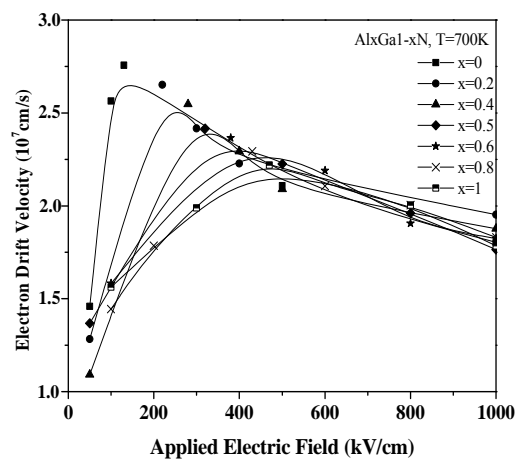


**Fig. 5** The electron drift velocity versus applied electric field for different molar fractions  $x$  at 700K, within  $\text{Al}_x\text{Ga}_{1-x}\text{N}$

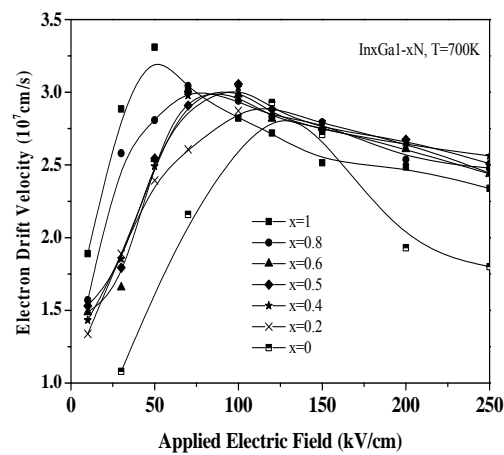


**Fig. 6** The electron drift velocity versus applied electric field for different molar fractions  $x$  at 700K, within  $\text{In}_x\text{Ga}_{1-x}\text{N}$



## Conclusion

GaN, InN, AlN, and their alloys, constitute a major research field of electronics in the solid state for microwave applications. They have several advantages: high voltage thanks to their large gaps, high output impedance, high peak and saturation velocities, and large thermal and chemical stabilities.

We studied the electron transport at low field in the  $\text{Al}_x\text{Ga}_{1-x}\text{N}$  and  $\text{In}_x\text{Ga}_{1-x}\text{N}$  ternary compounds, using Monte Carlo simulation, and considering a simplified model of three isotropic and nonparabolic valleys. We considered the acoustic, piezoelectric, ionized impurities and polar optical phonon scattering mechanisms.

We calculated the steady-state electron drift velocity versus applied electric field for different temperatures and various molar fractions  $x$  of aluminum and indium in the  $\text{Al}_x\text{Ga}_{1-x}\text{N}$  and  $\text{In}_x\text{Ga}_{1-x}\text{N}$  alloys.

The inclusion of alloy scattering influences the transport dynamics changing the peak velocity and the threshold electric field. However, if the alloy scattering is strong, the ternary compounds exhibit peak velocities below that of their constituent binaries.

Calculated at 300K; our results are in satisfactory agreement with those of (M. Farahmand & F. Brennan, 2001) where the authors use a nonparabolic effective mass energy band model, ensemble Monte Carlo simulation.

## References

- G. Roosen. (2003). Materials for Optoelectronics, Treaty Series Optoelectronics. Vol. 7, Hermes Science Publications.
- Fabrice Enjalbert (2004). Etude des hétérostructures semi-conductrices III-nitrures et application au laser UV pompé par cathode à micropointes. Ph.D. Thesis, University of Joseph Fourier, Grenoble 1, France.
- S. K. Pugh, D. J. Dugdale, S. Brand & R.A. Abram (1999). Electronic structure calculation on nitride semiconductors. *Semicond. Technol.*, 14, 23-31.
- Xu et al. (2000). Anomalous strains in the cubic phase GaN films grown on GaAs (001) by metalorganic chemical vapour deposition. *J. Appl. Phys.* 88(6), 3762-3764.
- R. C. Powell, N.E. Lee, Y.W. Kim & J. Greene. (1993). Heteroepitaxial wurtzite and zinc blend structure GaN grown by reactive ion molecular beam epitaxy, growth kinetic microstructure and properties. *J. Appl. Phys.* 73 (1), 189-204.
- Martinez Guerrero & Esteban. (2002). Elaboration en épitaxie par jets moléculaires des nitrures d'éléments III en phase cubique. National Institute of Applied Sciences, Lyon, France.
- François Dessenne. (1998). Etude thermique et optimisation des transistors à effet de champ de la filière InP et de la filière GaN. Ph.D. Thesis, University of Lille 1, France.
- I. Petrov, E. Majob, R.C. Powell & J.E. Greene. (1992). Synthesis of metastable epitaxial zinc blend structure AlN by solid reaction. *J. Appl. phys.* 60(20), 2491-2493.
- Okumaru et al. (1998). Growth of cubic III-nitrides by gas source MBE using atomic nitrogen plasma: GaN, AlGaIn and AlN. 198, 390-394.
- Thobel. (1992). Simulation Monte Carlo du transport électronique et des phénomènes de diffusion dans les systèmes à base de semi-conducteurs III-V. University of Lille 1, France.
- S. Galden. (1992). Etude du transistor bipolaire à double hétérojonction Si/SiGe/Si par la simulation Monte Carlo. University of south Paris.
- O. Mouton, J. L. Thobel, & R. Fauquemberg. (1993). Monte Carlo simulation of high-field electron transport in GaAs using an analytical band structure model. *J. Appl. Phys.* 10-74.
- A.F.M. Anwar, Senior Member, Shangli Wu, & Richard T. (2001). Temperature dependent transport properties in GaN,  $\text{Al}_x\text{Ga}_{1-x}\text{N}$ , and  $\text{In}_x\text{Ga}_{1-x}\text{N}$  semiconductors. *IEEE Transactions on Electron Devices*, 48(3), 567-572.
- M. Farahmand & F. Brennan. (2001). Monte Carlo Simulation of Electron Transport in the III-Nitride Wurtzite Phase Materials System: Binaries and Ternaries. *IEEE Trans. Electron Devices*, 48(3).

# The Potential for Climate Change Mitigation in Solid Waste Disposal: A Case Study of Lagos Landfills

Aboyade, A.O<sup>1</sup>, Rabiua, A.\*<sup>2</sup>, Amigun, B.<sup>3</sup>

<sup>1</sup>Department of Process Engineering, Stellenbosch University, Stellenbosch, South Africa

<sup>2</sup>Department of Chemical Engineering, Cape Peninsula University of Technology, Cape Town 8001, South Africa

<sup>3</sup>National Biotechnology Development Agency, Abuja, Nigeria

rabiua@cput.ac.za

**Abstract:** Solid waste disposal sites account for up to 20% of global emissions of methane the second most significant greenhouse gas. However, under proper management landfills can in fact have a positive carbon balance, by capturing the methane-rich landfill gas (LFG) produced from the dumpsites. This paper assesses the potential for implementing such a project in the Olusosun waste disposal site in Lagos, Nigeria. Data regarding municipal solid wastes (MSW) generation and composition, regulations as well as relevant aspects of the Nigerian energy market and its regulations and climate change policies were evaluated. This is employed to assess the potential for a viable implementation of a landfill gas to energy project at the site. The analyses revealed that the flaring only scenario was observed to be the most economically feasible. The cost of producing electricity from LFG (approx. US\$50/MWh) is higher than the estimated long term cost from natural-gas fed thermal plants (at US\$39/MWh).

**Key words:** Lagos landfill, Climate change, Solid waste disposal

## Introduction

Mounting scientific evidence linking climate change to anthropogenic greenhouse gas (GHG) emissions has given more urgency to the calls for adopting less carbon intensive economic growth (Watson, 2001). Increasing attention is being directed at developing countries where much of such future growth is expected. While it is recognized that economic growth is necessary for poverty reduction and sustainable development in these regions, global opinion leader and policy makers from both developing and developed countries agree that it would be undesirable for such growth to be sustained at current levels of carbon intensity.

There is therefore, general consensus on the need to integrate climate concerns into sustainable development objectives in all sectors of the economy; energy, transport, agriculture and waste management. Municipal solid wastes (MSW) contribute significantly to global GHG emission and are a major challenge to public health especially in lower income countries. Where proper management of solid waste disposal sites (SWDS) can be taken for granted in many developed countries, it still is a major problem for their less developed counterparts as many of these countries lack the funding and in most cases the technology to improve their disposal systems.

Emission trading schemes like the Kyoto protocol's Clean Development Mechanism (CDM) serves as a platform for overcoming such financial and technological barriers. Under the mechanism, investors or governments in developed countries can invest in projects in poorer countries, transferring environmentally sustainable technology to help these countries reduce their GHG emissions and contributing to their sustainable development. In the process these investors are allowed to offset the certified emission reductions (CER) generated from such projects against their own emission reduction targets as set by their various countries. Many developing countries are taking advantage of this opportunity already. By 2004, India, Brazil and China, already had 42 such projects between them at different stages of implementation (Ellis, Corfee-Morlot and Winkler, 2004). This paper investigates the potential of implementing a viable landfill gas to energy project (LFGTE) in Lagos, Nigeria under the CDM mechanism. To do this, the technical potential of the project (climate, waste generation quantities, etc) as well as the relevant regulatory and socio-economic environment will be analyzed.

## Methodology

### 1.1 Conceptual Approach

This study straddles three policy sectors, MSW, energy and climate and has clear and established benefits to sustainable development objectives in these sectors. Assessing the potential performance of an intervention such as proposed in this study requires the identification of the components and relations that could be potentially affected by that intervention (Villavicencio, 2003). In this case, introducing a technology like LFG capture will be influenced by the existing regulations and practices in

the MSW, energy and climate sectors as well as physical and socio economic characteristics of the immediate environment and their dynamic interactions (Figure 1).

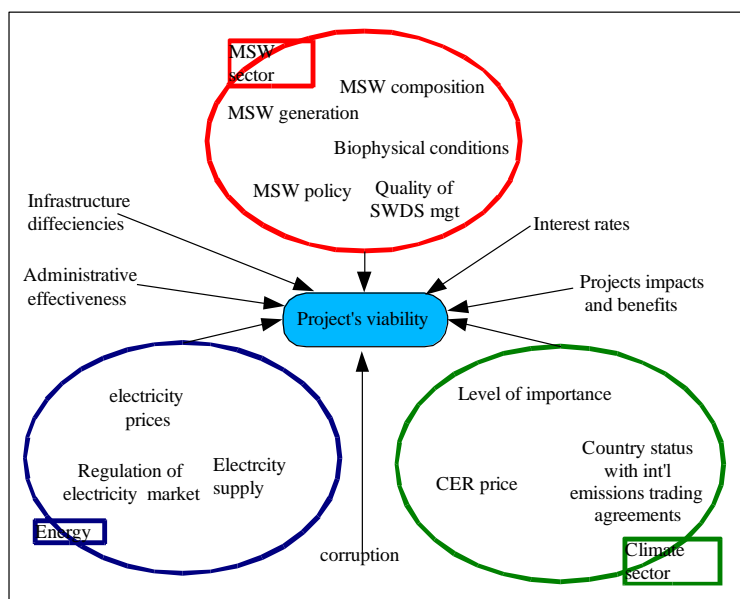


**Figure 1:** Conceptual map of system structure to be studied

The systems dynamics approach was used for much of the analysis done in this study. It is a method that aims to enhance the understanding of complex dynamic systems (Stermann, 2000) - dynamic, in the sense that the system variables evolve over time as the result of previous interactions (Ruth & Hannon, 1997). These variables and their interactions make up the structure of the system and determine the systems behavior. If those variables and relations can be identified, the system's behavior can then be simulated with reasonable levels of confidence (Bossel, 1994). Various permutations and combinations of the variables can also be simulated and the likely outcomes evaluated. System dynamics is here applied in analyzing the sectors shown in the conceptual map. Components within each sector interact dynamically with each other and with components in other sectors and influence the key outcome of interest i.e. the projects potential viability.

## 2.2 LFG Estimation Models

Many methods and models have been developed for projecting LFG generation potential from SWDS. The IPCC recommends two of these methods for LFG generation estimation for the purpose of establishing national GHG inventories – default and first order decay methodologies (World Bank, 2004). The first order decay method is the more accurate of the two and was employed in this work.

## Status of MSW Management and Climate Change Policy in Nigeria

### 1.2 MSW Management in Lagos, Nigeria

According to Bamgbose, Arowolo, Oresanya and Yusuf (2000), 70% of total waste generated in Lagos was from domestic sources and the rest from industry (Table 1). There are widely divergent views on waste generation in Lagos. A World Bank sponsored study reported a daily generation of about 0.21 kg per capita (Bamgbose *et al.*, 2000). This figure is very likely an underestimation because it was based on records of waste received at the various disposal sites across the city. In reality about 30% of waste generated never gets to disposal sites (Agunwamba, 1998). Another study reports daily per capita waste generation rates as 0.35kg (Cygnet Services Limited, 2002).

**Table 1:** Waste composition in Lagos obtained from different studies

Waste Composition (%)	(Bamgbose et al., 2000)	Rushbrook, Pugh, & Mundial (1999)	Cygnet Services Limited, (2002)
Paper	10	14	10
Textiles	4		2
Plastic	7		22
Non food putrescibles e.g. garden waste	68	60	45
Wood or straw			
Food waste			
Others	11	19	14

### 1.3 Olusosun SWDS

LAWMA currently operates 3 dumpsites; Olusosun, Solus and Abule-Egba. The focus of this work is the Olusosun SWDS which is the largest in Lagos. It is the only one fit to host an LFGTE project because it has a remaining life span left of more than 10 years, it receives a large amount of waste and, has the right depth. It was constructed under a World Bank loan secured in 1988 to use the trench system. It is at 60m above sea level and lies on a high density clay deposit under which there are two water aquifers (Bamgbose *et al.*, 2000). The average daily tonnage received in Olusosun between March and June 2004 is given in the Table 2.

**Table 2:** Average daily tonnage of refuse received at Olusosun site between March and June 2004 (Source: LAWMA)

Type of waste		Mon.	Tues	Wed.	Thurs	Fri	Sat	Sun	Weekly Averages
Domestic Waste	LAWMA	730	850	890	820	815	1130	610	835
	Local Government Sanitation Agencies	150	135	150	210	100	2665	60	
	Private Collectors	1340	1325	1215	1360	1220	1610	1140	
Commercial waste (from markets, non-hazardous waste from institutions etc)	LAWMA	220	190	210	170	180	130	180	835
Total domestic and commercial waste		2440	2500	2465	2560	2315	5535	1990	2829.29
Industrial waste and metal scraps	LAWMA, NAFDAC and SON	230	250	270	225	220	250	270	245.0

## Results and Discussion

The focus of the analysis is the assessment of the viability of a LFGTE plant in Olusosun SWDS in Lagos. This is done in two stages. First an analysis of the technical viability as determined by the availability of the methane resource is conducted, followed by a socio economic analysis of the project's survivability. Relevant factors and their interactions in each of these stages are first depicted in Causal Loop Diagrams (CLD), then the results of the STELLA analysis for that stage is presented along with the assumptions under which they were made. The model takes a modular design. The full structure and description of model can be obtained from Aboyade (2004).

### 1.4 Assessment of Resource Potential

The major factors affecting LFG and hence CH<sub>4</sub> emissions from MSW are mainly the amount of waste generated, the composition of the waste, the conditions under which the waste is disposed, and the climate of the region under study. All the factors, save the last, are dependent one way or the other on the socio-economic characteristics of the region. The CLD in Figure 2 captures the interactions that affect CH<sub>4</sub> emissions from MSW in Lagos.

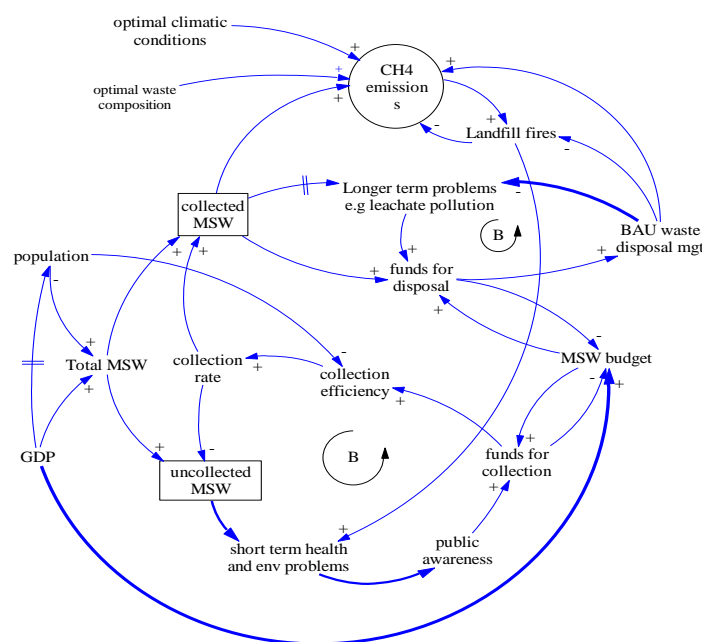


**Figure 2:** CLD showing factors affecting CH<sub>4</sub> emission from MSW disposal sites

The generated waste is either collected or littered as shown in the CLD. The amount of waste collected depends basically on the collection efficiency of LAWMA as dictated by its own administrative effectiveness, which in the past years has been poor. Where littered waste gets to the point where it becomes aesthetically unpleasant, and presents directly perceptible dangers to public health, public awareness influences government to increase the flow of funds for collection services. Such increase is of course limited by the municipality's budget which in itself is a direct function of the economic prosperity of the state. The poor economic status coupled with the low quality management enjoyed in public services ensures that such increased effort at collection services is hardly sustained. Usually however the limited successes of such efforts at least in reducing the amount of littered waste soon causes public pressure to relax. Also the ever increasing quantities of waste coupled with lack of sustained political will and increasing administrative inefficiencies ensures that the collection rates soon drops and uncleared waste again begins to mount. Interestingly, according to officials in LAWMA, this cycle (represented by the balancing loop in the CLD) very often coincides with the election or appointment of new leaders in the state. This is because in a bid to impress its constituents, the new administration (usually military controlled) pumps money towards reducing the amount of littered waste, only to relax after a while for the same reasons aforementioned.

#### 1.4.1 Methane emissions from Olusosun SWDS

The results of the emission modeling for methane are as shown in the Figure 3 under the following assumptions:

- $L_0$  – Methane generation potential (estimated using the formula,  $MFC \times DOC \times DOC_F \times \frac{16}{12}$  to be equal to  $150\text{m}^3/\text{mg}$ ). A conservative estimate when compared with  $190\text{m}^3/\text{Mg}$  for Brazil which has a similar waste composition (Maily, 2004).
- K- methane generation constant for lack of data is assumed to be the default suggested by IPCC - 0.05

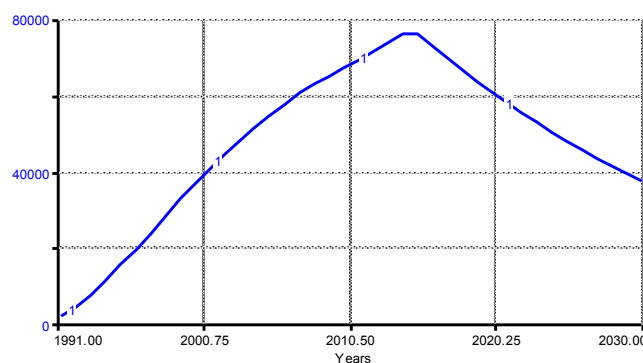


**Figure 3: Methane emissions from Olusosun SWDS**

The graph shows methane emission from Olusosun reaching its peak of about 76,000 tonnes of methane in 2014 thereabouts with an average annual emission of 63,000 tonnes during the project's lifetime. It also shows that Olusosun will still be generating emissions well beyond 2030. A sensitivity analysis varying  $k$  and  $L_0$  by  $\pm 15\%$  shows that this varies from a low of 47,000 tonnes to a high of 78,000 tonnes  $\text{CH}_4$ .

### 1.5 Assessment of Economic Viability

The economic viability of the proposed project is governed by policies in three different sectors; the MSW, energy and climate or emissions trading sectors. MSW policy and practices especially regarding, MSW collection efficiencies, choice of disposal method and so on are crucial to the waste stream which in turn forms the resource for LFG and electricity production. Energy policies relevant to the electricity prices and the level of regulation of electricity sales will to a large extent will ascertain how much income is to be expected from electricity generated from the site. Furthermore, the existence or not of a climate policy is important to determine if CER's can be sold. Economic viability as measured by net present value (NPV) and internal rate of return (IRR) is a direct consequence of the costs associated with the project and revenues accruing to it; all other factors that affect the projects viability e.g electricity price, CER price and interest rates could be said to feed in through these two components.

#### 1.5.1 Assumptions

Cost estimates for this analysis both capital and operational were obtained from representative estimates given in the US EPA's landfill gas-to-energy project development handbook (EPA, 1996). Apart from these, other important cost items are the transaction costs associated with CER sales; monitoring costs, verification and validation costs as well as registration and approval costs. Taking into account the value of emission reductions possible from this project (25 million  $\text{tCO}_2\text{e}$  over a 20 year crediting period) this project would qualify as a very large CDM project (UNFCCC, 2004) and according to Krey & Welt-Wirtschafts-Archiv (2004), the transaction costs associated with registering and validating emissions from the project under the CDM would be about US\$0.123/  $\text{tCO}_2\text{e}$ .

The revenue stream derives mainly from electricity and CER sales. In general it is assumed that the electricity generated from the project would be sold to the municipality for street lighting. Electricity prices in the analysis will be varied according to current obtainable rates. CER prices have typically been within the 3 to 6US\$/tCO<sub>2</sub>e range (Haites & Seres, 2004). Project lifetime of 20 years as consistent with projects of this nature (US EPA, 1999), and tax rate on all profits of 30% which is the prevalent corporate tax rate in Nigeria (NIPC, 2004). The analysis includes capital costs in the year they are incurred and as such it was not necessary to include depreciation (Barish, 1962).

Cash flow analysis of the viability of the project was done under three scenarios: a) Funding from local sources at current discount rates. b) Funding from foreign sources such as the World Banks Carbon Fund. c) Flaring only option (no electricity generated). The major distinguishing factor between the first two scenarios is the cost of capital for the project as determined by interest and discount rates. According to Barish (1962), high interest rates is one major impediment to project finance in developing countries.

#### 1.5.2 Scenario 1: Local funding

Consultations with officials from the state ministry of environment revealed that the government is investigating the possibilities of handing over operation of the landfills to private interests. This scenario simulates the project viability assuming the new private owner decides to borrow from local banks to implement the project. Interest rates in local financial institutions are pegged to the Central Bank's minimum discount rate for treasury bills which is set at 18%. In this scenario it is assumed the local investor borrows from local banks at 22.5% interest.

Putting all these parameters in the STELLA model yield the following results for NPV of the project after 21 years:

**Table 3:** NPV (in US\$) under different CER and electricity price ranges

		Electricity prices US\$/MWh		
		21	50	65
CER price (US\$)	0.00	-1,595,909.44	-874,063.87	-498,834.31
	3.00	-1,004,164.81	-279,299.14	95,631.38
	6.00	-384,284.00	340,581.67	715,512.19

Results show that the project cannot be viable under the price regimes given in the table, without additional revenue from CER's. The prices selected in the Table 6 are based on different assumptions under which electricity price for the project could be negotiated. US\$21 is the lowest price for which the national utility (Power Holding Company of Nigeria – PHCN) sells to its customers, US\$50 is the highest PHCN buys from IPP and US\$65 is the price municipalities pay for electricity for street lighting (all per MWh). Personal communication with PHCN officials revealed it is unlikely for PHCN to buy at higher price than US\$50/MWh given its recent attempts at commercialization. Even assuming that price could be negotiated, the project still isn't viable when CER's are sold for US\$3 as the project still returns a negative NPV. Also the IRR in this case is 13.5% which is clearly below local interest rates. The table shows the project can only be viable (i.e. returns positive NPV) at CER price of up to US\$6. Then IRR is at 23%, still too close to the interest rates.

#### 1.5.3 Scenario 2 foreign funding

In the general, the cost of funds from foreign sources are cheaper than that from local sources especially in Nigeria where interest rates are generally on the high side. This is especially true when the sources of the funds are public or non profit institutions, or specialized funds like the World Bank's Carbon Fund. In this scenario a simplified assumption that the project is funded at 8% interest rates yield the following

**Table 4:** NPV (in US\$) under different CER and electricity price ranges with 8% interest rates

		Electricity prices US\$/MWh		
		21	50	65
CER price (US\$)	0.00	-9,019,252.88	-3,366,784.37	-443,093.76
	3.00	-4,217,324.06	1,435,144.45	4,358,835.06
	6.00	736,240.20	6,442,369.50	9,366,060.11

Even here it is still obvious that the project cannot break even without additional revenue from CER's during the stipulated project life. However with IRR raging between 12 to 13%, i.e about 5% higher than the cost of funds, represented here by the interest rates, one can argue that the project stand a much better chance of been profitable under this scenario.

#### 1.5.4 Scenario 3 Flaring Only

Further analysis of the first two scenarios point to the fact that CERs makes up between 35% to 53% of revenues depending on whether it is sold for US\$3 or US\$6. The fact that CER revenues account for so much of the total is combined with the fact that the energy generation part of the costs actually accounts for 67% of the projects capital costs and 90% of the operation and



maintenance costs suggests higher rates of return if the project is run without electricity generation. Under this scenario therefore, the project's capital costs is reduced to US\$6,354,000 and maintenance costs to US\$299,000. This then yields an IRR of about 27% when CERs are sold for US\$3 per tCO<sub>2</sub>e. This implies the project has much higher returns even when the source of funding is local. This result in essence shows that the most commonly touted direct benefit of LFG capture – energy generation – holds little prospect as a driving force for such an intervention in Nigeria.

## Conclusions

The result of this study has shown that the cost of the local private funding is too high to allow the reasonable rate of return for a LFGTE project. Funding from foreign sources at lower lending rates increases the chances of the project being viable, but even that would be by only a slight margin. The flaring only option, without electricity generation on the other hand is the best scenario, as the bulk of the projects revenues are from CER sales. This is just as well, considering that electricity generated from the project will not be able to compete with conventional sources because the costs at which electricity from LFG is produced (approx. US\$50/MWh) is slightly higher than the marginal cost for which electricity from natural gas will be produced in the long term (US\$39/MWh). This conclusion is not very different from that arising from similar studies in countries where electricity prices are low.

## References

- Agunwamba, J. (1998). Solid waste management in Nigeria: problems and issues. *Environmental Management*, 22(6), 849–856.
- Bamgbose, O. A., Arowolo, T. A., Oresanya, O., & Yusuf, A. A. (2000). Assessment of Urban Solid Waste Management Practices in Lagos, Nigeria. *African Scientist*, 1(1), 23-31.
- Barish, N. N. (1962). *Economic Analysis for Engineering and Managerial Decision-Making* (Later Printing.). McGraw Hill Book Co.
- Bossel, H. (1994). *Modeling and Simulation*. A K Peters/CRC Press.
- Cygnnet Services Limited. (2002). *Technical and Commercial Proposal for Management of Olusosun Landfill Site*. Lagos: Lagos State Ministry of Environment.
- Ellis, J., Corfee-Morlot, J., & Winkler, H. (2004). Taking stock of progress under the Clean Development Mechanism (CDM). *Organisation for Economic Co-operation and Development, Paris*.
- EPA, U. (1996). Turning a Liability into as asset: A Landfill Gas-to-energy Project Development Handbook. *USA Environmental Protection Agency-EPA*.
- Haite, E., & Seres, S. (2004). Estimating the market potential for the clean development mechanism: review of models and lessons learned. *PCFplus Report*, 19.
- Krey, M., & Welt-Wirtschafts-Archiv, H. (2004). *Transaction costs of CDM projects in India: An empirical survey*. Hamburgisches Welt-Wirtschafts-Archiv (HWWA).
- World Bank, B. (2004). The World Bank handbook for the preparation of landfill gas to energy projects in Latin America and the Caribbean. *Waterloo, Ontario*.
- Rushbrook, P., Pugh, M., & Mundial, B. (1999). *Solid waste landfills in middle-and lower-income countries: a technical guide to planning, Design, and operation*. Banco Mundial.
- Ruth, M., & Hannon, B. (1997). *Modeling Dynamic Economic Systems* (1st ed.). Springer.
- Sterman, J. D. (2000). Business dynamics: systems thinking and modeling for a complex world. 2000. *Boston et al: Irwin McGraw-Hill*, 110.
- UNFCCC. (2004). Approved baseline methodology AM0003: Simplified Financial Analysis for Landfill Gas Capture Projects. UNFCCC.
- Villavicencio, A. (2003). *A systems view of sustainable energy development*. Discussion Paper. Quito.
- Watson, R. T. (2001). IPCC Third Assessment Report: Climate Change 2001: Synthesis report. IPCC.

# The Role of Desalinated Water in Integrated Water Resource Management in Abu Dhabi Emirate-UAE

Muthanna Al-Omar

Environmental Studies Dept., National Energy & Water Research Center  
Abu Dhabi Water & Electricity Authority/Abu Dhabi –UAE  
m.alomar@adwea.ae

**Abstract:** Water resources components in Abu Dhabi encompass the conventional sources (rain, springs, ponds and groundwater), and unconventional sources (desalinated water and reclaimed wastewater). The latter represent the most important resources for the time being, since ground water is brackish or salty and the annual rainfall is very low in Abu Dhabi Emirate. Thus conventional water resources are considered under sever depletion and exceeded their natural recharging capacity by 24 times. Per capita water consumption is considerably high, since the average daily domestic consumption in Abu Dhabi Emirate is estimated as 350 liters per person but it is intended to be slashed by 200 liters per day in the next few years, as proposed by the Environmental Authority. This should be accompanied by intensive awareness program. This article is aiming at discussing water resources components in Abu Dhabi and their Integrated Water Resources Management (IWRM) Plan.

**Key words:** Desalinated water, Abu Dhabi Emirate

## Introduction

United Arab Emirates (UAE) is the world's second largest consumer of water per capita after the United States and the first country in the world in the Ecological Footprints (WWF, 2008). The demand on water is increasing year-on-year due to rapid population growth, growth in hotel industry and rapid expansion of orchards and green areas in addition to the weak awareness of water scarcity and the weak water saving attitudes. All together, had led water issue in UAE to reach an alarming level, particularly because water scarcity issue could only be resolved through establishment of desalination industry which has many advantages and disadvantages (EAD 2009, Abdul-Wahab 2005) (Agashichev and Al-Nasher 2005).

According to the Environmental Agency of Abu Dhabi, water policy in the Emirate has principally emphasized on increasing water supply rather than improved demand management (EAD 2006a). This tendency has a great risk on both groundwater availability and seawater quality. Particularly, if we recall that the former is expected to be completely depleted in next 50 years (EAD 2006a) and the latter is already subjected to the threat of salinization.

It is estimated that the average daily domestic consumption in Abu Dhabi Emirate is ranging between 350-550 liters per person (EAD 2006) which is considered as considerably high rate as compared to 425 liters in the U.S. Flat residents consume on average from 170 to 200 liters of water per day, which may be considered as a reasonable range, but villa dwellers' water consumption is 270 to 1,760 liters per person per day (Teodrova 2009). On average, each Abu Dhabi resident uses 550 liters of water per day. However the Environmental Authority is planning to slash the rate of consumption by 200 liters per person per day in the next few years. On the other hand, water for agricultural uses is mostly ensured through groundwater (Dawoud 2007), whereas the rest of water demand particularly as drinking and household is fulfilled through desalination of seawater from the Arabian Gulf using multistage flash process (MSF) with a total capacity of 683 million gallon per day (MGD) (ADWEC 2011). Most of

these plants are planning to expand their production capacities, exposing in this way the fragile ecosystem of the Arabian Gulf to a greater risk due to discharge of warm brine water (Elshorbagy 2007).

This article is aiming at discussing water resources components in Abu Dhabi and their Integrated Water Resources Management (IWRM) Plan.

### The Study Area

Abu Dhabi Emirate is the largest of seven United Arab Emirates (UAE). It lays on the southwestern coastline of the Arabian Gulf (Fig. 1) with a coastline extending about 350 km. Total population of UAE is estimated to be 8 million

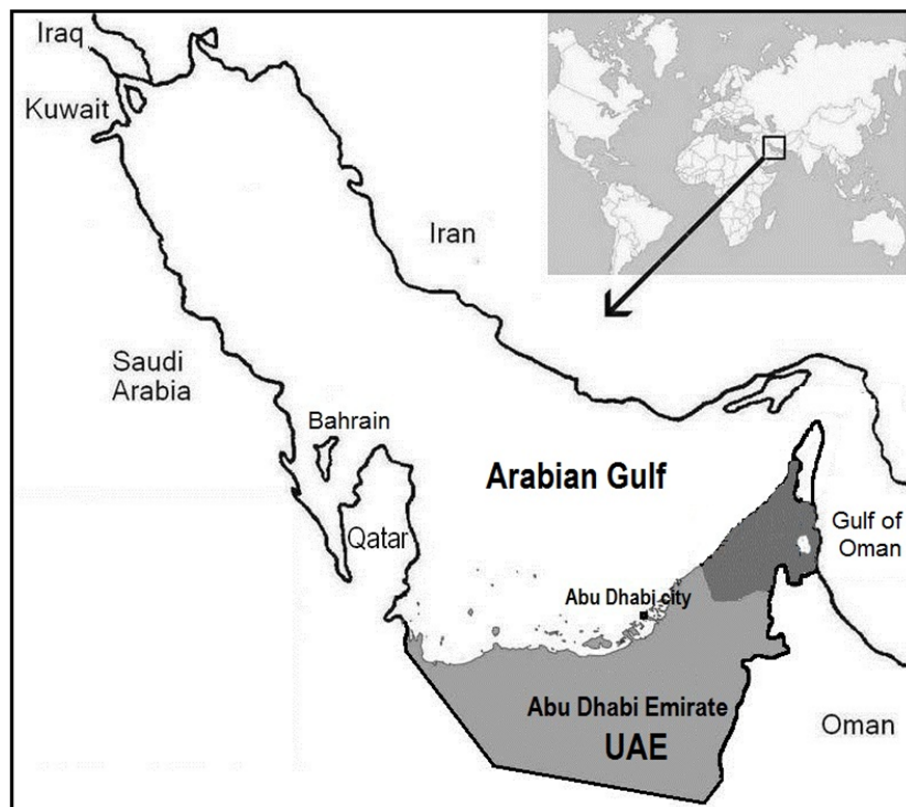


**Figure 1** Location of Abu Dhabi Emirate (marked in light grey) with respect to UAE in Arabian Gulf.

in 2011 , only 12% are nationals and the rest are expatriates, while Abu Dhabi population is estimated to be 1,305,060 with approximately the same percentage of nationals to expats. Population in Abu Dhabi is steadily increasing at an annual rate of 3.7% (EAD 2006b). Being part of a desert land in the Arabian Peninsula; climate is arid with prolonged hot summer and relatively short winter. The lowest atmospheric temperature was reported as 10.6 °C whereas the maximum temperature was reported as 47.4 °C (EAD 2006a). Relative humidity is considerably high and may reach more than 90% very often.

The majority of water demand is secured through the use of groundwater (brackish 38% ), which is mainly used in agriculture, followed by desalinated water (23%), then freshwater (13%). The former type is used for drinking or household and amenity (Fig. 2). Reclaimed water represent only 6% of the total and is only used in landscaping and forestry.

These water resources are generally categorized into two major groups of resources: conventional and unconventional water resources as follow:

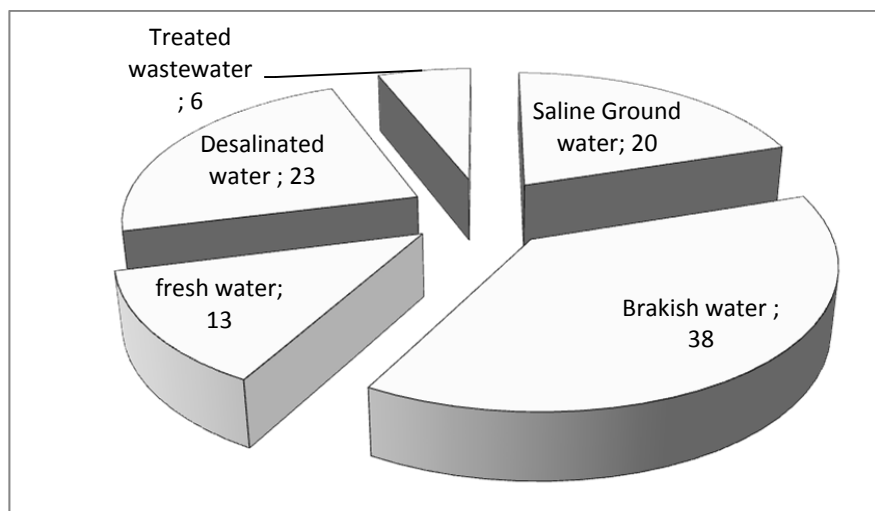


**Figure 2** Sources of water in Abu Dhabi Emirate.

### 1. Conventional Water Resources

These are rainfall, springs and groundwater resources:

**Rainfall:** The reported Annual Rainfall is considerably low, reaching 20.4 mm in Abu Dhabi City and 33.8 mm in Al Ain city (EAD 2006). Most of rainy days occur during February, however in a cycle of 4-5 years, rainfall may raise the rate above these average values. On the contrary, annual evaporation rate is relatively high reaching about 2,000 mm (EAD 2009). In general rain water stock is estimated to be 24 million cubic meter (Mcm) per year according to 2007 estimates. (EAD 2009)

Ground water falls into three different categories of salinity whose available stocks according to 2007 estimates are as follow: freshwater 26,000 Mcm, moderately brackish 89,000 Mcm and brackish 132,000 Mcm (EAD 2009).

Ground water contributes to 71.2% of total water demand, yet it is being over-exploited at a rapid rate. Groundwater supply had fallen by 18 % since 2003, while the consumption of water resources in the emirate exceeded their natural recharging capacity by 24 times. (Teodorova, 2009). Therefore it is envisaged that this resource can barely last for the next 50 years. Abu Dhabi's groundwater reserves stand at 641 Mcm. However, more than 97% is brackish, its reserves of sweet or moderately brackish water that can be easily tapped can last only 20 to 40 years, the study says. It is estimated that about 630 well fields exist in Abu Dhabi however the operating wells are only 363. Springs are confined to Al-Ain area. Water in both wells and springs is brackish, moreover water of springs is hot and run at a constant temperature of 39.3° C. It is worthy to mention that groundwater is not used for drinking due to the presence of relatively high levels of boron and nitrate.

### 2. Unconventional Water Resources

Seawater desalination represent the only source of potable water in Abu Dhabi Emirate, it is produced by five Giant power and desalination plants whose locations and capacities are shown on the map (Fig. 3). ADWEA oversees four of the power and desalination plants are located in Abu Dhabi Emirate and uses multistage flash (MSF) and multi-

effect systems (MED), whereas the fifth is in Fujairah Emirate and uses hybrid MSF and reverse osmosis (RO). The total annual water production has escalated from 66,772.58 million gallon (MG) in 1998 to 183,560.79 MG in 2010 in addition to 28,232.49 MG imported from Fujairah power and desalination plant (ADWEC 2011). As peak daily water supply, capacity was increased from 220MGD in 1999 to reach 673 MGD in 2010 (Fig. 4) (ADWEC 2011).

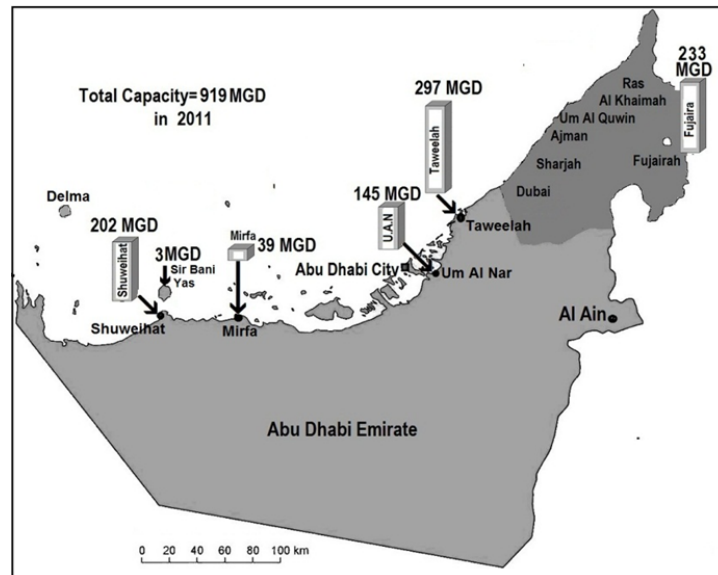


**Figure 3** Map of Abu Dhabi Emirate-UAE showing locations and capacities of desalination plants.

Desalination plants are in process to expand their capacities so that the daily production rate is to be doubled in 2030 to cope with the increasing demand. Nevertheless, environmentally, this expansion shall adversely affect marine environment in the Arabian Gulf by the discharge of hot brine water, which is already under great environmental stress.

A smaller desalination plant is located in Delma island has a total capacity of 3 MGD, among which one MGD is produced by MED and the rest is produced by reverse osmosis in addition to similar or smaller RO units owned by different entities or communities among them is the one in Sir Bani Yas which has only 2 MSF units of 0.28 MGD amounting to a total capacity of 0.56 MGD.

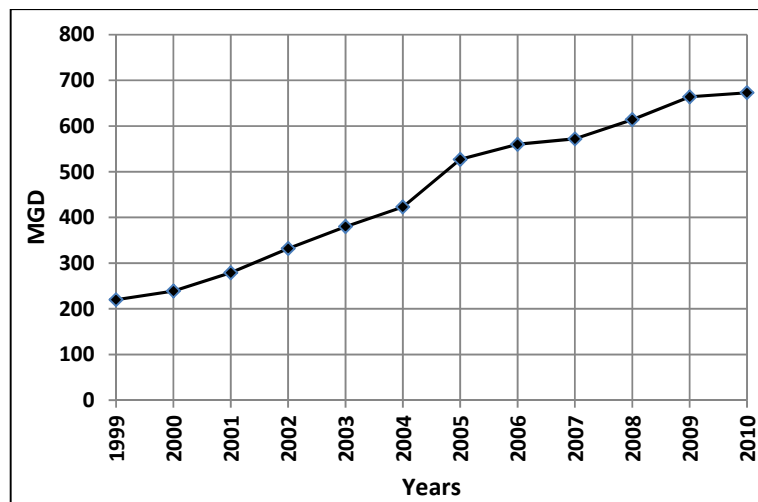


**Figure 4** Increase in daily desalinated water production capacity during 1999-2010

Majority proportion of desalinated water (43%) is consumed mostly as potable and household water. The second major use is for livestock 21%. Amenity water (public facilities) is mostly used for landscaping and roadside plantations

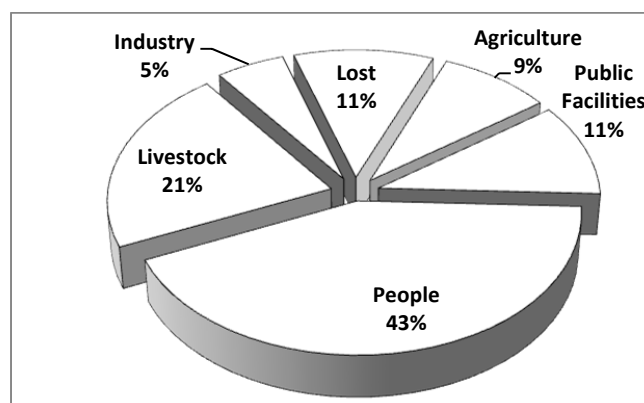


**Figure 5** Major uses of desalinated water in Abu Dhabi Emirate

which account 11%, other uses are demonstrated in Fig. 5. Losses in about 11% of water is attributed to breakage of pipes, and physical leakage.

The second unconventional water resource in Abu Dhabi is the reclaimed wastewater. There are two main sewage treatment plants in Abu Dhabi City and Al Ain city, both treat almost 95% of sewage and work slightly over their design capacity (EAD 2009). In the year 2003, population of Abu Dhabi Emirate was 1.3 million; a total of 140.8 Mm<sup>3</sup> of treated wastewater was reclaimed, representing 4% of the total water consumed that year (EAD 2006b) (ADSSC 2007). However, in 2005 a new sewage treatment plant was commissioned rising the total sewage effluents (TSE) to a level of about 139 Mm<sup>3</sup>/year, (Fig. 6) and about 182 Mm<sup>3</sup> in 2007 (EAD 2009). Abu Dhabi collects 146 Mm<sup>3</sup>/year whereas Al Ain collects 36 Mm<sup>3</sup>/year. The rest of 5% is treated by smaller units to serve smaller communities. TSE per person per day is estimated to be 130 based on the served population of 1.4 Million. Currently 35% of TSE (i.e. 51 Mm<sup>3</sup>) is disposed of into the Gulf, the rest is used for landscaping.



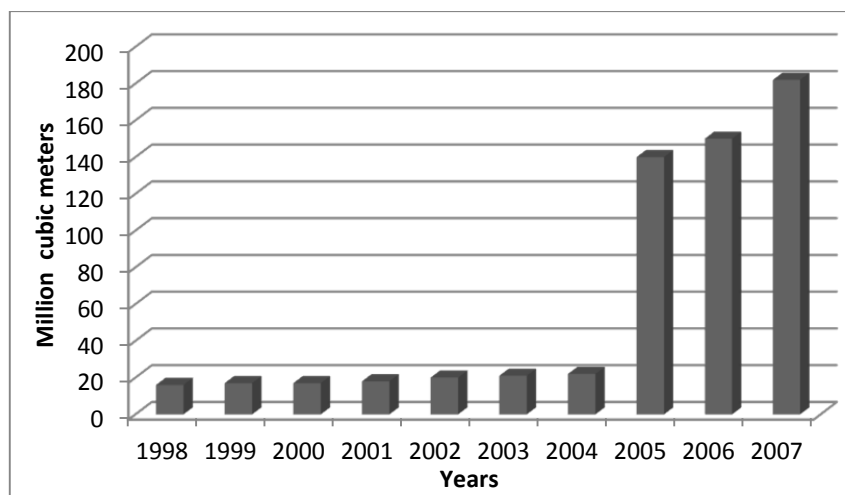


**Figure 6** Quantities of reclaimed water from sewage in Abu Dhabi Emirate.

### Water Scarcity Awareness

A couple of years ago, a survey of 2,363 people in the emirate showed that water conservation was the area of least concern. Only 42.8% of respondents were aware that water scarcity should be a concern in the UAE (Teodorova 2009). Taking into consideration that ground water is already under excessive extraction, surface water resources are scarce. Therefore water conservation should be considered as an essential practice disregarding its abundance or availability. Planners, engineers and policy makers are encouraged to shift toward green technologies (low-flow tabs and showers as well as low flush" toilets)...etc. Also to promote environmental awareness towards water saving behavior. On the other hand only 10 % say the task is exclusively the responsibility of consumers. (Gornall and Todorova, 2009)

### Conclusions

Per capita water consumption in Abu Dhabi Emirate is considerably high, with limited resources and continuously increasing population and agricultural practices. All these factors had led desalination plants to increase their production capacities in order to meet the demand. On the other hand desalination has different adverse effect of the fragile marine environment of the Arabian Gulf. Therefore, water conservation should be considered as an essential practice and people should made aware of its importance. Per capita daily water consumption should be slashed by 200 liters per day in the next few years to come.

### References

- Abdul-Wahab, S. A. (2005) Characterization of water discharge from two thermal power/desalination plants in Oman. *Environmental Engineering Science* 24(3) 321-337.
- ADSSC (2007) Annual Report 2007. Abu Dhabi Sewage Services Company (ADSSC).
- ADWEC (2011) ADWEC Statistical Report 1999-2010, Abu Dhabi Water and Electricity Company.
- Agashichev, S. and Al-Nasher A., (2005) Systemic approach for techno-economic evaluation of triple hybrid (RO, MSF and power generation) scheme including accounting of CO<sub>2</sub> emission. *Energy* 30 (2005) 1283–1303
- Anonymous (2009) Water Resources Strategy of Abu Dhabi. *World Environment Magazine*, No 02
- Dawoud, M. (2007) An Integrated approach for groundwater resources assessment, development and management in Abu Dhabi. *Water Summit 2007*, United Arab Emirate University and Shlumberger Water Services, 28 March 2007. p23

- EAD (2006a) The state of environment-Abu Dhabi. Environmental Agency Abu Dhabi. pp. 20-21
- EAD (2006b) Abu Dhabi Water Resources Statistics-2006, Environmental Agency Abu Dhabi.
- EAD(2008) Terrestrial Environment of Abu Dhabi Emirate. Environmental Agency Abu Dhabi-UAE.pp. 461
- EAD(2009) Abu Dhabi Water Resources Master Plan. G. Pitman, R. McDonnell and M. Daoud, (ed). Jan. 2009  
Environmental Agency Abu Dhabi.
- Elshorbagy, W. (2007) Desalination perspective and implication with coastal environment. Water Summit 2007, United Arab Emirate University and Shlumberger Water Services, 28 March 2007. p22
- Gornall, J. and Todorova, V. (2009) UAE's water woes need joint solution. The National Newspaper Retrieved from <http://www.thenational.ae/article>. Last Updated: Aug. 30, 2009
- IDS Water: Information Resource for Water Industry. retrieved from <http://www.idswater.com/water/asia/home.aspx>. last updated Sept 14, 2007.
- MoH (2010) UAE Biostatistics. Statistics and Research Department. Ministry of Health. UAE.
- Teodorova, V. (2009) Abu Dhabi faces water crisis. The National Newspaper Retrieved from <http://www.thenational.ae/article>. Last Updated: March 22. 2009.
- WWF (2008) Living Planet Report 2008, World Wide Fund for Nature. Chris Hails (ed.) p.14